2009

Fabricating New Miniaturized Biosensors for the Detection of Dna Damage and Dna Mismatches

N. Indika Perera
Cleveland State University

FABRICATING NEW MINIATURIZED BIOSENSORS FOR THE DETECTION OF DNA DAMAGE AND DNA MISMATCHES

N. INDIKA PERERA

BSc Special Degree in Chemistry
University of Colombo, Sri Lanka
January, 2002

submitted in partial fulfillment of the requirements
for the degree of

DOCTOR OF PHILOSOPHY IN CLINICAL-BIOANALYTICAL CHEMISTRY
at the

CLEVELAND STATE UNIVERSITY

December, 2008

This dissertation has been approved

for the department of CHEMISTRY

and the college of Graduate Studies by

_____

Mekki Bayachou, Ph.D.
Dissertation Committee Chairperson

_____

Department/Date

_____

Lily Ng, Ph.D.

_____

Department/Date

_____

Robert Wei, Ph.D.

_____

Department/Date

_____

John Masnovi, Ph.D.

_____

Department/Date

_____

Crystal Weyman, Ph.D.

_____

Department/Date

DEDICATION

This thesis is dedicated to my loving father late Mr. Naullage Maheepala Perera.

ACKNOWLEDGEMENT

I am deeply indebted to my supervisor, Professor Mekki Bayachou, for giving me the opportunity to carry on this research in his lab, and also for his help, stimulating suggestions, and encouragement that helped me in all the times of this research and writing of this thesis.

I would like to give my special thanks to my mother, Ms Mallika Perera, for her help and support in difficult times and to my wife, Dhanuja Perera, whose encouraging support and patience enabled me to complete this work.

I am also grateful to Dr Robert Wei for his help and support throughout my PhD career.

I have furthermore to thank my colleague, Dr John Moran, for his valuable advices in completing this thesis and *The Bayachou Lab* members for all their stimulating support.

FABRICATING NEW MINIATURIZED BIOSENSORS FOR THE DETECTION OF DNA DAMAGE AND DNA MISMATCHES.

N. INDIKA PERERA

ABSTRACT

A large number of genetic diseases and genetic disorders are simply caused by base alterations in the genome. Therefore, developing efficient and cost effective techniques for routine detection of these alterations is of great importance. Different methods involving gel electrophoresis and Polymerase Chain Reaction have been widely employed, but majority of these methods are costly, time consuming, and lack throughput, creating a fundamental gap between the current state-of-the-art and desired characteristics of low-cost, high-speed, simplicity, versatility, and potential for miniaturization. In this study, we attempt to bridge this gap by developing new sensing platforms to detect DNA base mismatches and DNA damage with higher throughput, better ease-of-use, and with the potential to be miniaturized for greater portability. Two electrochemical mismatch detection sensing platforms were developed. One uses the electrochemical reduction of trans-4-cinnamic acid diazonium tetrafluoroborate. The other takes advantage of the natural ability of MutS protein for single base mismatch recognition. Also, two DNA damage detection assays were developed and the first approach uses Atomic Force Microscopy to monitor minor DNA damage by labeling damaged sites with a biomarker. This site-specific biolabeling was achieved through well-established biotin-streptavidin chemistry. In the second approach, a new layer-by-layer biomolecular immobilization method was introduced and used to detect DNA chemical damage using electrochemical techniques.

TABLE OF CONTENTS

LIST OF FIGURES

LIST OF SCHEMES

LIST OF TABLES

GENERAL INTRODUCTION

Alterations in the DNA molecule introduce biochemical changes into cells with varying degrees of severity. The cause of these alterations can be divided into two major categories: replication errors by DNA polymerase, and exposure to harmful environmental conditions. DNA Polymerase replication errors result in random insertions[1], deletions[2, 3], or substitutions[4, 5] (also referred to as **DNA mismatches**) of the nucleotide bases in the macromolecular DNA, while the various, harsh oxidizing environmental conditions will cause more specific types of damage such as single-strand breaks and strand openings[6, 7]. These xenobiotic-induced DNA strand alterations are commonly referred to as **DNA damage**, and can be a consequence of direct exposure to harmful environmental conditions and various toxins[8-13]. In cells, most common type of DNA damage is a result of free-radical chemical attack to nucleotide bases.

The severity of the DNA mutation or damage depends on its location on the DNA strand, since only less than 10% of cellular DNA contains known and useful information that is used to make proteins and enzymes; the function of the remaining 90% of DNA nucleotides not involved in these processes is yet to be resolved[14].

When DNA base alterations are allowed to perpetuate uncorrected, they create biochemical havoc in the living organism[15], so it is of great importance to have the ability to correct or repair these alterations. One way for cells to correct mutations and the various degrees of DNA damage is to have multiple proofreading mechanisms and repair cascades that maintain genetic integrity. Failure of even one of these processes can result in a mutation of the DNA molecule, which is the origin of genetic diseases[15]. Though there are occasionally some positive long-term effects of genetic mutation through the

evolutionary process in all species of plant and animal, for the vast majority of cases these mutations are unwanted and undesirable[15]. Thus, early detection of DNA alterations can be a great benefit for avoiding the subsequent negative consequences that may arise from such mutations.

Recently, there has been enormous interest in developing and fabricating sensors for the detection of DNA mismatches and chemical damage. Since maintaining genomic integrity is vital, the development of reliable methods to identify and characterize early DNA abnormalities is especially important. Further, there is always an interest in efficient and reliable assays with high-throughput capability. Current methods and tools include gel electrophoresis and polymerase chain reaction (PCR). However, they lack simplicity, high-throughput, ease of use, and are limited in potential to be miniaturized. This creates a gap between the current state-of-the-art and the desired characteristics of the assay method mentioned above. The main goal of this work is to bridge the gap by developing new techniques to detect DNA base mismatches and DNA damage with higher throughput, better ease-of-use, and with the potential to be miniaturized for greater portability.

In the first three chapters, we will limit our discussion to the development of sensors that specifically target **DNA mismatches**. In chapters four and five we will address sensors that specifically target **DNA chemical damage**.

PART I

FABRICATING NEW MINIATURIZED SENSING PLATFORMS TARGETING DNA MISMATCHES

CHAPTER I

AN EXAMINATION OF THE CURRENT METHODS FOR DNA MISMATCH DETECTION

1.1 Introduction

Of all genetic alterations point mutations are the most difficult to detect[16]. A significant numbers of fatal diseases are caused by point mutations. For instance, sickle-cell disease and cystic fibrosis result simply from single base substitutions. In addition, single nucleotide polymorphisms can produce devastating effects within the genetic code, causing a myriad human diseases including cancer. For example, over 18 000 p53 mutations have a potential to develop various types of cancer including breast, lung, liver, prostate and skin carcinomas[17].

Various methods have been developed to detect the presence of mutations in DNA, and some methods are capable of characterizing the molecular nature of the mutation. Though detection of mutations in DNA sequences (which code a particular gene) is sufficient for diagnostic purposes, further characterization of the particular mutation may be important for certain diseases.

Sensitivity, selectivity, and high-throughput capabilities are important aspects to consider when developing DNA mismatch detection techniques. A large number of methodologies have been developed in various fields and the number of new methods is growing due to the increased demand for techniques that screen mutations both quantitatively and qualitatively. Chief among these methodologies for DNA mismatch detection are biochemical assays[18, 19], separations[20], molecular imaging[21], nano-gravimetric analysis[22], DNA microarrays[18], and spectroscopic probes[23]. Currently, biological assays such as electrophoresis, PCR, and DNA sequencing methods or their combinations are the most widely used in clinical diagnostics. PCR is used to replicate small segments of DNA using primers whereas gel electrophoresis is a biomolecular separation technique based on an electric field applied to the gel matrix.

Throughput, accuracy, speed, portability, and cost-effectiveness are among the most important criteria for large-scale screening of known mutations. Currently, there is nothing in the market that can meet all of these conditions. Therefore, the development of a method that bridges the gap between the current state-of-the-art and these desired criteria would be both novel and useful.

1.2 Molecular biological techniques

Many methods based on molecular biological assays have been developed for the detection of point mutations. DNA microarrays, ligation techniques, and DNA sequencing are among the widely used ones. Direct DNA sequencing is considered the "gold standard" for reliability in genetic testing[24]. DNA sequencing is relatively simple in that it determines the consecutive base sequence in a particular DNA strand with the help of PCR. Sequencing requires appropriate primers that target the sequence of interest, a pool of deoxynucleotides (dNTP), DNA polymerase enzyme, and labeled/unlabelled di-deoxynucleotides (ddNTP). All components (minus the ddNTP) are combined and then divided into four aliquots. Next, one of each of the four types of ddNTP chain terminator is added into each reaction vial. After the PCR reaction, the resulting amplified DNA strands are separated and analyzed via automated sequencing.

Sequencing is usually performed on relatively short DNA sequences (<700 bp), as the sequencing gets exponentially more complicated with the number of base pairs[25]. Despite significant advances in DNA sequencing technology, direct sequencing has not established itself as the method of choice for large scale analysis due to complexity, cost, and most importantly, lack of high throughput capability. Also, DNA sequencing has a very limited potential to be developed as a miniaturized device. Figure 1.1 illustrates the basics of the DNA sequencing process.

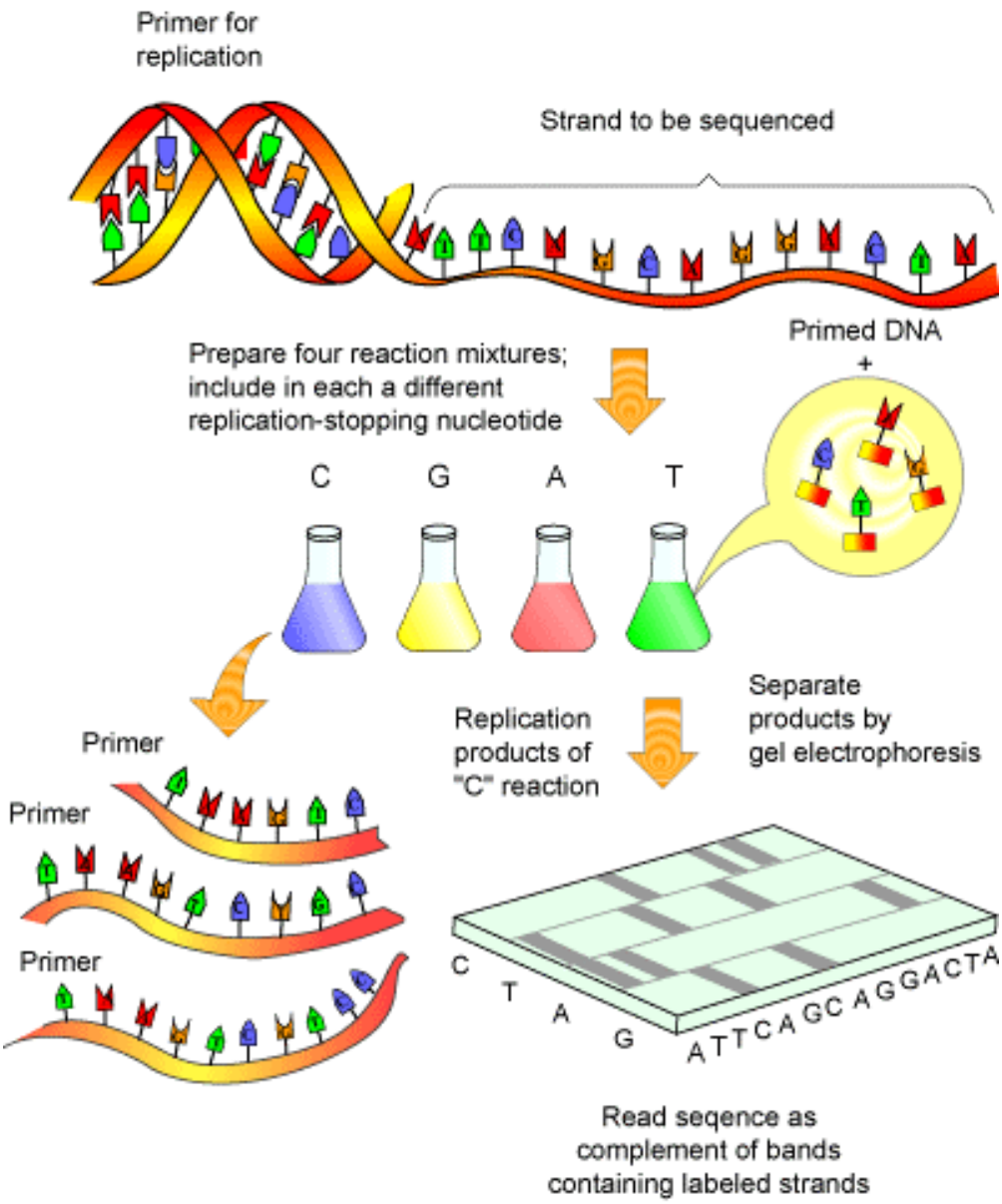

Figure 1.1 DNA sequencing methodology: Single stranded DNA is amplified in the presence of fluorescently labeled ddNTPs that serve to terminate the reaction and label all the fragments of DNA produced. The DNA fragments are then separated via gel-electrophoresis or capillary electrophoresis (CE) and the sequence read using a laser beam and a computer.

*(**Source:** GENOME PROJECTS: UNCOVERING THE BLUEPRINTS OF BIOLOGY by Helmut Kae)*

Besides DNA sequencing, numerous biotechnological methods have been developed and most of them are coupled to PCR and gel electrophoresis[26-30], two techniques that have revolutionized DNA testing. Advanced versions of gel electrophoresis called denaturing gradient gel electrophoresis (DGGE) and temperature gradient gel electrophoresis (TGGE) have been developed by Lerman, *et al* for the detection of point mutations[31]. Since then, many research groups have utilized these technologies to develop novel routes to screen for mutations[32]. However, these methods are tedious and difficult to handle, as they require radioactive phosphorous or fluorescent-labeled DNA molecules. If not handled carefully, radioactive phosphorous labels could lead to unwanted radiolysis reactions, which eventually interfere with the main assay.

Another technique incorporating electrophoresis is single-strand conformational polymorphism (SSCP)[30, 33]. The concept behind this technique is that when DNA is placed in a non-denaturing solution, it folds into a specific conformation that is determined by its base sequence. Any change in the sequence, as little as one base, results in a different conformation that can be visualized by differences in mobilities in the gel.

A similar approach to SSCP called conformation sensitive gel electrophoresis (CSGE)[34] is also reported. In CSGE, double-stranded DNA is exposed to mild denaturing conditions in order to induce conformational changes. Normal and mutated DNA will yield different conformations resulting in two distinct migration patterns in the gel. These techniques (CGSE and SSCP) are mostly suitable for shorter DNA fragments (<1kBP) in mismatch detection. For longer base pair sequences, another similar technique has been developed based on chemical cleavage of the mismatch (CCM)[35].

However, most of these methods suffer from the fact that some mutations fail to induce a conformational transition that is detectable by gel electrophoresis.

1.3 Use of mismatch detection proteins such as MutS

Another class of mutation detection methods uses the intrinsic capabilities of certain proteins to detect DNA mismatches. MutS is one such protein that has been extensively used to identify single-base mismatches. *In vivo*, MutS, a 90 kDa dimeric protein, plays a vital role in the mismatch repair cascade[36]. The MutS dimeric structure, with dimensions of ~125×90×70 Å[36], is shown in the ribbon diagram in Scheme 1.1-(a).

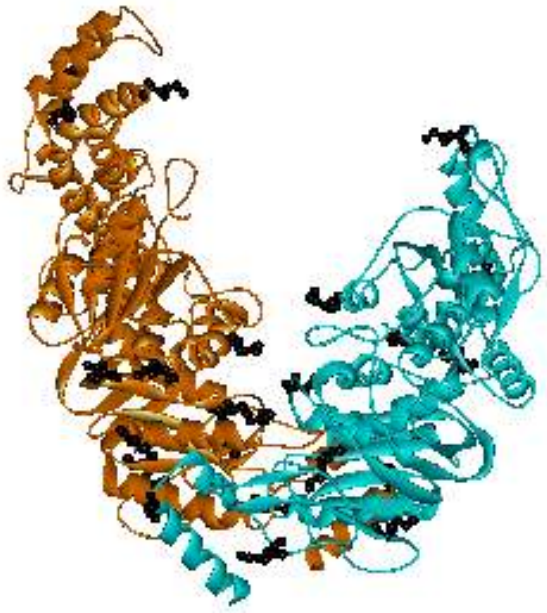

Scheme 1.1 (a) Solid ribbon diagram of MutS dimeric protein

Mismatched bases are often an unwanted byproduct of DNA replication errors that can prove to be harmful or fatal to the organism if left unchecked. Many of these mismatched bases are removed by the proofreading activity of DNA polymerase, however there is a need for a secondary detection system to ensure that nearly all mismatches are detected and eventually corrected. The mismatches that escape DNA polymerase detection are subject to later correction by the mismatch repair system (MMR) that scans newly synthesized DNA. If a mismatch is found, MutS initiates the MMR system by binding to it and specifically excising the mismatched base from the newly synthesized DNA strand after which the original sequence is restored[37]. MutS homologues have been identified in nearly all organisms examined to date, and the protein's ability to initiate the mismatch repair cascade has been well documented[38].

Each MutS subunit contains four domains, each with different characteristic features. The morphology of DNA does not promote binding to MutS. Only when the regular morphology of the DNA strand becomes perturbed or kinked by the presence of base mismatches, MutS specifically bind to the DNA macromolecule[36]. The kinked, mismatched DNA is then stabilized by extensive interaction with the four MutS domains to form a MutS-DNA complex. Scheme 1.1-(b) shows different views of MutS-DNA complex. The importance of MutS in the mismatch repair system is the initial recognition of mismatched base pairs on DNA, which are subsequently repaired by other members of the MMR cascade including MutL and MutH proteins[39].

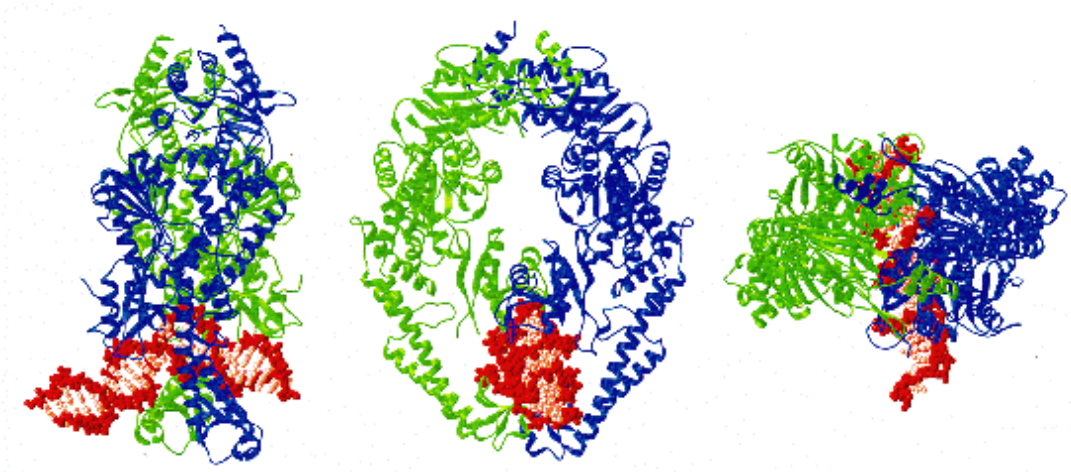

Scheme 1.1 (b) Crystal Structure of the MutS-DNA complex: different views[36] (MutS dimeric protein displayed in solid ribbon style in blue/green and DNA molecule in ball and stick display style in red)

MutS has been widely used as a major recognition element to screen mutations in various studies. The use of immobilized MutS protein on nitrocellulose membrane for base mismatch detection was first introduced by Wagner, *et al*[40]. The immobilized protein on nitrocellulose membrane recognizes all mismatch combinations as well as several unpaired bases. Wagner's modified nitrocellulose-membrane based method used chemiluminescence for detection. The method, however, is complicated due to the time-consuming, multiple steps of blotting, blocking, washing, and staining involved with the method.

Currently, the most extensively used MutS-based technique is gel electromobility shift assay (EMSA)[41, 42]. This method takes advantage of differences in the relative mobility of proteins during polyacrylamide gel electrophoresis to differentiate between

the MutS-DNA complexes and free MutS protein. Though reliable, the method lacks high throughput and is very time-consuming.

Recent advancements in imaging techniques enable identification of MutS-DNA complexes at the molecular level[43, 44]. Also, various other techniques such as nano-gravimetric analysis[45], DNA-microarray chips[46], capillary electrophoresis[47], surface plasmon resonance (SPR)[48] and electrochemistry[49] have exploited the mismatch detection capabilities of MutS protein to develop novel sensing stratergies of DNA base mismatches.

1.4 Atomic Force Microscopic (AFM) detection of DNA mismatches

Atomic force microscopy is another useful technique that has been exploited by various research groups in mismatch detection studies. AFM has been used to examine the details of molecular structures with exceptional resolution and without the need for rigorous sample preparation or labeling. AFM delivers topographical information at the nanometer scale.

In AFM, a sharp nanometer-scale tip attached to the end of a cantilever rasters across a given area while a laser and a photodiode are used to monitor the tip deflections as a result of the force experienced from the sample. A feedback loop between the photodiode and a piezo-crystal corrects and records tip deflections according to the scanning parameters set[50, 51].

The AFM can be used in two modes: *contact mode imaging* and *intermittent contact mode.* In contact mode, the cantilever tip maintains a constant force throughout the scan, while constant amplitude is maintained during intermittent contact mode imaging. Both

of these imaging modes have practical applications, depending upon the surface to be scanned and the features one is trying to detect.

The exceptionally low signal-to-noise ratio of the AFM allows individual biomolecules to be imaged at sub-nanometer resolution, presenting the opportunity to study the functionality of biomolecular assemblies. In addition to high-resolution capability, AFM can be used to directly measure intermolecular and intra-molecular interactions at the molecular level in order to acquire detailed insights about the function and structure of many biomolecular systems[51]. The resolution of topographical imaging has been tremendously improved mainly due to continuous developments of AFM instrumentation.

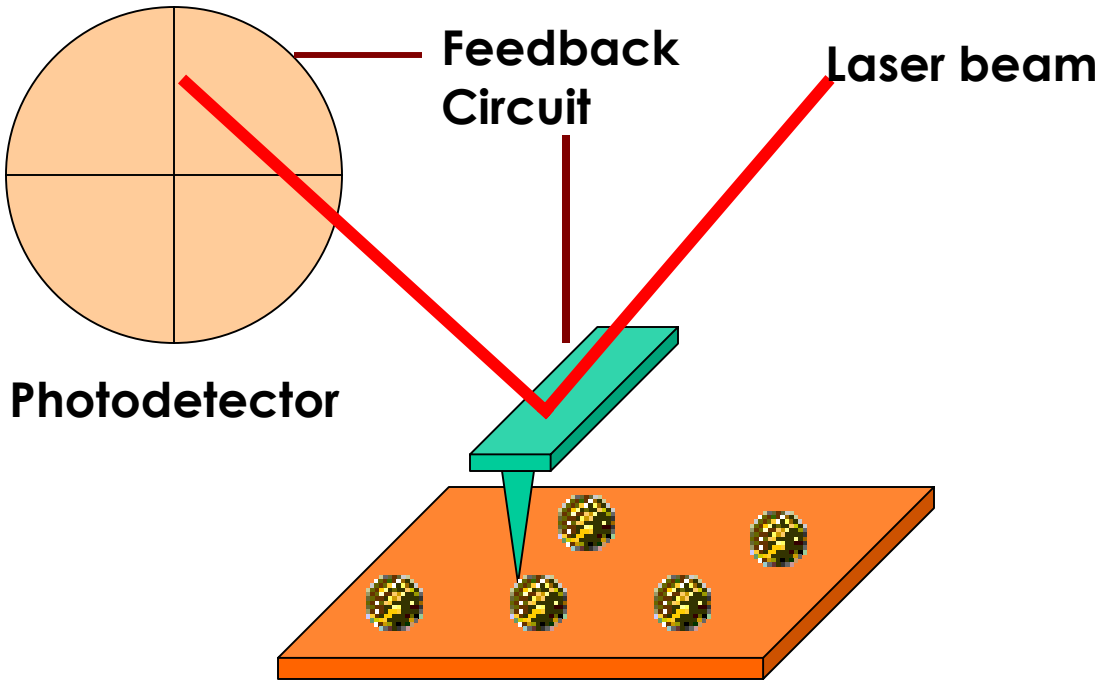

Scheme 1.2. Schematic representation of an Atomic Force Microscope

There is no AFM method currently reported that can directly visualize the mismatch site of a DNA double helix, but indirect methods using protein-DNA interactions or incorporating nano-particles to the mismatch site have been described[43, 52]. In the protein-DNA approach, DNA-MutS system has been successfully used to detect mismatched DNA [43, 53, 54]. Li, *et al* improved this approach by stretching the MutS-bound DNA in order to get more information specific to the location of the mutation[55].

Another MutS-based AFM imaging method to detect undesirable base substitutions was demonstrated by Tanigawa, *et al*[53]. Although Tanigawa's technique is attractive and effectively detects mutations in >1 kbp sequences, it is complicated by frequent aggregation of DNA during sample preparation. Some studies have also utilized the ability of AFM to measure intermolecular and intra-molecular forces to develop new mismatch detection methods[56]. One of the recent advancements of AFM, known as Topography and Recognition (TREC) imaging[57], has also proven effective in developing mutation detection techniques.

1.5 Microchip-based detection of DNA mismatches

DNA microarray technology has revolutionized genetic testing and research by enabling large numbers of analytes to be examined in parallel, resulting in a tremendous increase in throughput. This analytical technique is remarkably powerful and fast compared to other currently available techniques. The DNA microarray contains a million gene sites per square centimeter, making it possible to analyze the entire human genome without a large investment of time and resources[58]. The attached probes in each site are

hybridized to target and recognize specific sequences using chemical or electrochemical probes.

Numerous research groups have developed new methods and protocols in mutation screening research by utilizing this technology[59-62]. However, the need for optical detectors and X-ray films, widely used in microarray analyses to identify target sequences, make these methods either too complicated or too costly. Scanner cost, sample labeling requirements, and the complexity of the required optical systems are only a few of the drawbacks to these methods. Recently, a great deal of interest has been given to help develop microarray technologies that are more user-friendly devices, so that they can be used outside of highly specialized laboratories.

Several less expensive and highly sensitive detection procedures have already been developed using modified gold nano-particles in conjunction with optical and electrochemical detection techniques[63]. However, gold nano-particles need very specialized enhancements in order to grow them to a size where they are visible by optical methods, and usually require several trials to attain the desired size, contributing to added cost and an increase in overall detection time.

Use of MutS-DNA interaction in microarray technology has been reported in recent years. Begrensdorf, *et al*[46] and Bi, *et al*[64] each developed a DNA chip and a MutS protein chip for rapid screening of DNA mismatches. The recognition of MutS-DNA complexes is revealed by fluorescence images; again the method requires the added cost of labeling fluorescence detection devices.

1.6 Nano-gravimetric detection of DNA mismatches using Quartz Crystal Microbalance

Quartz crystal microbalance (QCM) is a sensitive nano-gravimetric detection technique that is widely used in various biological applications. The QCM is a piezoelectric mass-sensing device that works by sending an electrical signal through a gold-plated quartz crystal, which vibrates at a certain resonant frequency. The mass change on the crystal surface is monitored in terms of the change in resonant frequency of the crystal, based on the *Sauerbrey Equation*[65]*:*

$$\Delta f = -2f_0^2 mn/(\rho\mu)^{0.5} = -C_f \Delta m$$

Δf - Frequency Change (Hz) $\Delta \mathbf{m}$ - Mass Change (g)

ρ - Density of Qaurtz (2.648 g/cm^2) μ - Shear Modulus of Quartz

f_0 - Resonant Frequency (Hz)

QCM provides label-free real time measurements of interfacial binding events[66]. Moreover, the QCM detection principle provides additional information about the structural and viscoelastic properties of adsorbed molecules[67]. The ability of QCM to measure interfacial biomolecular binding events such as protein-protein and protein-DNA has been utilized by several groups to develop new methods to detect point mutations. One such approach uses horseradish peroxidase (HRP) as a detection element to screen

for DNA mismatches[22]. Ru-Qin, *et al* developed a similar method instead using Fe_3O_4/Au core/shell nanoparticle[68] as the detection element. Another approach using a laser gun to irradiate QCM crystals was recently developed, wherein DNA mismatches were effectively discriminated by analyzing the kinetics of laser responses[69]. Several groups have employed numerous other direct and indirect measurements of protein-DNA interactions using streptavidin–peroxide horseradish (SA–HRP)[20], MutS[45], and alkaline phosphatase[70] proteins to screen mutations using QCM.

QCM techniques are reliable, sensitive, and label-free, but they also have complicating factors associated with them. QCM requires expensive equipment and because the process cannot be miniaturized. The detection method can also be tedious and difficult at times due to problems with interference from non-specific binding events and/or background noise interference from stray electronic signals.

1.7 Capillary electrophoretic detection of DNA mismatches

Capillary electrophoresis (CE) has been an important technique for the characterization of biological systems due to its outstanding sensitivity and selectivity. It has been widely used as a detection element in various studies that are focusing to screen for gene defects.

A simple, robust, and miniaturized system for DNA mutation detection analysis has been developed using temperature gradient capillary electrophoresis (TGCE)[71, 72]. These methods have proven capable of performing simultaneous heteroduplex analyses for various mutations. An improved version of CE called multicapillary automated sequencers (MCAS) has also been reported for rapid and sensitive mutation

detection[73]. This technique is also known as conformation-sensitive capillary electrophoresis (CSCE). Another simple, highly sensitive method has been previously developed, especially for the analysis of large genes, using CE and with the help of laser-induced fluorescence detection[74]. A prior development in CE in the field of mutation detection is microchip electrophoresis[75]. Although these developments provide powerful platforms for simple, fast, automated, and high throughput detection, they are still costly and lack portability.

1.8 Mass spectrometric detection of DNA mismatches

Mass spectrometry (MS) is yet another tool that has been widely used in mutation detection research. Although mass spectrometry is well known for its high operational cost and complexity, lots of mutation detection methods have been developed around it due to its exceptional sensitivity. Mass Spectrometry can lead to the determination of molecular structure through an analysis of the ratio of mass to charge (M/Z) of the myriad ionized particles that are created upon fragmentation and ionization of a given analyte[76]. The fragmented ions pass through magnetic and electric fields, which have a separate, distinct effect on each ion fragment that passes through. These separated ionized fragments are then detected by various means. Among the more popular methods of MS technologies are the Quadrupole, Time-Of-Flight, Ion trap, and Linear Quadrupole Ion Trap[76].

Several research groups have developed rapid DNA sequencing methods using Matrix-Assisted Laser Desorption Ionization-Mass Spectrometry (MALDI-MS), and later used the sequenced DNA to effectively discriminate point mutations[77]. In addition to

MALDI-MS, various types of Electron Spray Ionization (ESI) mass spectrometric techniques have been utilized in mutation detection[78, 79]. Naviaux, *et al*`s ESI-MS based method for rapidly genotyping individuals for mitochondrial DNA (mtDNA) variants associated with mtDNA-based diseases[80] is the highlight of most recent advancements of MS in mutation detection.

1.9 Electrochemical detection of DNA mismatches

Many of the newer methods recently adapted for rapid screening appear to outperform the conventional methods in both sensitivity and selectivity. Recent advances in electrochemical techniques in this area have shown great promise, as having both of these desired characteristics, as well as faster throughput for biotechnological applications, better reliability, and ease of fabrication of microdevices[81, 82]. Electrochemical methods also provide direct readout, reducing the complexity of the detection assay.

Several electrochemical biosensors have been developed to specifically recognize target DNA sequences. Mikkelsen, *et al* developed an early electrochemical approach by hybridizing test DNA samples to single-stranded DNA probes immobilized on a carbon paste electrode[83]. When the test DNA recognizes a correct complementary DNA strand, it hybridizes to the immobilized sequence and allows for an enhanced electrochemical response from the positively charged electro-active probe $Co(phen)_2^{3+}$ in solution. Mismatches, on the other hand, will cause a reduction in $Co(phen)_2^{3+}$ current that signals the presence of the mismatch.

Heller, *et al* later employed a similar approach using immobilized single-stranded probe DNA on a redox-active polymer and attaching soybean peroxidase to the target DNA[84].

When the probe DNA strand recognizes the target strand, the attached soybean peroxidase interacts with the polymer to release hydrogen peroxide, which is then detected on the electrode. Another novel method is reported based on a "sandwich" hybridization assay using ferrocene as a signaling probe[85]. Furthermore, DNA mismatch detection methods are also reported based on DNA guanine base oxidation to 8-oxoguanine, as catalyzed by $Ru(bpy)^{3+}$ and other transition metal complexes[86]. The rate of guanine base oxidation is monitored electrochemically and thus the mutation is detected.

Although the aforementioned electrochemical biosensors can accurately detect mutations, they are limited in sensitivity. These assays are also dependant on hybridization efficiencies, which do not yield a marked difference in pairing energies between normal and mutated strands. Thus, determination of the mutation becomes harder without further method development.

The sensitivity of these hybridization assays have recently been enhanced by incorporating nano-particles such as gold. In 2004, Aamiya, *et al* developed a very sensitive electrochemical-based assay to detect base mismatches by incorporating gold nano-particles into the mismatch site[87]. In Amiya's study, a double-stranded DNA probe is immobilized on the electrode surface and is exposed to four different solutions containing mono-base modified colloidal gold nanoparticles in the presence of DNA polymerase I. When there is a mismatch in the probe sequence, only the gold nano-particles that are modified with the correct complementary monobases will accumulate on the electrode surface, resulting in a significant change in the electrochemical signal due to gold oxidation. Similar approaches are also reported using chemically modified

magnetic beads[49, 88] and various proteins such as MutS[49]. In addition, electrochemical impedance studies have been utilized by several research groups to detect DNA mutations[89].

DNA has been extensively studied for its unique characteristic of long-range charge transport through the fully hybridized molecule[90]. The molecule's extraordinary charge transport has been exploited by several research groups to design new methods to detect DNA mutations[91, 92]. A method has been reported whereby the reduction of anthro quinone is used to indicate DNA damage. The anthro quinone is attached juxtaposed to a mutation site and the amount of charge that passes via the subsequent reduction of the anthro quinone molecule is directly related to the number of mutations on the DNA molecule[93].

Among other current methods utilizing the charge transport concept through DNA, the technique developed by Barton and co-workers is the most commonly known. The barton group was able to detect DNA mismatches by monitoring charge transport through immobilized double-stranded oligonucleotides on gold electrodes with the help of DNA intercalators such as methylene blue and daunomycin[94-98]. Barton's electrochemical method seemed simpler and relatively cost-effective than the methods previously described.

1.10 Use of portable sensors in biological applications

Although most of the previously discussed detection methods of direct sequencing and electrophoretic assays are sensitive and reliable, they lack portability in their current and foreseeable embodiments. Thus, development of a portable biosensor methodology has

received considerable attention. Portable biosensors can offer great advantages such as rapid screening, high throughput, low cost, excellent sensitivity, and the possibility for further miniaturization. The recent increase in demand for these devices is also linked to their potential to be used by the general public directly in the field without any specific training or skill[99].

For a portable sensor to satisfy all these requirements the device needs to be exclusively selective for the target analyte, especially in cases where less skilled technicians and/or the untrained general public is the end user. Most real-world samples involve complex matrices such as blood and urine, where it is possible to have false reads when using a detection method that is not exclusive to the analyte, making this characteristic a key to the success of the innovation.

Most successfully innovated portable sensors currently on the market achieve this high level of specificity by using specific biological recognition molecules such as enzymes, DNA, antibodies, or peptides[100]. An example of this is the use of glucose oxidase in reliable, low-cost, home glucose monitoring.

Most portable biosensor surfaces are modified with one of these aforementioned biorecognition molecules and connected to a signal transducer to give a reagentless, quantitative detection that is easily displayed and interpreted by the end user. Devices such as amperometric electrodes, optical waveguides, and mass-sensitive piezoelectric crystals are often used as transducers[101, 102] that turn sophisticated data into a simple readout that consumers can easily use in biosensor applications with very little training or skill. Scheme-1.3 illustrates a representation of an electrochemical biosensor.

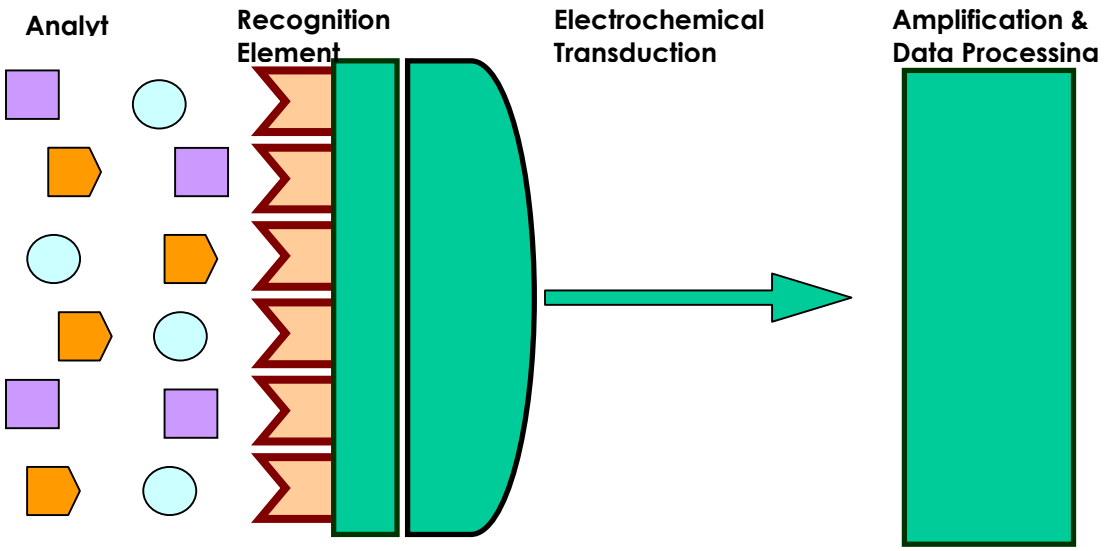

Scheme 1.3 Schematic representation of an electrochemical biosensor

1.11 The potential for electrochemical detection techniques to be developed as portable devices

Unlike other techniques that use optical devices and separation methods, electrochemical detection techniques can be more easily developed and incorporated into portable devices. The biggest advantage of using electrochemical instrumentation is that it can be made compact and lightweight. Since electrochemical detectors do not require much voltage and only measure very small currents, usually in the nanoamp to microamp range, these devices only require a small, inexpensive power supply. This gives an option to power up the device through batteries or even smaller power sources. This feature enables significant applications of electrochemical detectors in the market in which small, inexpensive, and portable systems are always needed.

Most electrochemical methods do not require complex separation steps or expensive optical components such as light sources, mirrors, filters, or optical detectors. As a result, electrochemical detectors become easier to handle and are inexpensive.

The other major advantage of using electrochemical detectors is that they have generally higher signal-to-noise ratio giving a greater sensitivity and lower detection limit. They have negligible incident background noise as compared to optical detectors. The only existing noise comes from the inherent background currents in the measurement systems and from the capacitive charging currents at the detector surface. These currents are small enough that they typically do not interfere with the signal.

1.12 Electrochemical techniques used in this study

Various electrochemical techniques will be used in our biosensor development studies, including cyclic voltammetry (CV), square wave voltammetry (SWV), and chronocoulometry (CC). These methods were chosen because of their simplicity, sensitivity, cost effectiveness, and ability to gather much information within a few potential cycles.

1.12.1 Cyclic Voltammetry (CV)

In CV, voltage (potential) is first decreased as a function of time to induce reductions. A current results as electrons are transferred to or from the analyte when the electrode reaches a specific voltage that matches the standard redox potential of the species in the cell. This is the reduction peak. Voltage is then increased back to allow oxidations to take place at the electrode, again when the potential matches the electron transfer potential of

the analyte. The resulting current from electron transfer makes an oxidation peak. Current is measured as a function of applied potential at a given scan rate, and the resultant data is represented by a curve that is called a voltamogram[65].

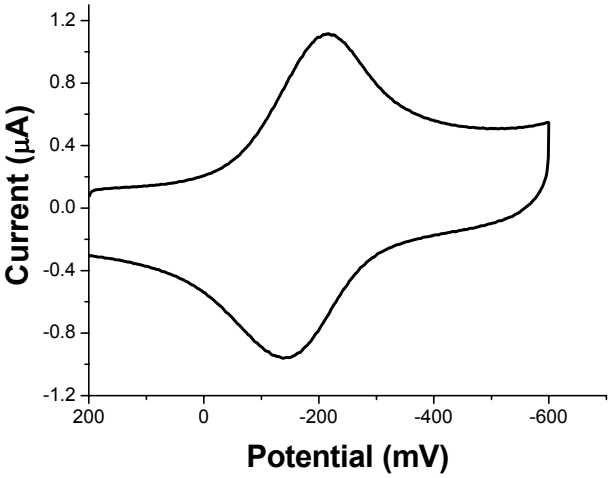

A typical Cyclic Voltammogram

1.12.2 Square Wave Voltammetry (SWV)

In contrast to CV, SWV`s potential sweep is a series of stair steps. The current difference between the cathodic and anodic pulses in each step is measured before the next step is taken. During the cathodic pulse, the electro-active species gets reduced at the electrode, while the anodic pulse oxidizes those reduced species back to original form. The resultant current is measured as a function of voltage potential and is displayed as a square wave voltamogram. Since the currents obtained during cathodic and anodic processes have opposite signs, the difference in current that is measured at each step in potential will be higher compared to the currents obtained in CV at a given potential. This, combined with

the low charging currents associated with SWV, makes SWV relatively more powerful with regard to CV[65].

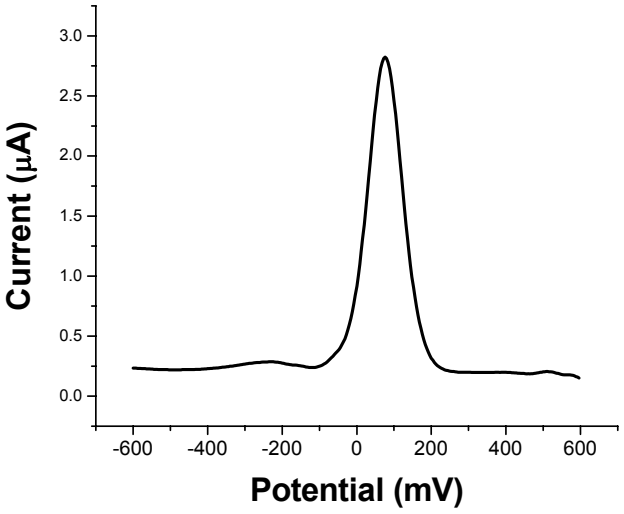

A typical Square Wave Voltammogram

1.12.3 Chronocoulometry (CC)

In CC, the applied potential on the electrode is stepped from a non-redox reactive starting point to a final point where the redox reaction occurs. The transient charge passes through the electrode and is measured as a function of time[65]. CC is very useful in calculating the surface area of sensors, and obtaining the amount of adsorbed molecules on sensor surfaces, as well as determining mechanisms and kinetics of electron transfer reactions that occur on the sensor surface. CC can also be used to calculate diffusion constants for different analytes.

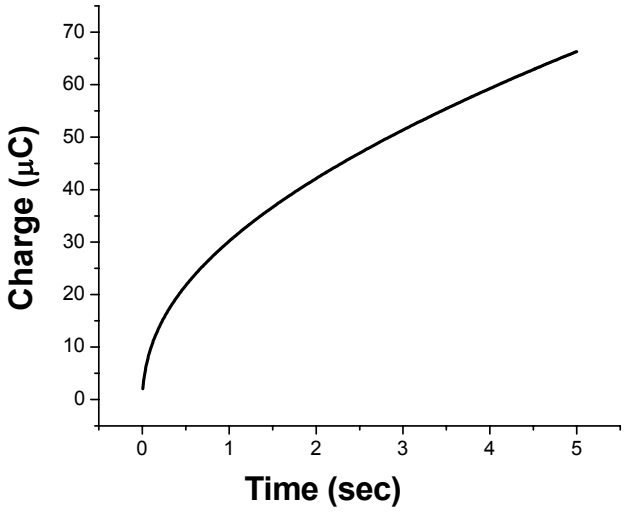

A typical Chronocoulogram

The advantages associated with these three aforementioned electrochemical techniques enable them to be used in the characterization and analysis of our mismatch and damage detection biosensors described in the following chapters.

1.13 Importance of biomolecular immobilization in developing biosensors for mutation detection.

In order to make an electrochemical biosensor that incorporates biorecognition molecules in conjunction with a signal transducer, the recognition molecule needs to be immobilized onto conductive surfaces. This biomolecular immobilization of biomacromolecules such as enzymes, antibodies, or oligonucleotides plays a key role in biosensor development, as it directly influences the sensitivity and the selectivity of the sensor. However, the stable and reproducible immobilization of these biomacromolecules

with complete retention of their recognition properties remains a crucial problem. For this reason, use of a proper immobilization method is vital to achieving high throughput capability in manufactured biosensors.

Although many established strategies are available for the immobilization of these biomolecules on sensor surfaces, the actual method of immobilization varies depending on ligand type, analyte, and the purpose of the experiment. The most challenging component in any immobilization is to preserve the activity of the biomolecule during the immobilization process, which is where many of the current immobilization methods fail.

Biomolecular immobilization methods can be categorized into various groups. However, two methods are widely employed. The first method is based on covalently attaching biomolecules onto a solid support via various linker groups; thiols, amines, and aldehydes are among well-established linkers for covalent immobilization[103-106].

The second immobilization category is called *layer-by-layer methodology*, which is based on electrostatic interactions between a pre-charged solid support and alternating layers of biomolecules. The solid support, in this case the bare surface of a biosensor, can be easily charged, either positively or negatively, using monovalent or multivalent substrates, cations, or anions. Although the majority of available substrates are monovalent, a few multivalent substrates are being used, divalent Mg^{2+} being one example. Polylysine, PDDA, and polyglutamate are some examples of monovalent substrates that are used[107-109]. Both covalent and layer-by-layer techniques have their own advantages as well as disadvantages.

1.4 References

1. Akbari, M., et al., Mitochondrial base excision repair of uracil and AP sites takes place by single-nucleotide insertion and long-patch DNA synthesis. DNA Repair (Amst), 2008. 7(4): p. 605-16.
2. Wilson, R.C. and J.D. Pata, Structural insights into the generation of single-base deletions by the Y family DNA polymerase dbh. Mol Cell, 2008. 29(6): p. 767-79.
3. Milunsky, J.M., et al., TFAP2A mutations result in branchio-oculo-facial syndrome. Am J Hum Genet, 2008. 82(5): p. 1171-7.
4. Shin, C.Y. and M.S. Turker, A:T --> G:C base pair substitutions occur at a higher rate than other substitution events in Pms2 deficient mouse cells. DNA Repair (Amst), 2002. 1(12): p. 995-1001.
5. Satta, Y., H. Ishiwa, and S.I. Chigusa, Analysis of nucleotide substitutions of mitochondrial DNAs in Drosophila melanogaster and its sibling species. Mol Biol Evol, 1987. 4(6): p. 638-50.
6. Dong, M., et al., Development of enzymatic probes of oxidative and nitrosative DNA damage caused by reactive nitrogen species. Mutat Res, 2006. 594(1-2): p. 120-34.
7. Setlow, P., Mechanisms for the prevention of damage to DNA in spores of Bacillus species. Annu Rev Microbiol, 1995. 49: p. 29-54.
8. Dahle, J., et al., Overexpression of human OGG1 in mammalian cells decreases ultraviolet A induced mutagenesis. Cancer Lett, 2008. 267(1): p. 18-25.

9. Pfeifer, G.P., Y.H. You, and A. Besaratinia, Mutations induced by ultraviolet light. Mutat Res, 2005. 571(1-2): p. 19-31.

10. Harbottle, A. and M.A. Birch-Machin, Real-time PCR analysis of a 3895 bp mitochondrial DNA deletion in nonmelanoma skin cancer and its use as a quantitative marker for sunlight exposure in human skin. Br J Cancer, 2006. 94(12): p. 1887-93.

11. Li, H.H., J. Aubrecht, and A.J. Fornace, Jr., Toxicogenomics: overview and potential applications for the study of non-covalent DNA interacting chemicals. Mutat Res, 2007. 623(1-2): p. 98-108.

12. Harder, A., B.I. Escher, and R.P. Schwarzenbach, Applicability and limitation of OSARs for the toxicity of electrophilic chemicals. Environ Sci Technol, 2003. 37(21): p. 4955-61.

13. Brellier, F., et al., Ultraviolet responses of Gorlin syndrome primary skin cells. Br J Dermatol, 2008. 159(2): p. 445-52.

14. Kalyanmoy Deb, I., Genetic And Evolutionary Computation. Springer, 2005.

15. Stryer, L., Biochemistry. W.H. Freeman and Co, 1998.

16. Binder, Alexander; 1996, Alleles of the Human β_2 Adrenegic Receptor Gene and Possible Effects on the Phenotype*,* Masters Thesis, Der Karl-Franzens-University Graz, Germany.

17. IARC TP53 Mutation Database, International Agency for Research on Cancer.

18. Gunderson, K.L., et al., Mutation detection by ligation to complete n-mer DNA arrays. Genome Res, 1998. 8(11): p. 1142-53.

19. Triques, K., et al., Mutation detection using ENDO1: application to disease diagnostics in humans and TILLING and Eco-TILLING in plants. BMC Mol Biol, 2008. 9: p. 42.

20. Jens, B.G., G; Per Olaf, E, Melting gel techniques in single nucleotide polymorphism and mutation detection: From theory to automation. GAUDERNACK Gustav (1) ; EKSTR?M Per Olaf, 2002. 25: p. 637-647.

21. Fiche, J.B., et al., Point mutation detection by surface plasmon resonance imaging coupled with a temperature scan method in a model system. Anal Chem, 2008. 80(4): p. 1049-57.

22. Feng, K., et al., QCM detection of DNA targets with single-base mutation based on DNA ligase reaction and biocatalyzed deposition amplification. Biosens Bioelectron, 2007. 22(8): p. 1651-7.

23. Yeh, H.C., et al., Homogeneous point mutation detection by quantum dot-mediated two-color fluorescence coincidence analysis. Nucleic Acids Res, 2006. 34(5): p. e35.

24. Bakker, E., Is the DNA sequence the gold standard in genetic testing? Quality of molecular genetic tests assessed. Clin Chem, 2006. 52(4): p. 557-8.

25. Mount, D., Bioinformatics. CSHL Press, 2004.

26. Chen, J. and P.D. Hebert, Directed termination PCR: a one-step approach to mutation detection. Nucleic Acids Res, 1998. 26(6): p. 1546-7.

27. Theophilus, B.R., R, PCR Mutation Detection Protocols. 2001. 187.

28. Bjorheim, J., et al., Mutation detection in KRAS Exon 1 by constant denaturant capillary electrophoresis in 96 parallel capillaries. Anal Biochem, 2002. 304(2): p. 200-5.

29. Hestekin, C.N., et al., An optimized microchip electrophoresis system for mutation detection by tandem SSCP and heteroduplex analysis for p53 gene exons 5-9. Electrophoresis, 2006. 27(19): p. 3823-35.

30. Richard, G.C., EE; Sue, F, Mutation Detection. Oxford University Press, 1998.

31. Fischer, S.G. and L.S. Lerman, DNA fragments differing by single base-pair substitutions are separated in denaturing gradient gels: correspondence with melting theory. Proc Natl Acad Sci U S A, 1983. 80(6): p. 1579-83.

32. Cariello, N.F., et al., Resolution of a missense mutant in human genomic DNA by denaturing gradient gel electrophoresis and direct sequencing using in vitro DNA amplification: HPRT Munich. Am J Hum Genet, 1988. 42(5): p. 726-34.

33. Hakkarainen, J.W., JA; Vohokangas, KH, TP53 Mutation Detection by SSCP and Sequencing. Methods in Molecular Medicine, 2004. 97: p. 191-208.

34. Hinks, J.W., PR; Makris, M; Preston, FE; Peake, IR; Goodeve AC, A rapid method for haemophilia B mutation detection using conformation sensitive gel electrophoresis. British Journal of Haematology, 1999. 104: p. 915-918.

35. Taylor, G., Laboratory Methods for the Detection of Mutations and Polymorphisms. CRC Press, 1997: p. Chapter 2.

36. Obmolova, G., et al., Crystal structures of mismatch repair protein MutS and its complex with a substrate DNA. Nature, 2000. 407(6805): p. 703-10.

37. Repair affairs. Nat Genet, 2000. 24(4): p. 325-6.

38. Manelyte, L., et al., Structural and functional analysis of the MutS C-terminal tetramerization domain. Nucleic Acids Res, 2006. 34(18): p. 5270-9.

39. Mendillo, M.P., CD; Kolodner, RD, Escherichia coli MutS Tetramerization Domain Structure Reveals That Stable Dimers but Not Tetramers Are Essential for DNA Mismatch Repair in Vivo*. J. Biol. Chem., 2007. 282(22): p. 16345-16354.

40. Wagner, R., P. Debbie, and M. Radman, Mutation detection using immobilized mismatch binding protein (MutS). Nucleic Acids Res, 1995. 23(19): p. 3944-8.

41. Smith, J. and P. Modrich, Mutation detection with MutH, MutL, and MutS mismatch repair proteins. Proc Natl Acad Sci U S A, 1996. 93(9): p. 4374-9.

42. Lishanski, A., E.A. Ostrander, and J. Rine, Mutation detection by mismatch binding protein, MutS, in amplified DNA: application to the cystic fibrosis gene. Proc Natl Acad Sci U S A, 1994. 91(7): p. 2674-8.

43. Sun, H.B. and H. Yokota, MutS-mediated detection of DNA mismatches using atomic force microscopy. Anal Chem, 2000. 72(14): p. 3138-41.

44. Zhang, Y.H., X; Kong, X; Li, B; Zhao, G, Surf Interface Anal, 2002. 33: p. 122-125.

45. Xiaodi, S.R., R; Yinngju, W.; Guangyu, W; Koll, W, Detection of point mutation and insertion mutations in DNA using a quartz crystal microbalance and MutS, a mismatch binding protein. Analytical chemistry, 2004. 76: p. 489-494.

46. Behrensdorf, H.A., et al., Rapid parallel mutation scanning of gene fragments using a microelectronic protein-DNA chip format. Nucleic Acids Res, 2002. 30(14): p. e64.

47. Han, A., et al., Gene mutation assay using a MutS protein-modified electrode. Nucleic Acids Res Suppl, 2002(2): p. 287-8.

48. Brooks, P., MutS-DNA Interactions and DNase Protection Analysis with Surface Plasmon Resonance. Methods In Molecular Biology, 2000. 152: p. 119-132.

49. Cho, M., et al., Electrochemical detection of mismatched DNA using a MutS probe. Nucleic Acids Res, 2006. 34(10): p. e75.

50. Shao, Z. and Y. Zhang, Biological cryo atomic force microscopy: a brief review. Ultramicroscopy, 1996. 66(3-4): p. 141-52.

51. Zhang, Y., S. Sheng, and Z. Shao, Imaging biological structures with the cryo atomic force microscope. Biophys J, 1996. 71(4): p. 2168-76.

52. Sato, K., K. Hosokawa, and M. Maeda, Non-cross-linking gold nanoparticle aggregation as a detection method for single-base substitutions. Nucleic Acids Res, 2005. 33(1): p. e4.

53. Tanigawa, M., et al., Detection and mapping of mismatched base pairs in DNA molecules by atomic force microscopy. Nucleic Acids Res, 2000. 28(9): p. E38.

54. Wang, H., et al., DNA bending and unbending by MutS govern mismatch recognition and specificity. Proc Natl Acad Sci U S A, 2003. 100(25): p. 14822-7.

55. Zhang, Y.L., Y; Hu, J;Kong, X; Li, B; Zhao, G; Li, M, Direct detection of mutation sites on stretched DNA by atomic force microscopy. Surface and Interface Analysis, 2000. 33(2): p. 122-125.

56. Schafer, A.J. and J.R. Hawkins, DNA variation and the future of human genetics. Nat Biotechnol, 1998. 16(1): p. 33-9.

57. Chtcheglova, L.A., et al., Nano-scale dynamic recognition imaging on vascular endothelial cells. Biophys J, 2007. 93(2): p. L11-3.

58. Gershon, D., DNA microarrays: more than gene expression. Nature, 2005, 437(7062): p. 1195-8.

59. Sato, Y., et al., Surface plasmon resonance imaging on a microchip for detection of DNA-modified gold nanoparticles deposited onto the surface in a non-cross-linking configuration. Anal Biochem, 2006. 355(1): p. 125-31.

60. Qu, X., F. Sang, and J. Ren, Fabrication of PDMS/glass microchips by twofold replication of PDMS and its application in genetic analysis. J Sep Sci, 2006. 29(15): p. 2390-4.

61. Lu, M.L., et al., Impact of alterations affecting the p53 pathway in bladder cancer on clinical outcome, assessed by conventional and array-based methods. Clin Cancer Res, 2002. 8(1): p. 171-9.

62. Scoggan, K.A. and D.E. Bulman, Single-strand conformational polymorphism analysis (SSCP) and sequencing for ion channel gene mutations. Methods Mol Biol, 2003. 217: p. 143-51.

63. Chen, Y.T., C.L. Hsu, and S.Y. Hou, Detection of single-nucleotide polymorphisms using gold nanoparticles and single-strand-specific nucleases. Anal Biochem, 2008. 375(2): p. 299-305.

64. Bi, L.J., et al., Construction and characterization of different MutS fusion proteins as recognition elements of DNA chip for detection of DNA mutations. Biosens Bioelectron, 2005. 21(1): p. 135-44.

65. Bard, A.F., LR, Electrochemical Methods. John Wiley & Sons, 2005. Second Edition.

66. Matsuda, T., et al., Novel instrumentation monitoring in situ platelet adhesivity with a quartz crystal microbalance. Asaio J, 1992. 38(3): p. M171-3.

67. Wang, J., et al., Mismatch-sensitive hybridization detection by peptide nucleic acids immobilized on a quartz crystal microbalance. Anal Chem, 1997. 69(24): p. 5200-2.

68. Panga, L.L., JS; Jianga, JH; Lea, Y; Li, G; Yu, RQ, novel detection method for DNA point mutation using QCM based on Fe3O4/Au core/shell nanoparticle and DNA ligase reaction. Sensors and Actuators B: Chemical, 2008. 127(2): p. 311-316.

69. Junichi, K.T., K; Yoshio, Q, Detection of Mismatch of DNA by Using a Laser-QCM Method. Nippon Kagakkai Koen Yokoshu, 2005. 85(2): p. 1386.

70. Patolsky, F.L., A; Willner, I, Highly Sensitive Amplified Electronic Detection of DNA By Biocatalyzed Precipitation of an Insoluble Product onto Electrodes. Chemistry - A European Journal, 2003. 9(5): p. 1137 - 1145.

71. Zhang, H.D., et al., DNA mutation detection with chip-based temperature gradient capillary electrophoresis using a slantwise radiative heating system. Lab Chip, 2007. 7(9): p. 1162-70.

72. Zhu, L., et al., Spatial temperature gradient capillary electrophoresis for DNA mutation detection. Electrophoresis, 2001. 22(17): p. 3683-7.

73. Davies, H., et al., High throughput DNA sequence variant detection by conformation sensitive capillary electrophoresis and automated peak comparison. Genomics, 2006. 87(3): p. 427-32.

74. Kozlowski, P. and W.J. Krzyzosiak, Combined SSCP/duplex analysis by capillary electrophoresis for more efficient mutation detection. Nucleic Acids Res, 2001. 29(14): p. E71.

75. Tian, H., et al., Capillary and microchip electrophoresis for rapid detection of known mutations by combining allele-specific DNA amplification with heteroduplex analysis. Clin Chem, 2001. 47(2): p. 173-85.

76. Gross, J., Mass Spectrometry. Springer, 2004.

77. Elso, C., et al., Mutation detection using mass spectrometric separation of tiny oligonucleotide fragments. Genome Res, 2002. 12(9): p. 1428-33.

78. Wang, L., R. Luhm, and M. Lei, SNP and mutation analysis. Adv Exp Med Biol, 2007. 593: p. 105-16.

79. Bertagnolo, V., et al., Vav1 modulates protein expression during ATRA-induced maturation of APL-derived promyelocytes: a proteomic-based analysis. J Proteome Res, 2008. 7(9): p. 3729-36.

80. Jiang, Y., et al., Mitochondrial DNA mutation detection by electrospray mass spectrometry. Clin Chem, 2007. 53(2): p. 195-203.

81. Napier, M.T., H.H, Electrocatalytic Oxidation of Nucleic Acids at Electrodes Modified with Nylon and Nitrocellulose Membranes. Journal of Fluorescence, 1999. 9(3): p. 181-186.

82. Mikkelsen, S., Electrochemical Biosensors for DNA Sequence Detection. Electroanalysis, 1996. 8: p. 15-19.

83. Millan, K.M., A. Saraullo, and S.R. Mikkelsen, Voltammetric DNA biosensor for cystic fibrosis based on a modified carbon paste electrode. Anal Chem, 1994. 66(18): p. 2943-8.

84. Lumley-Woodyear, T.C., C.N.; Heller, A, Direct Enzyme-Amplified Electrical Recognition of a 30-Base Model Oligonucleotide. J. Am. Chem. Soc, 1996. 118(23): p. 5504–5505.

85. Suyea, S.M., T; Kimuraa, T; Zhenga, T; Horia, Y; Katayama, H, Amperometric DNA sensor using gold electrode modified with polymerized mediator by layer-by-layer adsorption. Microelectronic Engineering, 2005. 81(2-4): p. 441-447.

86. Wang J.; Kawde, A., Pencil-based renewable biosensor for label-free electrochemical detection of DNA hybridization. Anal. Chim. Acta, 2001. 431(219-224).

87. Kerman, K., et al., Electrochemical coding of single-nucleotide polymorphisms by monobase-modified gold nanoparticles. Anal Chem, 2004. 76(7): p. 1877-84.

88. Kerman, K.M., Y.; Morita, Y.; Takamura, Y.; Tamiya, E, Peptide nucleic acid modified magnetic beads for intercalator based electrochemical detection of DNA

hybridization. Science and Technology of Advanced Materials, 2004. 5: p. 351-357.

89. Li, C.Z.L., Y.T.; Lee, J.S.; Kraatz, H.B., Protein-dna interaction: impedance study of muts binding to a DNA mismatch. Chemical communications, 2004. 5: p. 574-575.

90. Li, X., et al., Chip-based microelectrodes for detection of single-nucleotide mismatch. Anal Chem, 2005. 77(17): p. 5766-9.

91. Boal, A.K. and J.K. Barton, Electrochemical detection of lesions in DNA. Bioconjug Chem, 2005. 16(2): p. 312-21.

92. Drummond, T.G., M.G. Hill, and J.K. Barton, Electron transfer rates in DNA films as a function of tether length. J Am Chem Soc, 2004. 126(46): p. 15010-1.

93. Kumamoto, S.W., M.; Kawakami, N.; Nakamura, M.; Yamana, K, 2'-Anthraquinone-Conjugated Oligonucleotide as an Electrochemical Probe for DNA Mismatch. Bioconjugate Chem., 2008. 19: p. 65-69.

94. O'Neill, M.A. and J.K. Barton, DNA-mediated charge transport requires conformational motion of the DNA bases: elimination of charge transport in rigid glasses at 77 K. J Am Chem Soc, 2004. 126(41): p. 13234-5.

95. O'Neill, M.A. and J.K. Barton, DNA charge transport: conformationally gated hopping through stacked domains. J Am Chem Soc, 2004. 126(37): p. 11471-83.

96. Williams, T.T., et al., Effects of the photooxidant on DNA-mediated charge transport. J Am Chem Soc, 2004. 126(26): p. 8148-58.

97. Boon, E.M., et al., DNA-mediated charge transport for DNA repair. Proc Natl Acad Sci U S A, 2003. 100(22): p. 12543-7.

98. Boon, E.M. and J.K. Barton, DNA electrochemistry as a probe of base pair stacking in A-, B-, and Z-form DNA. Bioconjug Chem, 2003. 14(6): p. 1140-7.

99. Thevenot, D.R.T., K.; Durst, R.A.; Wilson, G.S., Electrochemical Biosensors: Recommended Definitions and Classification. Analytical Letters, 2001. 34: p. 635-659.

100. Hall, E., Biosensors. Open University Press, Buckingham, 1990.

101. Weimar, T., Recent Trends in the Application of Evanescent Wave Biosensors. Angewandte Chemie-International, 2000. 39: p. 1219.

102. Salamon, Z.M., H.A.; Tollin, G, Surface Plasmon Resonance Spectroscopy as a Tool for Investigating the Biochemical and Biophysical Properties of Membrane Protein Systems. I: Theoretical Principles. Biochimica Et Biophysica Acta, 1997. 1331: p. 117–129.

103. Boecking, T.K., K.A.; Gaus, K.; Gooding, J.J, Langmuir, 2006. 22(8): p. 3494-3496.

104. Ligaj, M.J., J.; Musial, W.; Filipiak, M.;, Electrochimica Acta, 2006. 51(24): p. 5193-5198.

105. Heise, C.B., F. F., Topics in Current Chemistry, 2005. 261: p. 1-25.

106. Feng, C.L.Z., Z.; Foerch, R.; Knoll, W.; Vancso, G. J.; Schoenherr, H., Biomacromolecules, 2005. 6(6): p. 3243-3251.

107. Suye, S.K., T.; Zheng, H.; Hori, T.; Amano, Y.; Katayama, H, Sensors and Actuators B: Chemical. 20: p. 512-513.

108 Pedano, M.L.M., L.; Desbrieres, J.; Defrancq, E.; Dumy, P.; Coche-Guerente, L.; Labbe, P.; Legrand, J.; Calemczuk, R.; Rivas, G. A., Analytical Letters, 2004. 37(11): p. 2235-2250.

109. Ivanova, E.P.P., D. K.; Brack, N.; Pigram, P.; Nicolau, D. V., Biosensors & Bioelectronics, 2004. 19(11): p. 1363-1370.

CHAPTER II

A NEW APPROACH TO IMMOBILIZING DNA ON BIOSENSORS USING ELECTROCHEMICAL DIAZONIUM REDUCTION: APPLICATIONS IN BASE MISMATCH DETECTION USING INTERCALATOR-MEDIATED CHARGE TRANSPORT

2.1 Introduction

Recently, considerable interest has been focused on the current DNA/Oligonucleotide immobilization techniques being used for mismatch detection. Most of these current methods have various drawbacks that will adversely affect the sensitivity of the assay. A variety of methods have been developed for assembling nucleic acid monolayers on biosensor surfaces such as metals (e.g. gold), polymers, and glasslike surfaces (e.g. silica, oxidized silicon, microscope slides)[1-6].

DNA/oligo-attachment to gold surfaces with free thiol labels is the most commonly used immobilization method because of the well-established thiol-gold chemistry[7-11]. Free thiol moieties of terminated DNA/oligos are attached via chemisorption to the gold surface. However, it has been identified that the thiol-gold based methods have serious limitations including long immobilization time, cost, and restrictions on the type of metal

used. As well, it has been determined that the dithiothreitol (DTT) used to reduce the disulfide bond to generate the free thiol moieties significantly interferes with the efficiency of self-assembly of the monolayer on the gold surface[12]. Recent studies have also revealed that the length of the oligos can affect the immobilization efficiency when using thiol-gold immobilizations[13].

In another study conducted by Mirkin and colleagues, single linkage thiol-gold attachments are shown to be more susceptible to desorbing from the surface as compared to multi-linkage thiol-gold attachments[14, 15]. Other investigators have further noted significant instability of thiol-terminated DNA due to their tendency to oxidize under normal atmospheric conditions[16]. By considering all of the drawbacks associated with the thiol-gold immobilization, it is apparent that there is a growing need to develop an immobilization technique that is sensitive, fast, low in cost, and applicable to any conductive surface.

Surface grafting of biological molecules using diazonium chemistry is appealing in this regard. Electrochemical reduction of diazonium ions results in a highly reactive radical which attaches covalently to the electrode surface[17-19] and can be used to immobilize macromolecules[20, 21] on almost any type of conductive surface. To this end, we describe a fast and reliable method for the immobilization of DNA/oligonucleotides.

Our particular approach involves grafting a glassy carbon electrode surface with carboxylic acid groups by electrochemical reduction of *4-cinnamic acid diazonium tetrafluoroborate.* This is followed by the coupling of amino-terminated oligonucleotide to the pre-activated cinnamic acid groups on the electrode surface using 1-Ethyl-3-(3-dimethylaminopropyl) carbodiimide Hydrochloride (EDAC) and N-hydroxysuccinimide

(NHS). The oligonucleotide immobilization is confirmed using electroactive probes such as $K_3Fe(CN)_6$ and $Ru(bpy)_3^{2+}$. In addition, each surface-modification step is characterized by Atomic Force Miroscopy (AFM). Barton's DNA-mediated charge transport technique, introduced earlier in Chapter 1, is used to investigate the applicability and the sensitivity of our proposed immobilization technique.

2.2 Experimental design

2.2.1 Chemicals and biomolecules

15'mer single-stranded oligonucleotides, C6 5' amino modified, purchased from Biosynthesis (**1.** 5'-amino-C6-AGT ACA GT*C* ATC GCG-3', **2.** 5'-CGC GAT GAC TGT ACT-3'**, 3.** 5'-CGC GAT GAA TGT ACT -3') are suspended in deionized water to prepare stock solutions of 2 μg/μl concentrations. Equal volumes of each ssDNA (1+2:complementary oligo and 1+3:mismatched oligo) are hybridized in pH 7.0 phosphate buffer (5 mM phosphate, 0.1 mM NaCl) by heating for 5-8 min at 95°C in a heat block and cooling slowly to room temperature over 3-4 hrs. The final DNA concentration is estimated by absorption spectroscopy at 260 nm.

Highly Oriented Pyrolytic Graphite (HOPG) surfaces (SPI-1 Grade) are purchased from SPI suppliers. All other chemicals, trans-4-aminocinnamic acid, sodium nitrite, 1-Ethyl-3-(3-dimethylaminopropyl) carbodiimide Hydrochloride (EDAC), 2-[N-morpholino]ethane sulfonic acid (MES), N-hydroxy succinimide (NHS), methylene blue, Potassium hexacyanoferrate (III), and tris(2,2`-bipyridyl) dichlororuthenium (II) hexahydrate are reagent grade and purchased from Sigma-Aldrich. Deionized water is obtained from a Barnstead ultra-pure water purification system (specific resistance >18

MΩ/cm). Trans-4-cinnamic acid diazonium tetrafluoroborate is synthesized and purified according to published procedures[22].

2.2.2 Procedures and apparatus

A BAS electrochemical workstation is used for all electrochemical experiments. Potentials are recorded against an Ag/AgCl (3.0 M KCl) reference electrode with a platinum counter-electrode, and 3.0 mm glassy carbon working electrode.

2.2.3 Electrochemical measurements

All electrochemical measurements are carried out at room temperature in buffers as indicated in each specific trial, which are purged for 10 min and blanketed with nitrogen immediately before readings. Cyclic Voltammetry (CV) and Square Wave Voltammetry (SWV) are performed in a three- neck electrochemical cell.

2.2.4 Grafting carboxylic acid groups

This is performed with glassy carbon electrodes, which are polished with 0.3 and 0.05 μm alumina respectively on a Buehler microcloth and ultrasonically cleaned in acetone, and then in deionized water for 15 min before grafting. The synthesized diazonium compound (10mM) is then dissolved in acetonitrile containing 0.1 M $Bu_4N^+BF_4^-$ as the electrolyte. The acetonitrile electrolyte solution is purged and kept under nitrogen atmosphere. Cyclic voltammetry is performed on the glassy carbon electrode (GC) in a potential window of 0.8 V to -0.8 V (scan rate 0.1V/s). Two consecutive scans are used in these conditions (scheme 2.1, Figure 2.1).

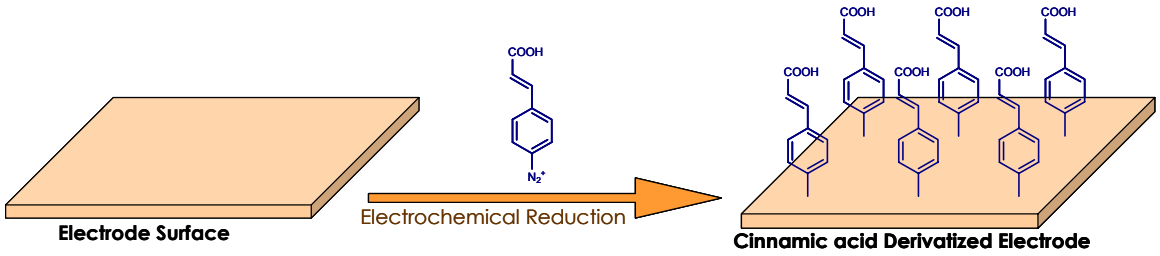

Scheme 2.1 Grafting of the electrode surface with carboxylic acid groups.

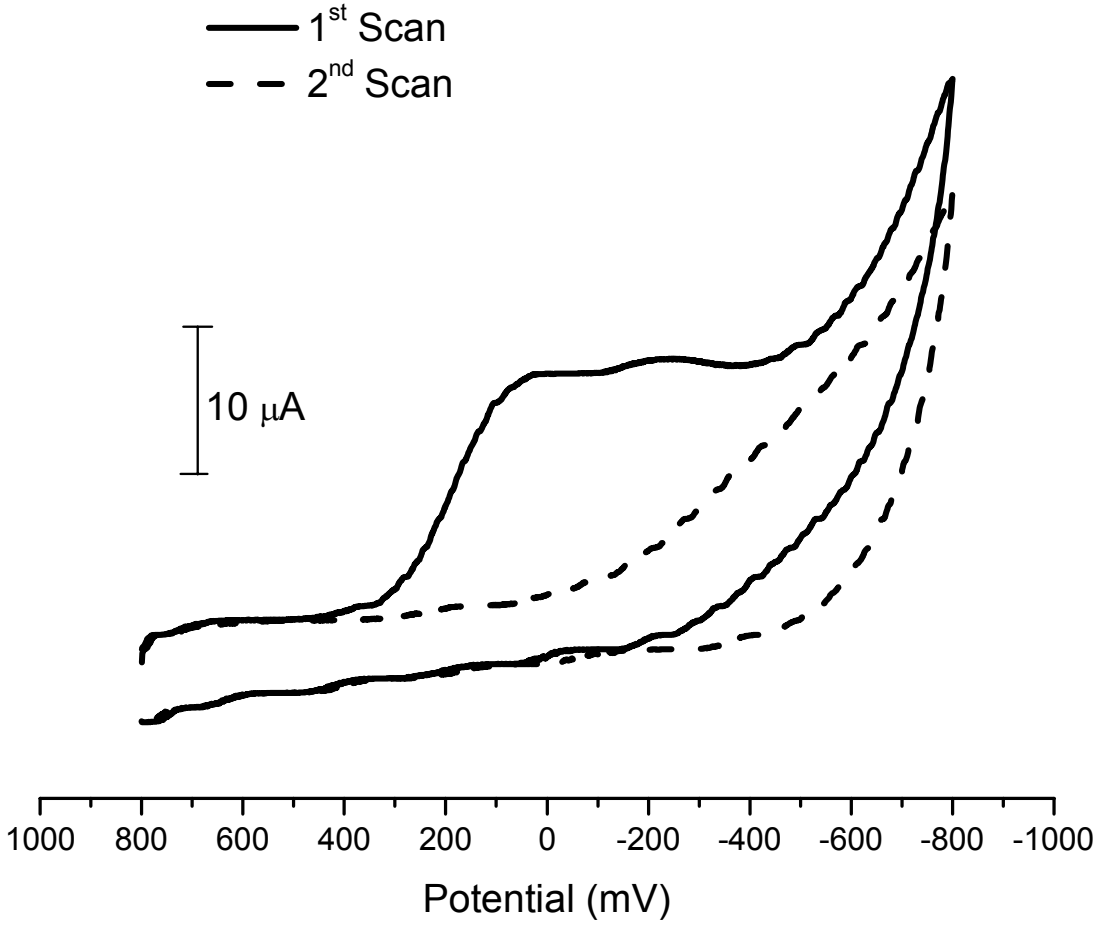

Figure 2.1 Cyclic voltamograms (ν=100 mV/s) for the first (–) and second (---) scans of the 15 mM Trans-4-cinnamic acid diazonium tetrafluoroborate in acetonitrile.

2.2.5 DNA immobilization on electrode surface

The modified electrode grafted with carboxylic acid groups is washed thoroughly with acetone followed by deionized water before proceeding with DNA immobilization (scheme 2.2). A 50 µl drop of EDC/NHS solution (10:1 mg of EDC to NHS in 1.0 ml solution of 50 mM MES buffer, pH 6.5) is carefully cast on the surface of the electrode. The electrode is incubated in this solution in a closed environment for 20 min. After incubation, the modified GC electrode is washed immediately with deionized water. Then, 50 µl of 50 µM amino-terminated oliginuceotides in 5 mM phosphate buffer (pH 7.0) containing 50 mM NaCl and 0.1 M $MgCl_2$ is cast on the electrode surface in a closed chamber for 2 hours. After immobilization of the oligonucleotides, the electrode is thoroughly washed with 5 mM pH 7.0 phosphate buffer (50 mM NaCl) followed by deionized water.

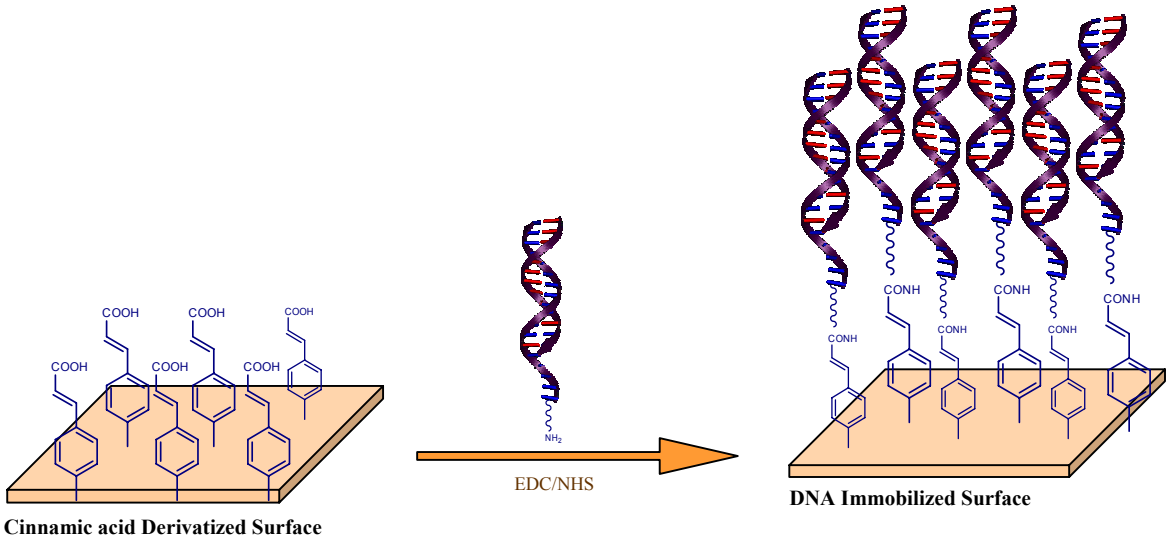

Scheme 2.2 Immobilization of DNA on the electrode surface

2.2.6 Atomic Force Microscopy

AFM is performed with a pico-SPM scanning probe microscope controlled by a magnetically coated MAC-mode module and interfaced with a PicoScan controller from Molecular Imaging Corp., Tempe, Arizona. All the AFM are performed with a multi-purpose small scanner with a scan range of 9 μm in x-y dimension and 2 μm in the z-dimension (Molecular Imaging Corp.). Silicon Type II MAClever cantilevers (Molecular Imaging Corp.) of 225 μm length, 2.8 N/m spring constant, and 60-90 kHz resonant frequencies are used in Acoustic AC mode. All AFM measurements are performed in air at ambient conditions.

2.3 Results and discussion

2.3.1 Characterization of the DNA modified electrode

2.3.1.1 Characterization of DNA modified electrodes using electroactive probes

C_6-5'-amino modified oligos are immobilized on the carboxylic acid derivatized glassy carbon electrode using the technique described in Section 2.2.5. The derivatized electrode is treated for 20 minutes with 1-Ethyl-3-(3-dimethylaminopropyl) carbodiimide Hydrochloride (EDAC)/ N-Hydroxysuccinimide (NHS) to activate the carboxylic acid groups. The available carboxylic acid groups on the para- position of the benzene ring react with EDC/NHS to form stable esters, which hydrolyze slowly in aqueous media, in contrast with their rates of reaction with amino groups. Slow hydrolysis of the ester enhances the coupling efficiency of carbodiimide (EDC) for conjugating amine functionality of modified DNA to carboxyl groups on the surface. (See scheme 2.2) The

presence of immobilized DNA is characterized electrochemically using a ferricyanide redox probe.

Figure 2.2 shows the cyclic voltamograms for the bare, carboxylic groups grafted and the DNA modified electrode in 2 mM potassium ferricyanide. The reversible ferricyanide redox couple in the figure is clearly seen around 200 mV on the bare electrode. Derivatization of the electrode surface with carboxylic acid groups drastically reduces the electrochemical signal due to electrostatic repulsion between the negatively charged probe and the electrode surface. DNA immobilization further enhances the negative charge density on the electrode surface that results in complete reduction of the electrochemical signal (see scheme 2.3).

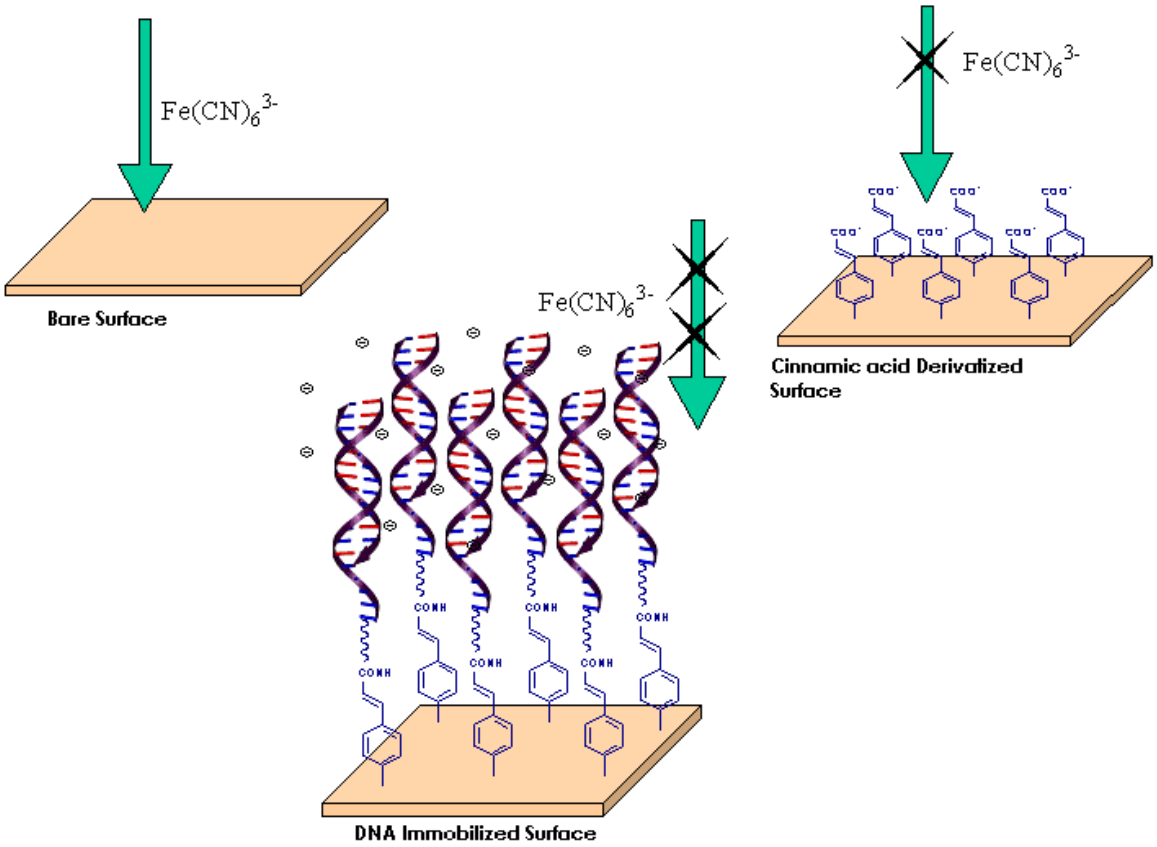

Scheme 2.3 Accessibility of ferricyanide redox probe

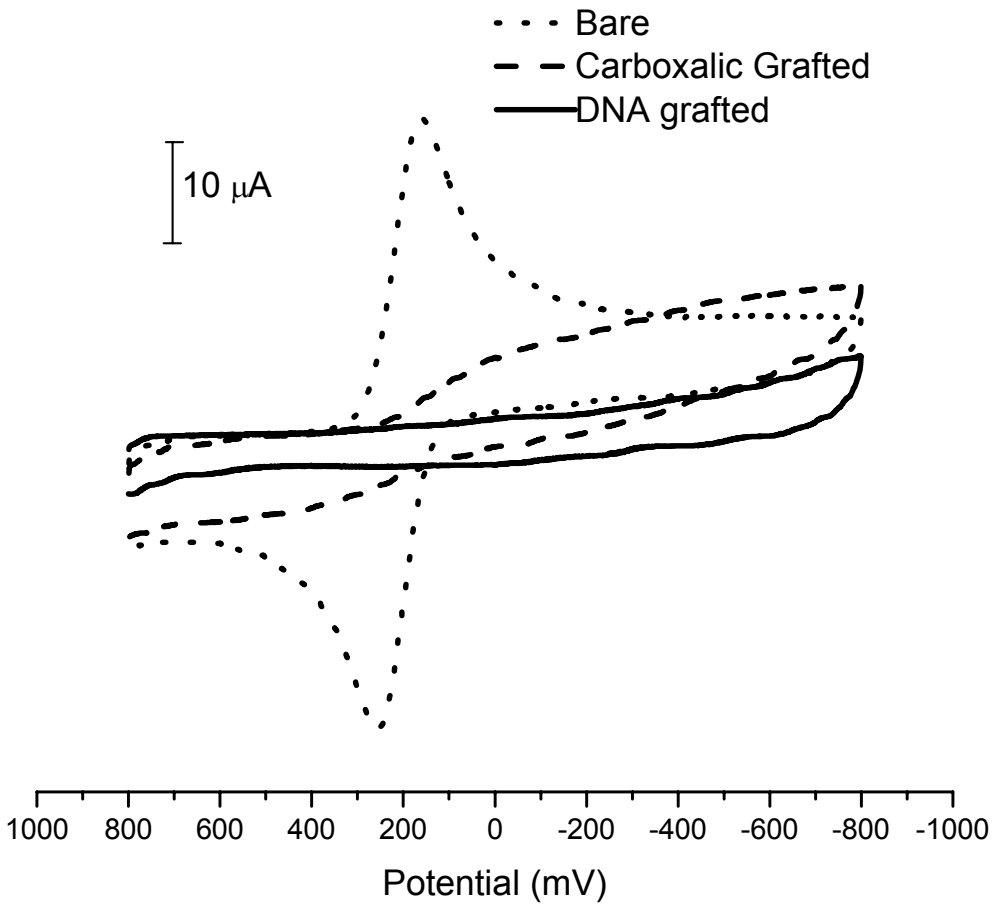

Figure 2.2 Cyclic voltammograms (ν=100 mV/s and A=0.07 cm^2) for the bare, carboxylic grafted and DNA modified electrode surfaces in 2 mM $Fe(CN)_6^{4-}$ in pH 7.0 phosphate buffer.

The presence of DNA on the electrode surface is further characterized using tris(2,2'-bipyridyl) dichlororuthenium (II) complex. This transition metal complex shows enhanced electrochemical oxidation in DNA[23-25]. Figure 2.3 shows the square wave voltammograms for the bare, carboxylic acid derivatized, and DNA modified electrodes in 50 μM $Ru(bpy)_3^{2+}$ complex in pH 5.5 acetate buffer. The reversible redox couple for ruthenium bipyridyl complex is observed around 1.05 V for the bare electrode. The presence of DNA shifts the redox potential slightly towards more positive values while significantly increasing the peak current compared to the bare electrode in the same solution.

Ruthenium bipyridyl, a positively charged metal complex, interacts with negatively charged DNA molecules via electrostatic attraction. Charge transport through DNA oxidizes $Ru(bpy)_3^{2+}$ complex. The oxidized ruthenium probe is reduced back to the Ru^{2+} form by oxidizing guanine bases in attached DNA layer as described in Scheme 2.4[26]. This two-step catalytic mechanism of $Ru(bpy)_3^{2+}$ mediated DNA oxidation leads to an overall increase in catalytic current as shown in the voltammogram for the DNA-modified electrode in the figure. This provides additional evidence for DNA immobilization on the electrode surface.

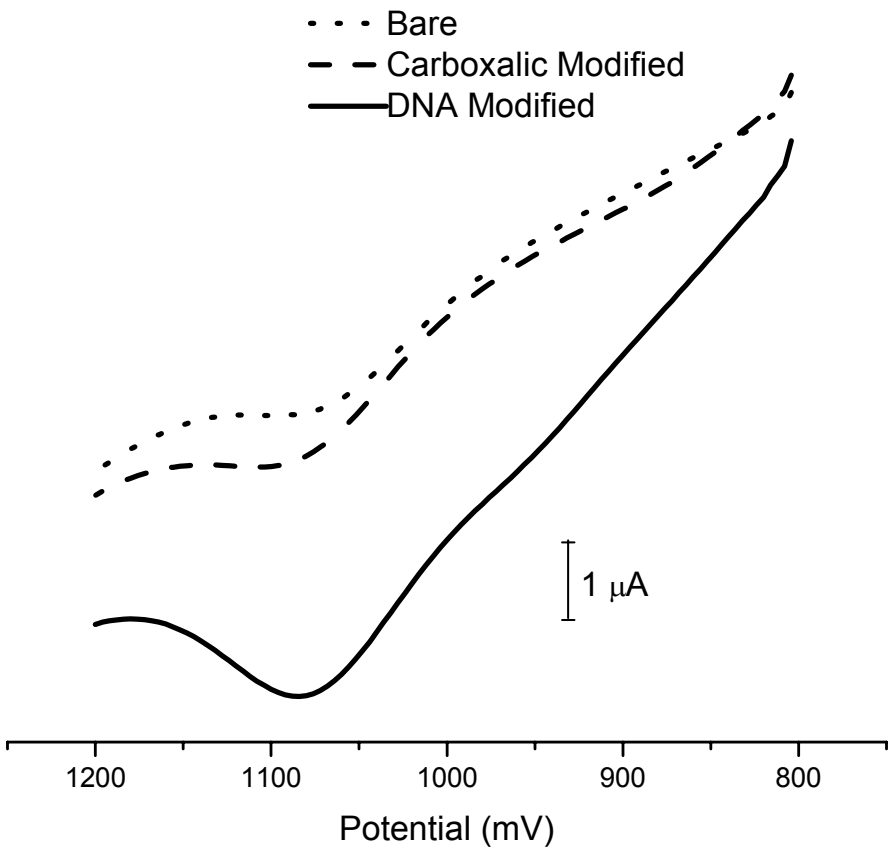

Figure 2.3 Square wave voltammograms for bare and DNA modified electrode in 50 μM $Ru(bpy)_3^{2+}$ complex in pH 5.5 acetate buffer.

$$Ru(bpy)_3^{2+} \rightleftharpoons Ru(bpy)_3^{3+} + e^-$$

$$Ru(bpy)_3^{3+} + DNA(Guanine) \rightleftharpoons DNA(Ox\text{-}Guanine) + Ru(bpy)_3^{2+}$$

Scheme 2.4 Ruthenium-mediated guanine base oxidation.

2.3.1.2 Characterization of the DNA modified electrode using Atomic Force Microscopy

Bare, carboxylic acid derivatized, and DNA immobilized HOPG surfaces were characterized using AFM for detailed analysis of each step involved in the previously described immobilization technique, and also to support the results obtained from the electrochemical studies.

Figure 2.4-(a) illustrates typical 3-D AFM image of the freshly cleaved, bare HOPG substrate used in the surface analysis experiments. As expected, the bare HOPG is extremely smooth, giving a *z* height of 0.4 nm, which enables the identification of the topographical changes when the surface is modified with DNA using this technique.

Figure 2.4-(b) shows the three-dimensional AFM image for the carboxylic acid grafted HOPG surface that occurs after step one of the immobilization technique. The modified surface now has a comparatively rough topography with perforations and a z height of 1.5 nm, which is consistent with surfaces grafted using electrochemical diazonium reduction. The 1.5 nm height is also comparable to other published results involving diazonium reduction[27].

Figure 2.4-(c) shows the three-dimensional topographical image for the DNA immobilized HOPG that is present after the second, final step of the immobilization process. AFM images of the DNA modified HOPG surface clearly shows a non-uniform thin film of DNA immobilized on the HOPG surface with a z height of 5 nm, which is in agreement with the width of the double stranded DNA.

When taking all AFM images into consideration, it is noteworthy that the DNA can effectively and conveniently be immobilized using the proposed technique based on

electrochemical diazonium reduction. Our AFM results are in agreement with what was obtained with the electrochemical studies using electroactive probes.

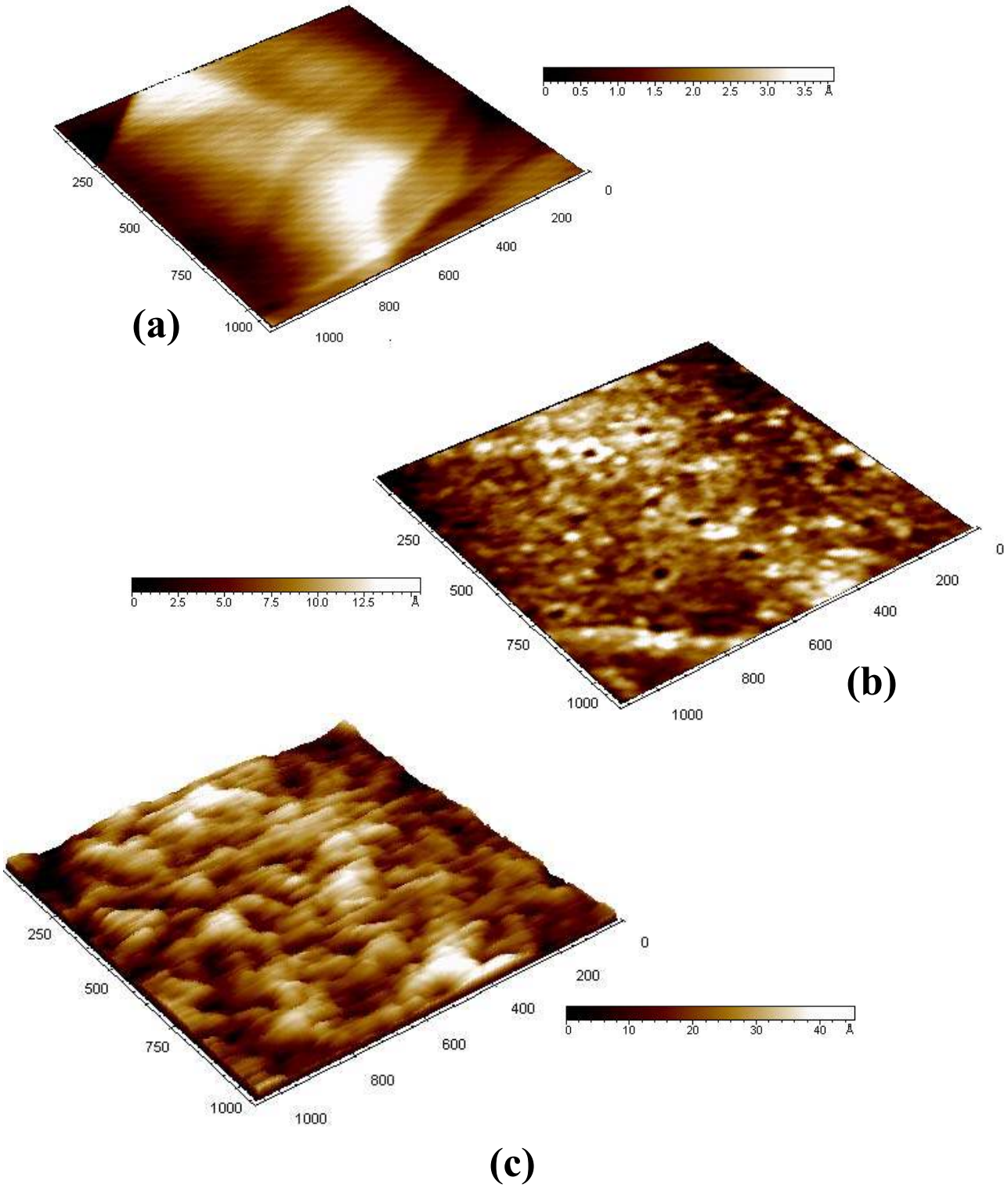

Figure 2.4 Tapping mode AFM images of (a) Bare HOPG, (b) HOPG modified with carboxalic acid. (c) DNA immobilized HOPG.

2.3.2 Application of DNA modified electrodes in DNA mismatch detection

2.3.2.1 Using methylene blue as an intercalator probe to detect DNA base mismatches

The developed immobilization method that we developed was tested for its applicability in DNA base mismatch detection using Barton's intercalator-mediated charge transport technique. The mismatch detection experiment is initiated by immobilizing two identical 15-base oligonucleotide probe sequences on two identical glassy carbon electrodes, and hybridizing one probe to a complementary target. The second probe is hybridized to another target with a mismatched base. Experimental parameters such as sequence of the oligonucleotide, type of mismatch, location of the mismatch, scan rate, probe concentrations, and buffers are optimized. The analysis is performed using two voltammetric approaches, cyclic voltammetry and chronocoulometry, and the sensitivity is compared to the thiol-gold method used in Barton`s assay[28].

Single base mismatch detection of hybridized oligos on the electrode surface is performed using methylene blue (MB), a redox-active DNA intercalator. Because of the packed DNA layer on the electrode surface, MB intercalates only at the top of the layer. MB on the bare electrode surface gives a reversible redox couple around –0.2V. When the electrode is modified with complementary oligos, a higher peak current at slightly more negative potentials is obtained. The higher peak current obtained for the electrode with complementary DNA is a result of π-stacking that facilitates electron transport through the DNA film to reduce intercalated MB[28]. The observed shift to negative potentials indicates increased energy of electron transfer, which is likely due to the

additional energy needed to move the flow of electrons through the negatively charged DNA, as compared to bare electrode.

The π-stack of aromatic nucleotide bases within the DNA molecule is a unique medium for electron transport. When a base mismatch is present, the π-base stack is disturbed resulting in diminished electron flow, thus reducing the peak current. Figure 2.5 shows how the introduction of only a single mismatch in the DNA strand results in a considerable reduction in peak current.

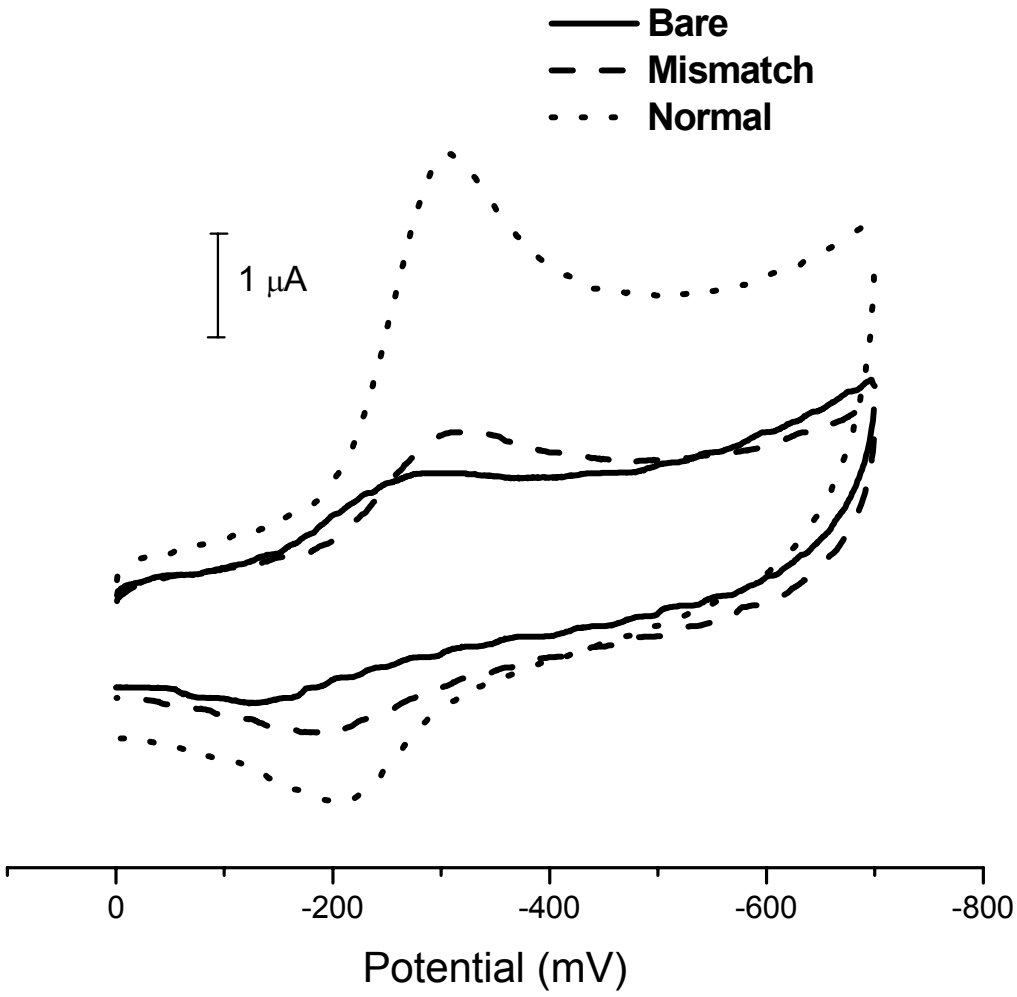

Figure 2.5 Cyclic Voltammograms in 2 μM MB in pH 7.0phosphate buffer for bare electrode (—), complementary DNA modified electrode (---) and mismatched DNA modified electrode (….).

2.3.2.2 Using MB/Ferricyanide to enhance detection of DNA mismatches

The sensitivity for the aforementioned intercalated MB-based detection assay depends mainly on the electrochemical signal, which in turn is directly related to the surface concentration of the MB. It is reported that this process of MB reduction can be coupled to a freely diffusing redox active molecule (*i.e.* ferricyanide) in solution to enhance the electrochemical response through electrocatalysis[29, 30].

The cyclic voltammograms for the DNA modified electrodes, with and without mismatch, in MB/ferricyanide solution are shown in Figure 2.6. An enhanced electrocatalytic current for the complemetary DNA-modified electrode is observed due to the efficient charge transport. During this two-step catalytic process, MB intercalated at the end of each DNA strand is first reduced. The reduced MB then oxidizes back to its original form by reducing the ferricyanide in solution resulting in a catalytic response. Scheme 2.5 shows the catalytic reduction cycle between intercalated MB and ferricyanide in solution. The presence of a mismatched base pair in the DNA strand drastically decreases the electron flow to the MB intercalated at the top of the DNA layer resulting in an almost total shutdown of the electrocatalytic signal. The difference in catalytic current between normal DNA and mismatched DNA is much greater than that shown previously in Figure 2.5 indicating enhanced detection of the mismatch.

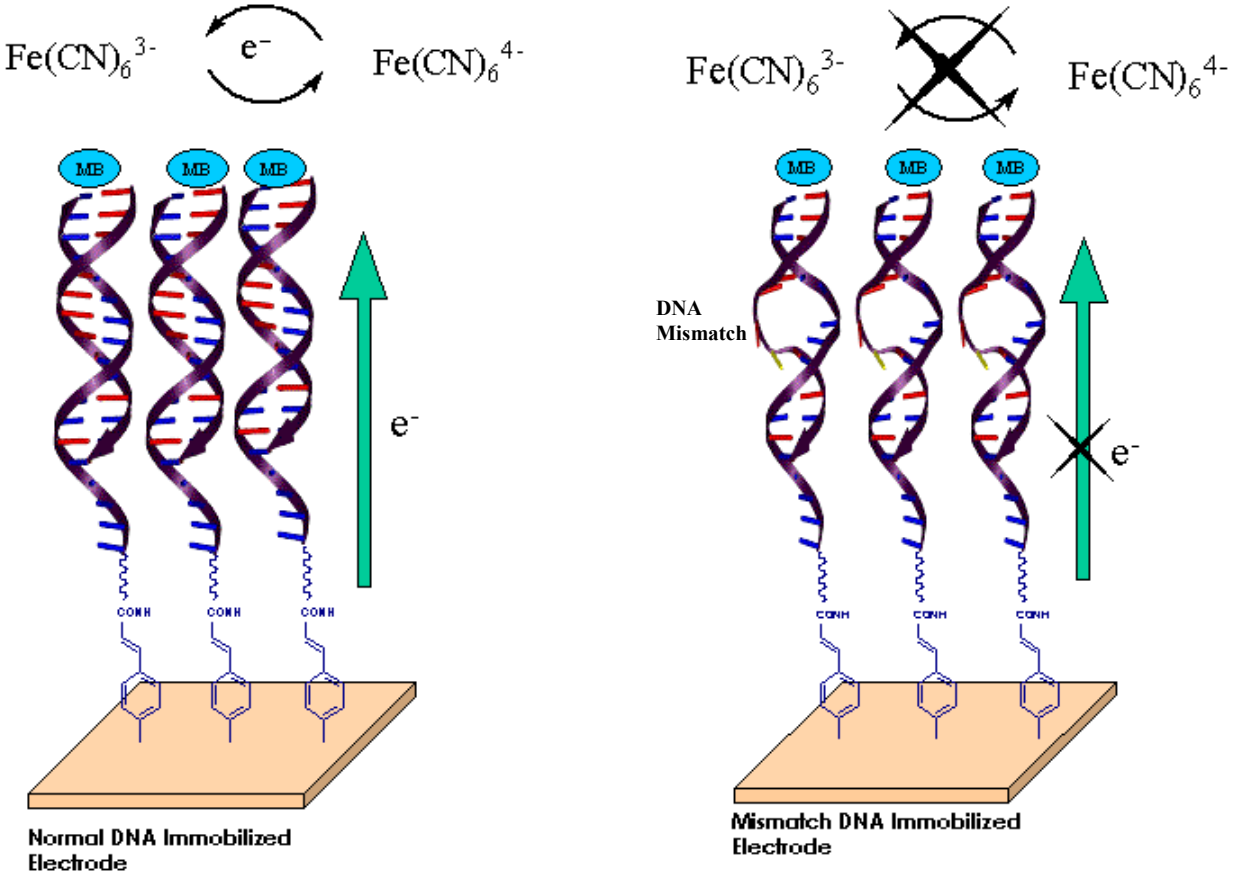

Scheme 2.5 Catalytic reduction of MB intercalated at the top of the packed DNA layer in the presence of ferricyanide in solution.

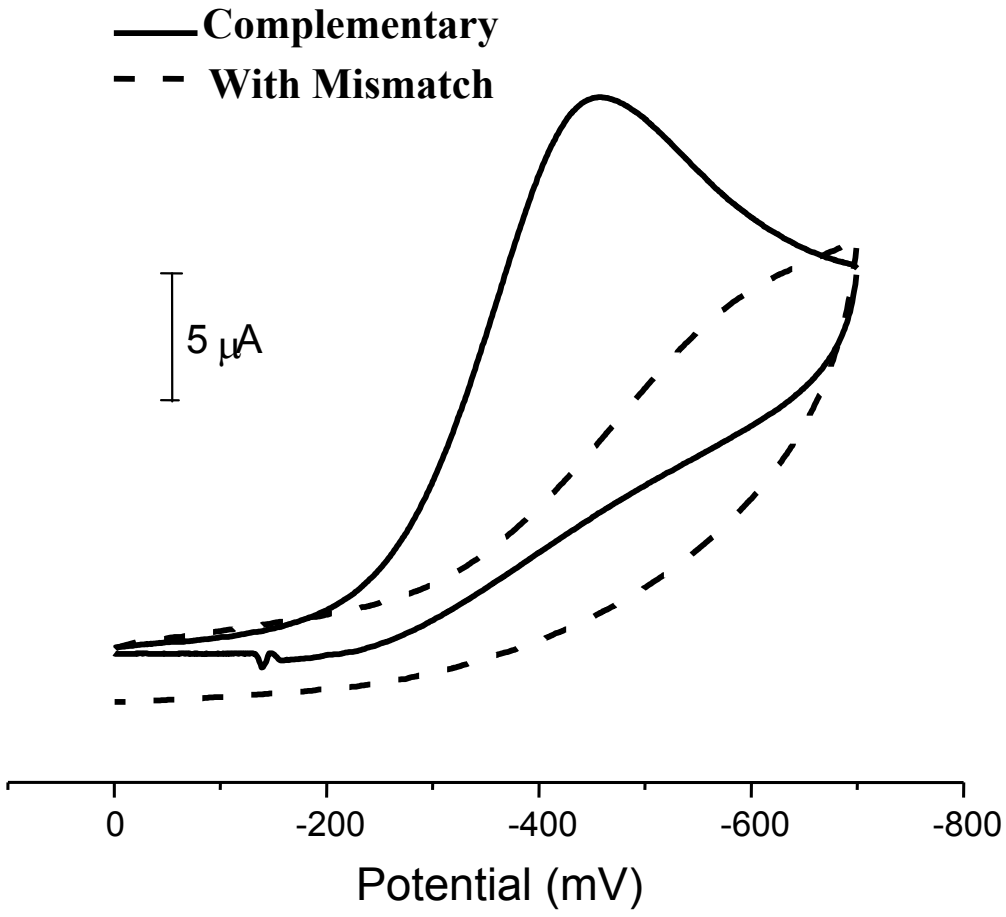

Figure 2.6 Cyclic voltammograms in 2 mM Ferricynide + 2 μM Methylene Blue solution in pH 7.0 phosphate buffer. Scan rate 0.1 mV/s. DNA modified electrodes with single base mismatch and complementary DNA.

2.3.2.3 Using chronocoulometry to monitor MB/Ferricyanide detection of DNA mismatches

To further elucidate the signal enhancement of the MB/ferricyanide method in the detection of single base mismatches, another sensitive electrochemical technique, chronocoulometry, is used on modified electrodes with mismatched and complementary DNA. In this experiment, the potential applied to the electrode is stepped from 0 V to -0.4 V, and the transient charge is monitored as a function of time. As a result of electron flow perturbation, the two electrodes with mismatched and complementary DNA gave significantly different faradaic charges. The complementary DNA immobilized electrode allows the passage of significant faradaic charge, whereas the electrode with mismatchd DNA yields significantly less charge, consistent with our previous voltammetric results. Figure 2.7 clearly illustrates how chronocoulometric monitoring using the MB/ferricyanide system can readily distinguish normal DNA from mismatched DNA.

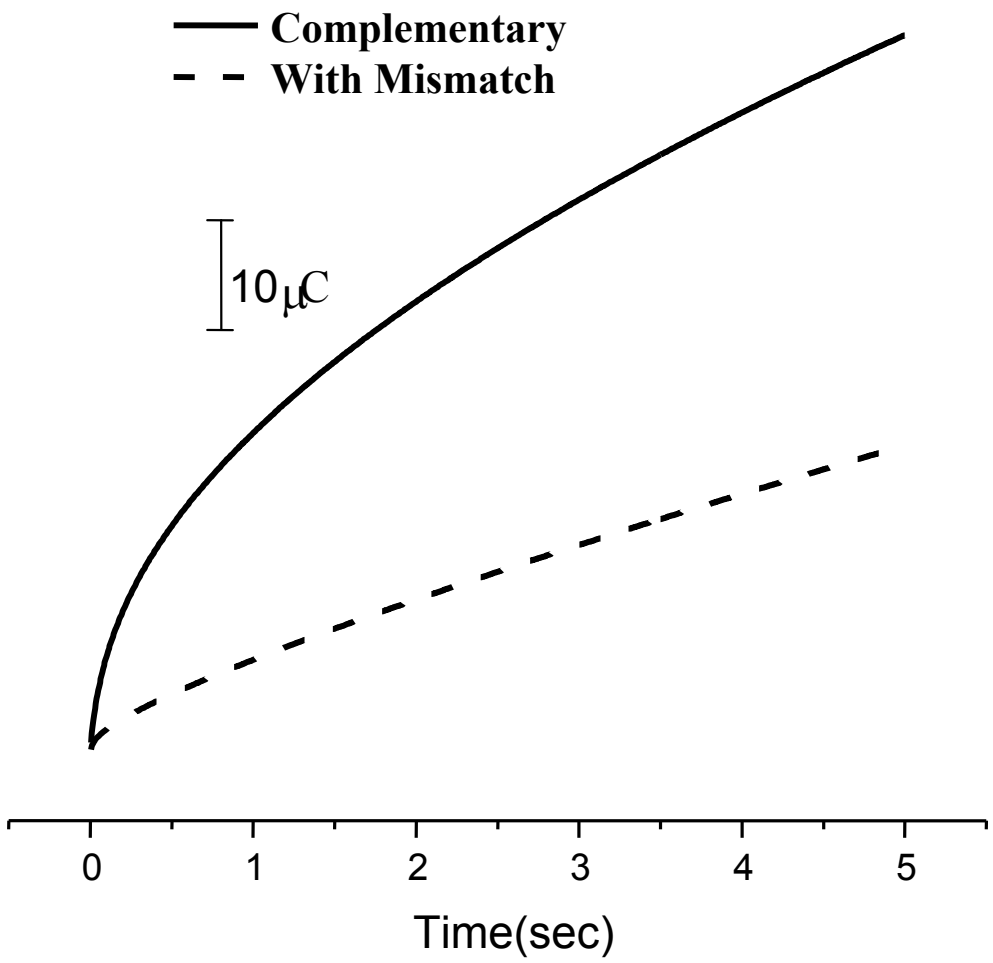

Figure 2.7 Chronocoulometry at – 400 mV of 2.0 mM ferricyanide and 2 μM methylene blue at pH 7.0 for mismatched and complementary DNA modified electrodes.

2.3.3 Comparison of the diazonium method with thiol-gold method

The sensitivity of our diazonium based mismatch detection assay was compared with the conventional Thiol-gold based detection assay. The comparison was performed using the current density values obtained for the diazonium method and the current density values reported for Gold-thol method in literature. The comparison results are given in Table 2.1. The results clearly show that the sensitivity of the diazonium method is slightly higher than the widely used Thiol-gold method.

	Current Density for 2 µM MB/ 2 mM $Fe(CN)_6^{3-}$
Diazonium Method (Electrode Area, A=0.07cm^2)	**265.5 µA/cm^2**
Thiol-Gold Method (Electrode Area, A=0.02cm^2)	**250 µA/cm^2**

Table 2.1 Comparison of the proposed diazonium method with Thiol-gold method.

2.4 Conclusion

The sensitivity of our DNA sensing platform using the new diazonium method for the detection of DNA mismatches was compared to the method using thiol-gold sensor developed by the Barton group. Though comparable to thiol-gold, the data statistically proves that our diazonium sensor has slightly higher sensitivity. In addition, our diazonium sensor has many other distinct advantages over the existing thiol-gold based sensor.

(1) Fast, reliable, simple and economical compared to thiol-gold method.

(2) No surface restrictions can be used with any conductive surface.

(3) No chemical interferences, doesn't need prior reduction with DTT.

2.5 References

1. Chrisey, L.A., G.U. Lee, and C.E. O'Ferrall, Covalent attachment of synthetic DNA to self-assembled monolayer films. Nucleic Acids Res, 1996. 24(15): p. 3031-9.
2. Du, W., et al., Functionalized self-assembled monolayer on gold for detection of human mitochondrial tRNA gene mutations. Anal Biochem, 2003. 322(1): p. 14-25.

3. Mark, S.S., et al., Dendrimer-functionalized self-assembled monolayers as a surface plasmon resonance sensor surface. Langmuir, 2004. 20(16): p. 6808-17.

4. Gore, M.R., et al., Detection of attomole quantities [correction of quantitites] of DNA targets on gold microelectrodes by electrocatalytic nucleobase oxidation. Anal Chem, 2003. 75(23): p. 6586-92.

5. Johnson, P.A., Levicky, R., Langmuir, 2003. 19: p. 10288-10294.

6. Charles, P.T., Vora, G.J., Andreadis, J.D., Fortney, A.J., Meador, C.E., Dulcey, C.S., Stenger, D.A., Langmuir, 2003. 19: p. 1586-1591.

7. Okahata, Y., Matsunobu, Y., Ijiro, K., Mukae, M., Murakami, A., Makino, K., Hybridization of Nucleic Acids Immobilized on aQuartz Crystal Microbalance. J. Am. Chem. Soc., 1992. 114: p. 8299-8300.

8. Georgiadis, R., Peterlinz, K.P., Peterson, A.W., Quantitative Measurements and Modeling of Kinetics in Nucleic Acid Monolayer Films Using SPR Spectroscopy. J. Am. Chem. Soc., 2000. 122: p. 3166-3173.

9. He, L., Musick, M.D., Nicewarner, S.R., Salinas, F.G., Benkovic, S.J., Natan, M.J., Keating, C.D., Colloidal Au-Enhanced Surface Plasmon Resonance for Ultrasensitive Detection of DNA Hybridization. J. Am. Chem. Soc., 2000. 122: p. 9071-9077.

10. Walti, C., Wirtz, R., Germishuizen, W.A., Bailey, D.M.D., Pepper, M., Middelberg, A.P.J., Davies, A.G., Direct Selective Functionalization of Nanometer-Separated Gold Electrodes with DNA Oligonucleotides. Langmuir, 2003. 19: p. 981-984.

11. Li, C.Z., Long, Y.T., Kraatz, H.B., Lee, J.S., Electrochemical Investigations of M-DNA Self-Assembled Monolayers on Gold Electrodes. J. Phys. Chem. B, 2003. 107: p. 2291-2296.

12. Lee, C.y.G., P.; Harbers, G.M.; Grainger, D.W.; Castner, D.G.;Gamble, L.J., Surface Coverage and Structure of Mixed DNA/Alkylthiol Monolayers on Gold: Characterization by XPS, NEXAFS, and Fluorescence Intensity Measurements. Anal Chem, 2006. 78(10): p. 3326–3334.

13. Steel, A.B., Levicky, R.L., Herne, T.M., Tarlov, M.J., Immobilization of Nucleic Acids at Solid Surfaces: Effect of Oligonucleotide Length on Layer Assembly. Biophysical Journal, 2000. 79: p. 975-981.

14. Li, Z., Jin, R., Mirkin, C.A., Letsinger, R.L., Multiple thiol-anchor capped DNA-gold nanoparticle conjugates. Nucleic Acid Research, 2002. 30: p. 1558-1562.

15. Letsinger, R.L., Elghanian, R., Viswanadham, G., Mirkin, C.A., Use of a Steroid Cyclic Disulfide Anchor in Constructing Gold Nanoparticle-Oligonucleotide Conjugates. Bioconjugate Chemistry, 2000. 11: p. 289-291.

16. Li, Y., Huang, J., McIver, R.T., Hemminger, J.C., Characterization of Thiol Self-Assembled Films by Laser Desorption Fourier Transform Mass Spectrometry. J. Am. Chem. Soc., 1992. 114: p. 2428-2432.

17. Bourdillon, C., Delarmar, M., Demaille, C., Hitimi, R., Moiroux, J., Pinson, J., Journal of Electroanalytical Chemistry, 1992. 336: p. 113.

18. Allongue, P.d.V., C. Henry; Pinson, J., Structural characterization of organic monolayers on Si111 from capacitance measurements. Electrochimica Acta, 2000. 45: p. 3241-3248.

19. Brooksby, P.A., Downard, A.J., Electrochemical and Atomic Force Microscopy Study of Carbon Surface Modification via Diazonium Reduction in Aqueous and Acetonitrile Solutions. Langmuir, 2004. 20: p. 5038-5045.

20. Blankespoor, R., Limoges, B., Schollhorn, B., Magale, J.L.S., Yazidi, D., Langmuir, 2005. 21: p. 3362-3375.

21. Ricci, A.B., C; Calvo, E.J., An FT-IRRAS study of nitrophenyl mono- and multilayers electro-deposited on gold by reduction of the diazonium salt. Phys. Chem. Chem. Phys, 2006. 8: p. 4297 - 4299.

22. Yang, X., Hall, S.B., Tan, S.N., Electroanalysis, 2003. 15: p. 885-891.

23. Thorp, H.H., Cutting out the middleman: DNA biosensors based on electrochemical oxidation. Trends in Biotecnology, 1998. 16: p. 117-121.

24. Sistare, M.F., Holmberg, R.C., Thorp, H.H., Journal of Physical Chemistry B, 1999. 103: p. 10718-10728.

25. Brooksby, P.A., Downard, A.J., Nanoscale Patterning of Flat Carbon Surfaces by Scanning Probe Lithography and Electrochemistry. Langmuir, 2005. 21: p. 1672-1675.

26. Ontko, A.C., Armistead, P.M., Kircus, S.R., Thorp, H.H., Electrochemical Detection of Single-Stranded DNA Using Polymer-Modified Electrodes. Inorg. Chem.,, 1999. 38(8): p. 1842-1846.

27. Tuite, E., Kelly, J.M., Biopolymers, 1995. 35: p. 419-33.

28. Kelley, S.O., Boon, E.M., Barton, J.K., Jackson, N.M., Hill, M.G., Single-base mismatch detection based on charge transduction through DNA. Nucleic Acid Research, 1999. 27(24): p. 4830-4837.

29. Drummond, T.G., Hill, M.G., Barton, J.K., Electrochemical DNA Sensors. Nature, 2003. 21: p. 1192-1199.

30. Liu, T., Barton, J.K., DNA Electrochemistry through the Base Pairs Not the Sugar-Phosphate Backbone. J. Am. Chem. Soc., 2005. 127: p. 10160-10161.

CHAPTER III

ADVANCING THE CAPABILITIES OF DNA MISMATCH DETECTION USING MUTS: A HIGH-THROUGHPUT APPROACH TO MULTIPLE-USE SENSORS

3.1 Introduction

Most of the DNA sensing approaches for mismatch detection[1-4], including the diazonium based attachment previously discussed, use covalent methods to immobilize DNA probes on the sensor surface. As a result, reusability of these sensors for a different target sequence is not possible, as the probe sequence is permanently fixed to the sensor surface. This *sequence specific detection* is a drawback that reduces the capability of these sensors in high throughput use. In finding a solution to this problem, it is important that the original sensitivity is not sacrificed over throughput capability.

Ones solution to overcome this sequence-specific detection problem is to immobilize a more generic biomacromolecule on the sensor surface instead of the sequence-specific, single-stranded DNA probe. The desired biomolecule should be able recognize DNA mutations, regardless of base sequence. In order to maintain better sensitivity and selectivity, the biomolecule for this particular task should also have a high binding

constant to the target mutated DNA. Also, to reuse the sensor, the binding between the biomolecule and the target DNA should easily reversible by changing a simple parameter such as chemical composition, pH, or ionic strength of the solution. Finding such a biomacromolecule that satisfies all of these conditions is challenging.

MutS is a protein able to reliably recognize mispaired bases in heteroduplex DNA, as well as small insertions/deletions of one to four bases (*vide supra*). MutS strongly binds to DNA with high specificity. Strong, consistent binding of MutS to mismatched bases is a tremendous advantage that makes it an ideal candidate for use as a recognition biomolecule in mismatch detection sensors. Moreover, the bound MutS is easily detached from DNA by changing the ionic strength of the medium[5], providing another reason to consider MutS as the recognition element of choice. MutS forms the strongest complexes with G-T mismatches and single unpaired bases; whereas weaker, yet still significant binding is observed at C-C mismatches[6-8].

In this study, we take advantage of MutS' natural ability to recognize unpaired and mismatched bases to develop a high throughput assay using electrochemical techniques. Studies of MutS' interaction with DNA are conducted by immobilizing biotin-tagged MutS protein on an electrode surface through a new approach. Biotin-streptavidin chemistry[9-11] is used to immobilize MutS on the electrode surface.

Atomic Force Microscopy and electrochemistry are used to confirm the immobilization efficiency. Scheme 3.1 shows an illustration of the proposed MutS immobilization method for mismatch detection. This label-free electrochemical method has the advantage of simple and direct detection, allowing the protein and DNA to be used in more diverse environments. Moreover, the MutS-immobilized sensor can be

differentiated from other mismatch probing sensors because its reusability increases its versatility and reduces the overall cost of the tests performed.

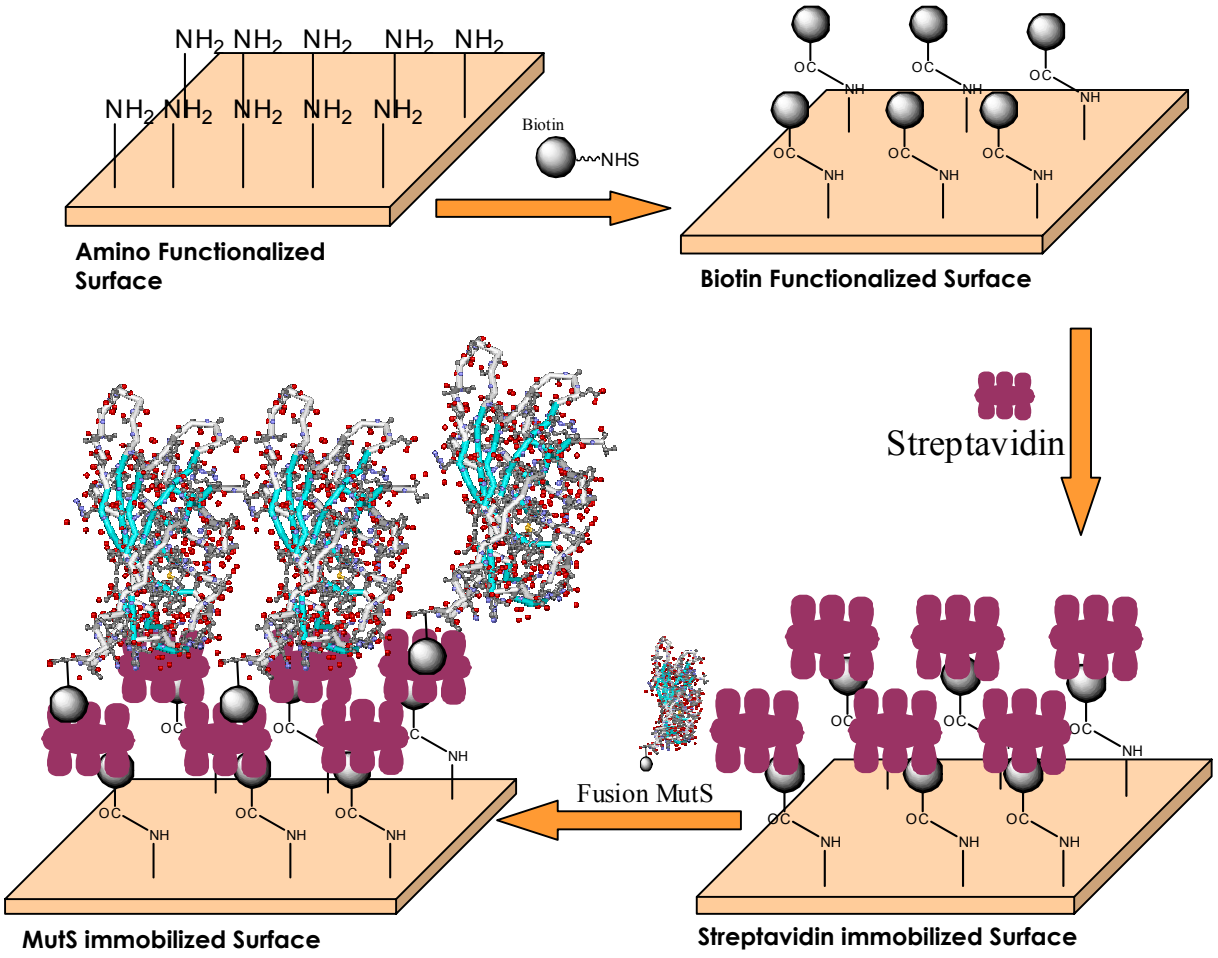

Scheme 3.1 Schematic illustration of the new immobilization method for MutS.

3.2 Experimental

3.2.1 Chemicals, apparatus, and procedures

3.2.1.1 Chemicals

All the chemicals used were of analytical grade. Nanopure deionized water (specific resistance >18.2 Ω.cm) used in all experiments was supplied by a Barnstead water purification system. Biotin-NHS, streptavidin, para-nitrodiazonium tetrafluoroborate, aminopropyltriethoxysilane (APTES), and tetrabutylammonium tetrafluoroborate ($Bu_4N^+BF_4^-$) were all purchased from Sigma-Aldrich.

3.2.1.2 Electrochemical measurements

A BAS (Bio-Analytical Systems) electrochemical workstation is used for all electrochemical experiments. All electrochemical measurements are carried out at room temperature in buffers that are purged for 10 min with nitrogen immediately before readings and blanketed with nitrogen throughout the experiment. Cyclic Voltammetry (CV) and Square Wave Voltammetry (SWV) are performed in a three-neck electrochemical cell with Ag/AgCl reference electrode, platinum counter electrode and 3.0 mm diameter glassy carbon working electrodes. The working electrodes were polished prior to experiment with alumina slurry (successively with 0.3 and 0.05 micron), and cleaned in ultrasound bath in deionized water.

3.2.1.3 Atomic Force Microscopic imaging

AFM is performed with a Pico SPM® scanning probe microscope controlled by a magnetic alternating current MACmode® module and interfaced with a PicoScan®

controller from Molecular Imaging Corp., Tempe, Arizona. All AFM scans are performed with a multi-purpose small scanner from Molecular Imaging Corp. with a scan range of 9 μm in the x-y plane and 2 μm along the z axis. Silicon Type II MAClever® cantilevers (Molecular Imaging Corp.) of 225 μm length, 2.8 N/m spring constant, and 60-90 kHz resonant frequencies are used in acoustic AC mode in deionized water.

3.2.1.4 DNA hybridization

30 base single stranded oligonucleotides from Biosynthesis (**1.** 5'-GCA CCT GCA TCC TGT GGA GAA GTC TGC CGT-3', **2.** 5'-ACG GCA GAC TTC TCC ACA GGA GTC AGG TGC-3', **3.** 5'-ACG GCA GAC TTC TCC GCA GGA GTC AGG TGC-3') are dissolved in deionized water to prepare stock solutions of 2 μg/μl concentrations. Equal volumes of each ssDNA (1+2: complementary oligo and 1+3: mismatched oligo) are hybridized in pH 7.0 phosphate (5 mM phosphate, 0.1 mM NaCl) buffer by heating for 5-8 min at 95°C in a heat block and cooling slowly to room temperature over 3-4 hrs. The final DNA concentration is estimated by UV absorption at 260 nm[12].

3.2.1.5 GST fusion protein expression and purification

The MutSb expression plasmid (pMutSb) was kindly provided by Stanley F. Nelson, *et al*. The plasmid is engineered with a biotin tag at the N-terminal lysine of the MutS gene. Expression and purification of biotinylated MutS is carried out according to a published protocol[13]. pMutSb is transformed into BL21(DE3). Cell cultures are grown to mid log phase (0.6 OD) and 1mM IPTG is added for optimized protein expression at room temperature overnight. 5g of wet cell pellets are harvested from 1L cell culture and

suspended in 20 mL lysis buffer (50mM Hepes pH 7.8, 50mM KCL, 1mM DTT, 0.1mM EDTA). 100μg/μL lysozymes are added to the cell suspension on ice. Cells are lysed by sonication for complete cell lysis. The soluble fraction is isolated by centrifugation for 20min at 20,000 x g. Purification of the MutSb is carried out using the same procedure mentioned above, with additional step of adding 5% to 31% ammonium sulfate while stirring for 45 minutes in order to precipitant and isolate MutSb. The MutSb is pelletized by centrifugation at 15,000 x g for 30min, and then resuspended in 2mL of MutSb buffer. The protein is isolated using a column consisting of monomeric avidin-agarose beads (Pierce). The protein is eluted from the column using an elution buffer containing 0.2M NaCl and 20mM Biotin. The eluted protein is dialysed against the MutSb buffer and concentrations are determined using Bradford assay.

3.2.1.6 Protein immobilization on mica surface

A freshly cleaved mica surface is used to immobilize the protein. The mica surface is derivatized with amino functionalities by incubating it for 20 minutes in aminopropyltriethoxysilane (APTES) solution, which is prepared by mixing 950μL of acetone, 50μL of deionized water and 30 μL of APTES from the original bottle. After incubation, the mica surface is washed three times with acetone followed by deionized water. The mica surface is then incubated for 45 minutes in biotin-NHS ester solution that is prepared by dissolving 0.1mg of biotin-NHS in 500μL of DMF. After biotin functionalization, the surface is thoroughly washed with DMF followed by deionized water. This modified surface is then exposed to 1μg/mL solution of streptavidin for 5 minutes. Next, the surface is thoroughly washed with deionized water to remove any non-

specifically adsorbed proteins. Bare mica surface, streptavidin-immobilized mica with biotin linkages, and MutS immobilized on the streptavidin-modified, biotin-linked mica will all be further characterized by AFM imaging.

3.2.1.7 Protein immobilization on electrode surface

3.2.1.7.1 Electrode derivatization with amino functionalities

Glassy carbon electrodes are polished consecutively with 0.3 and 0.05 μm alumina on a Buehler microcloth, follwed by 5 minutes ultrasonication in acetone, and 15 minutes ultrasonication in deionized water. The cleaned electrodes are next derivatized electrochemically with nitrobenzene functionalities using a 1 mM solution of para-nitrodiazonium tetrafluoroborate in acetonitrile containing 0.1 M tetrabutylammonium tetrafluoroborate ($Bu_4N^+BF_4^-$) as the electrolyte. Cyclic Voltammetry is performed twice on each electrode in a potential window of 0.8 V to -0.8 V at a scan rate of 0.1V/s.

After cyclic voltammetry, the electrodes are rinsed several times with acetone followed by through washing with deionized water. Nitro functionalities on these modified electrodes are then electrochemically reduced to amino functionalities by performing another cyclic voltammetric run (potential window of 0 V to 1.0 V and with a scan rate of 0.1 V/s) in a protic solvent containing 20% Methanol and 80% water (v/v).

3.2.1.7.2 Protein immobilization on the electrode surface

The amino-functionalized electrodes are incubated for 45 minutes in biotin-NHS ester solution that is prepared by dissolving 0.1mg of biotin-NHS in 500μL of DMF. After biotin functionalization, the electrodes are thoroughly washed with DMF followed by

deionized water. These modified electrodes are then exposed to a 1μg/mL solution of streptavidin for 5 minutes. Next, the electrodes are thoroughly washed with deionized water to remove any non-specifically adsorbed proteins. Protein-immobilized electrodes will be characterized by cyclic voltammetry using potassium ferricyanide as an interrogative probe.

3.3 Results & discussions

3.3.1 AFM characterization of MutS immobilized on mica

Two different characterization techniques, atomic force microscopy and electrochemistry, are performed to examine the immobilization efficiency of MutS through the new immobilization approach discussed in the experimental section. The results from the first set of characterizations are shown by the AFM images in Figure 3.1. All AFM images are obtained on mica substrate. Figure 3.1 presents the topographic images of (a) bare mica, (b) streptavidin-immobilized mica with biotin linkages, and (c) MutS immobilized on streptavidin-modified, biotin-linked mica, as well as (d) a zoom 3-D image of the MutS immobilized on streptavidin-modified, biotin-linked mica.

As expected, the bare mica surface in figure 3.1 (a) is extremely smooth, with a *z* height of only 0.3 nm[14]. The streptavidin-immobilized surface in figure 3.1 (b) gives relatively rough topography with peaks heights around 6 nm, which is very close to the theoretical height of immoblized streptavidin[15]. The image also shows a high density of immobilized streptavidin on the surface, which confirms literature reports of an unusually strong binding ($K_d \sim 10^{-15}$ M) between biotin and streptavidin[16]. The appearance and the z height for both bare and streptavidin-immobilized mica substrates

are compatible with other published experiments[17]. The peak density on the topography image is almost unchanged for the streptavidin-modified surface after several washings indicating a robust adherence of the streptavidin to the biotin functional groups on the surface. Due to static repulsions, the negatively charged mica surface reduces the possibility for any non-specific attachment of streptavidin, which is also negatively charged in the pH 7.0 phosphate working buffer.

The MutS immobilized on streptavidin-modified, biotin-linked mica in figure 3.1 (c) shows a surface that is relatively uneven in peak heights with a significant number of peaks relatively larger and taller than the streptavidin peaks in figure 3.1 (b). X-ray crystallographic height of the MutS dimeric structure is around 7 nm. The large features on the image have a height around 13 nm, which is consistent with the additive height of MutS (about 7 nm) being immobilized on top of the surface streptavidin proteins (around 6 nm). Moreover, the significant difference in height between MutS-bonded and MutS-free streptavidin in the zoomed 3D (figure 3.1 (d)) image verifies the binding between MutS and streptavidin. We further investigated the MutS immobilized surface and found that the MutS remained attached to the streptavidin even after thorough washings. This proves beyond reasonable doubt that MutS is attached to streptavidin through the strong `biotin-streptavidin' interaction, but not through weak hydrophobic interactions. Attempts to immobilize $MutS_b$ on a surface modified with *inactive* streptavidin (streptavidin with no active sites for biotin recognition) as a control experiment showed no attachment of MutS after 10 minutes of incubation (see Figure 3.2). This observation further clarifies the nature of the binding between MutS and streptavidin.

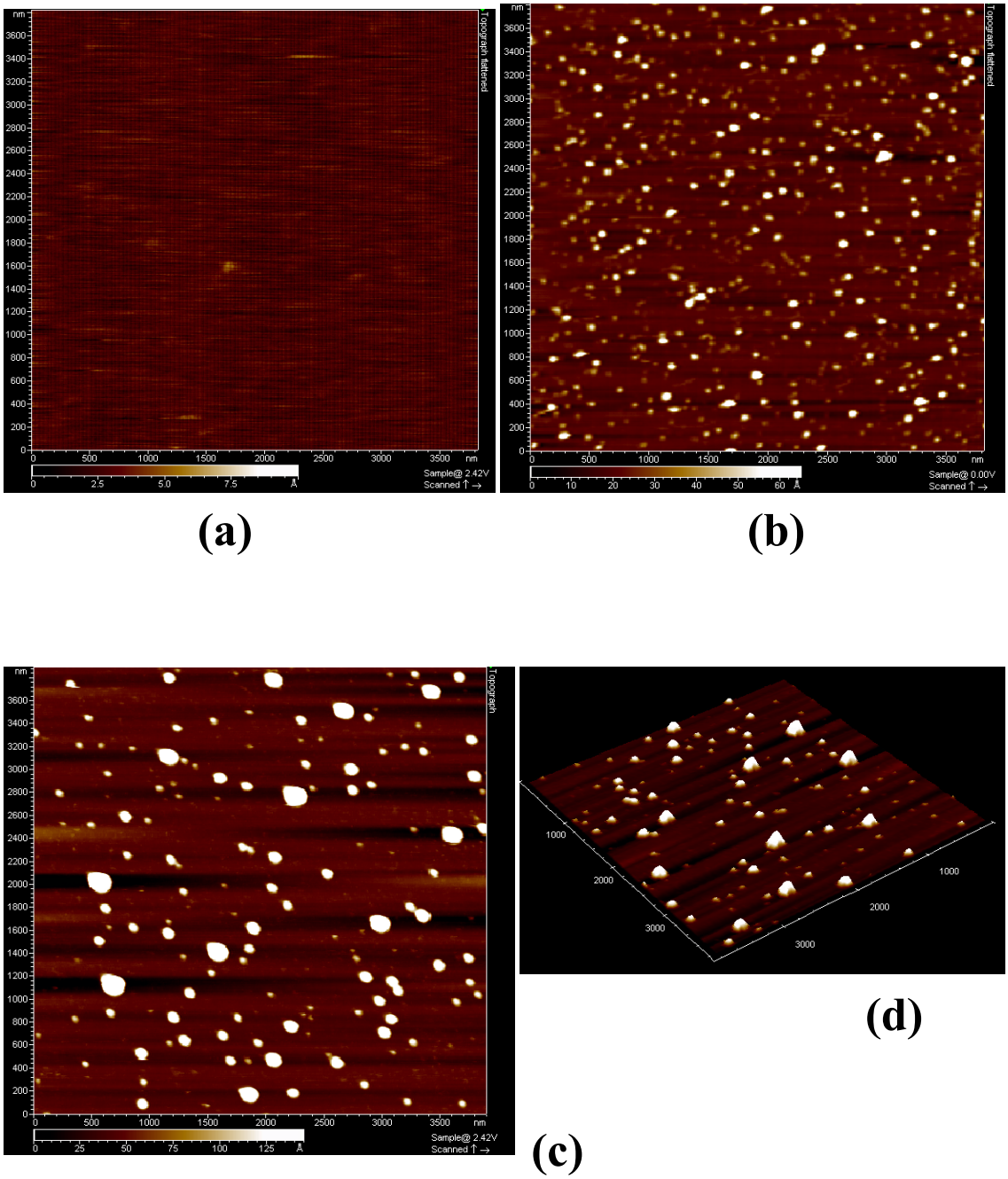

Figure 3.1 Tapping mode AFM images in water. (a) Bare Mica, (b) Streptavidin immobilized Mica through biotin linkages, (c) Immobilized MutS on streptavidin modified Mica, and (d) 3-D image of the MutS immobilized Mica.

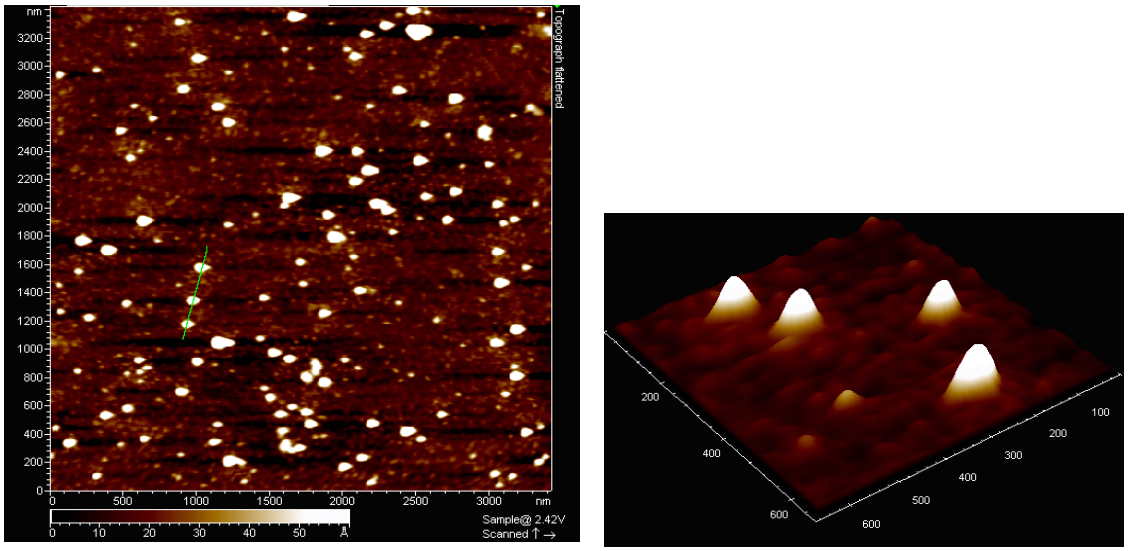

(a)

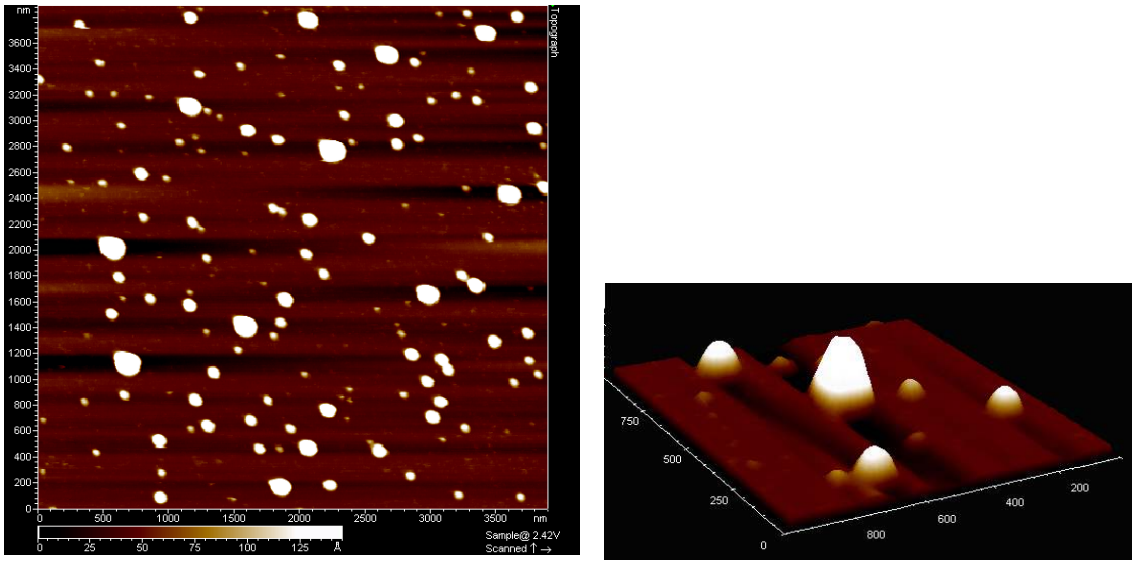

(b)

Figure 3.2 – Comparison of 2D and 3D images of (a) Control experiment for MutS immobilization after blocking active sites of streptavidin. (b) MutS immobilization without blocking active sites of streptavidin.

3.3.2 Electrochemical characterization of MutS immobilized glassy carbon electrodes

The second characterization was carried out using cyclic voltammetry (CV), in the presence of an electro-active probe, potassium ferricyanaide ($K_3Fe(CN)_6$). The immobilization efficiency at each step of the new method is directly detected by observing the change in redox currents of $Fe(CN)_6^{3-}$ via CV. Figure 3.3 shows the cyclic voltamograms for the bare, biotin modified, streptavidin immobilized, and MutS immobilized electrodes in 2 mM $Fe(CN)_6^{3-}$ in pH 7.4 phosphate buffer. A bar chart comparing the average peak currents obtained for each immobilization step is shown in Figure 3.4. The reversible redox couple for the $Fe(CN)_6^{3-}$ probe occurs around 200 mV (vs. Ag/AgCl) for the bare electrode with a current density of about 586 $\mu A/cm^2$. Derivatizing the electrode with biotin functionalities significantly reduces the current density to about 443 $\mu A/cm^2$. This significant reduction of the current is due to the decrease in the surface concentration of the probe ion on the electrode surface, probably as a result of the formation of a blocking layer of biotin on the electrode surface. The formation of the biotin monolayer is important, as the efficiency of streptavidin and MutS immobilization is totally dependant on the amount of the available biotin functionalities on the surface. We also obtained AFM images supporting our electrochemical data and showing a formation of a fine layer of biotin after NHS coupling.

The immobilization of the two proteins further reduces peak currents by blocking the electrochemical reaction on the electrode surface. Moreover, both streptavidin and MutS are negatively charged in the pH 7.4 phosphate buffer and the negatively charged $Fe(CN)_6^{3-}$ probe is further electrostatically repelled by the immobilized proteins. This is

possibly the reason why a very low average current density (181 $\mu A/cm^2$) is observed for the MutS-immobilized electrode with respect to the bare electrode. Another noticeable observation in Figure 3.3 is that the corresponding peak potentials for biotin, streptavidin, and MutS move towards more negative potentials as compared to bare electrode. The shift in peak potentials is mainly due to the obstruction of electron flow from the electrode surface to the redox probe through the immobilized molecules. Since both streptavidin and MutS are negatively charged in the operating buffer, the electron movement across the negatively charged interface is disturbed by static repulsions. As a result, the electrons need to be further energized to reduce ferricyanide, resulting in the observed negative shift in peak potentials for both streptavidin and MutS immobilized electrodes.

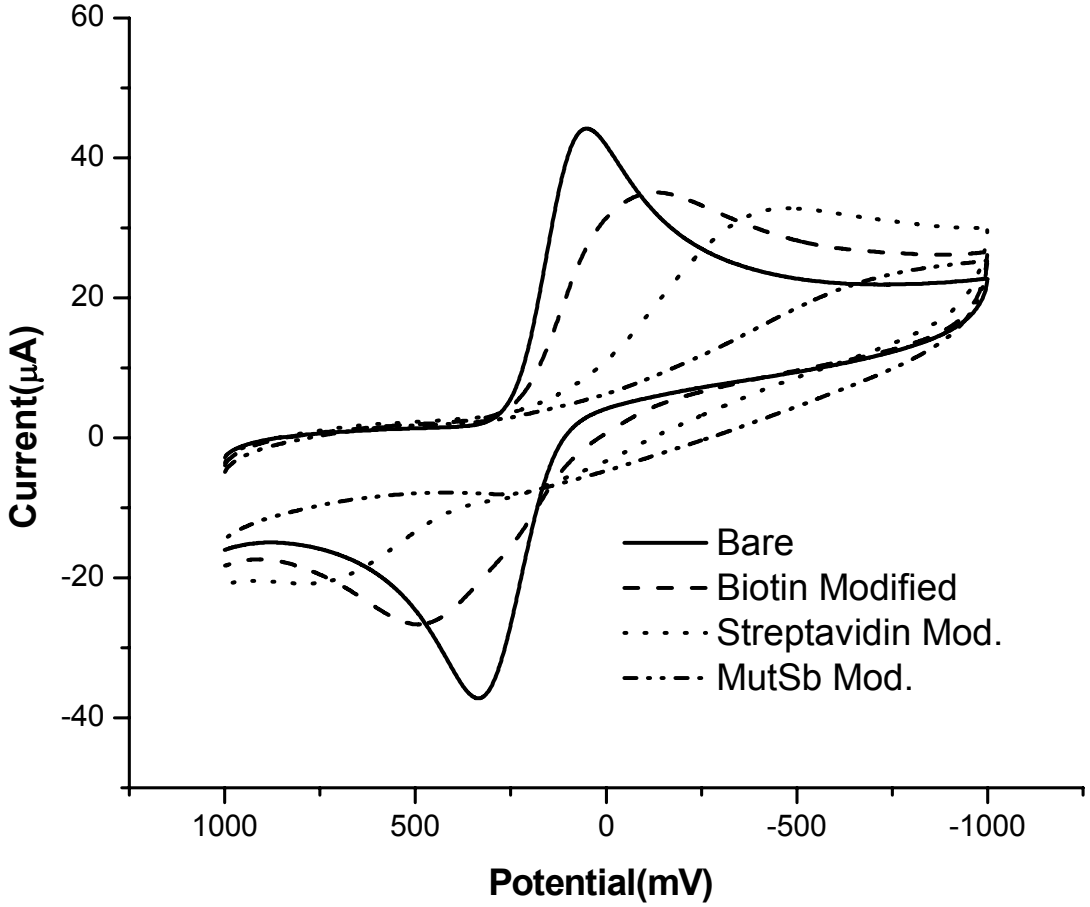

Figure 3.3 Overlaid cyclic voltammograms (vs Ag/AgCl) for the bare, biotin-modified, streptavidin-modified, and MutS-modified electrodes in 2mM $Fe(CN)_6^{3-}$ in pH 7.4 phosphate buffer.

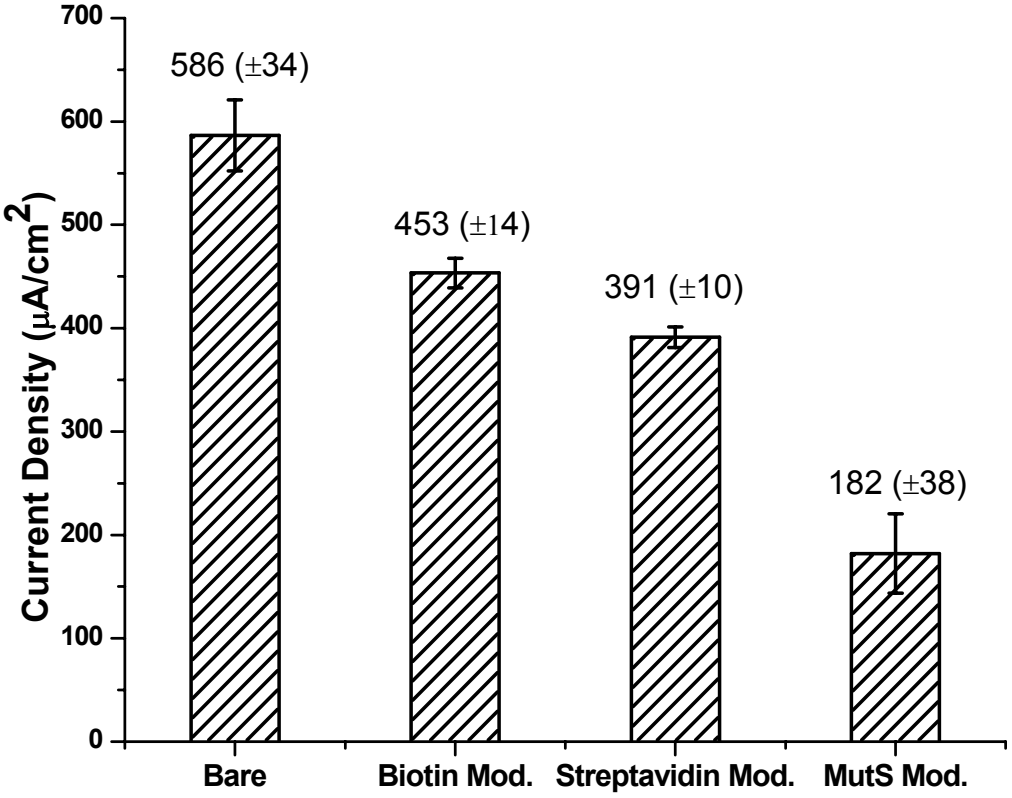

Figure 3.4 Comparison bar graphs for the bare, biotin modified, streptavidin modified, and MutS modified electrodes in 2mM $Fe(CN)_6^{3-}$ in pH 7.4 phosphate buffer.

3.3.3 DNA mismatch detection

In a typical experiment, we derivatized two identical glassy carbon electrodes with MutS protein in order to evaluate our ability to detect DNA mismatches using our proposed method. The two MutS-modified electrodes are exposed to mismatched and complementary DNA. Finally, we performed cyclic voltammetry (1.0 V to -1.0 V at 100 mV/sec) using the electrodes in methylene blue/ferricyanide solution.

Methylene blue (MB) is an electrochemically active flat aromatic molecule, which binds to DNA predominantly via intercalation. The intercalation is driven by the π-π^* interaction between nucleotide bases and methylene blue molecules. As we found earlier (section 2.3.2.2), the use of methylene blue/ferricyanide coupled catalytic reduction enhances the current via a two-stage catalytic reduction, whereby intercalated methylene blue is reduced, which in turn reduces ferricyanide in solution. As a result of this recognition, we get a positive signal enhancement that magnifies the original methylene blue reduction current, making the detection of mismatches easier to identify.

Figure 3.5 shows two cyclic voltammograms obtained in 2μM MB/2mM $Fe(CN)_6^{3-}$ solution for the two electrodes that were exposed to mismatched and complementary DNA. The mismatched-DNA electrode yields a significantly higher catalytic reduction peak indicating a positive recognition between mismatched DNA and immobilized MutS, which is a clear indication of the success of the proposed method. The experiment performed by incubating the electrode with complementary DNA does not show any reduction peak, suggesting that the increase in peak current with the mismatched DNA is a direct result of preconcentration of methylene blue on DNA recognized by immobilized MutS. We checked reproducibility by performing repetitive experiments. The bar graph with error bars in Figure 3.6 is a typical average of the three replicates, showing that peak

currents for DNA with single-base mismatches are significantly higher than currents recorded for complementary DNA.

As a control, we performed another cyclic voltammetric experiment in 2μM MB/2mM $Fe(CN)_6^{3-}$ by incubating only streptavidin immobilized electrodes in normal and mismatched DNA solutions to confirm mismatch DNA binds only to immobilized MutS, but not to streptavidin. Figure 3.7 shows the voltammograms we obtained for bare, with mismatched DNA, and streptavidin immobilized electrode incubated with normal DNA.

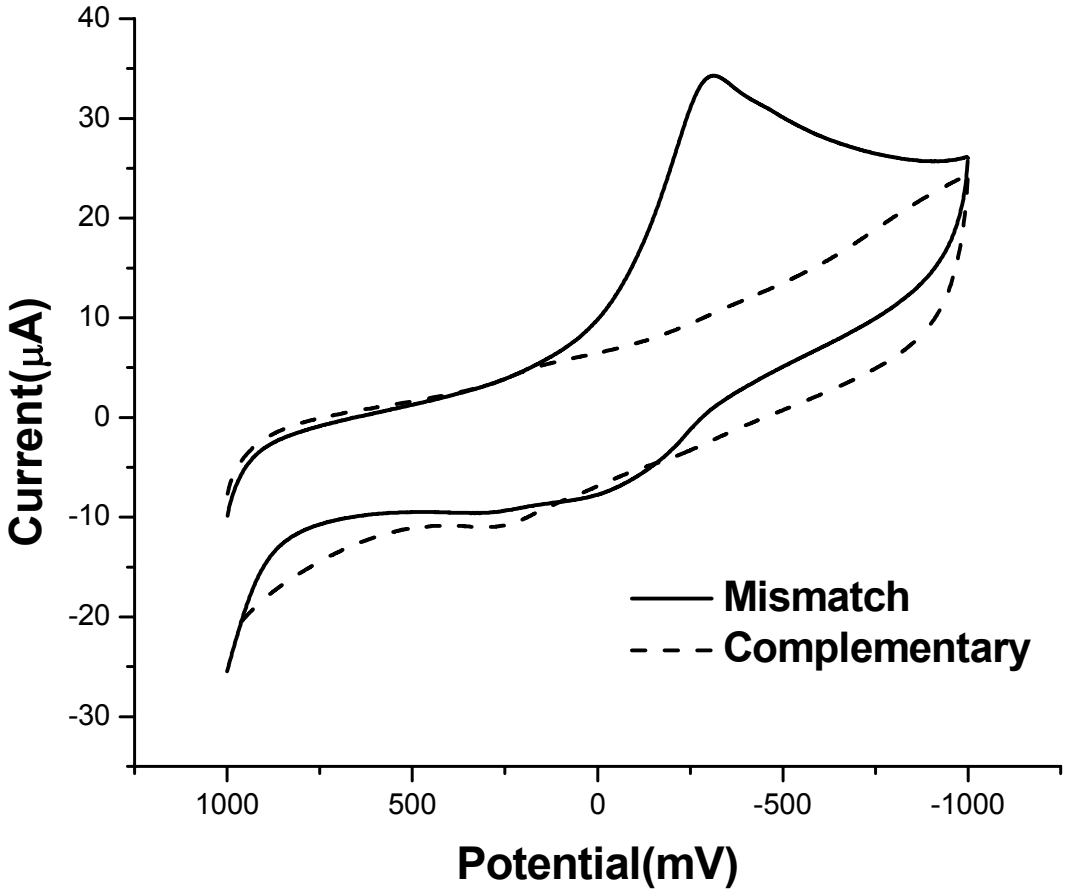

Figure 3.5 Overlaid cyclic voltamograms (vs Ag/AgCl) for the mismatched and complementary DNA incubated electrodes in 2μM MB-2mM $Fe(CN)_6^{3-}$ in pH 7.4 phosphate buffer.

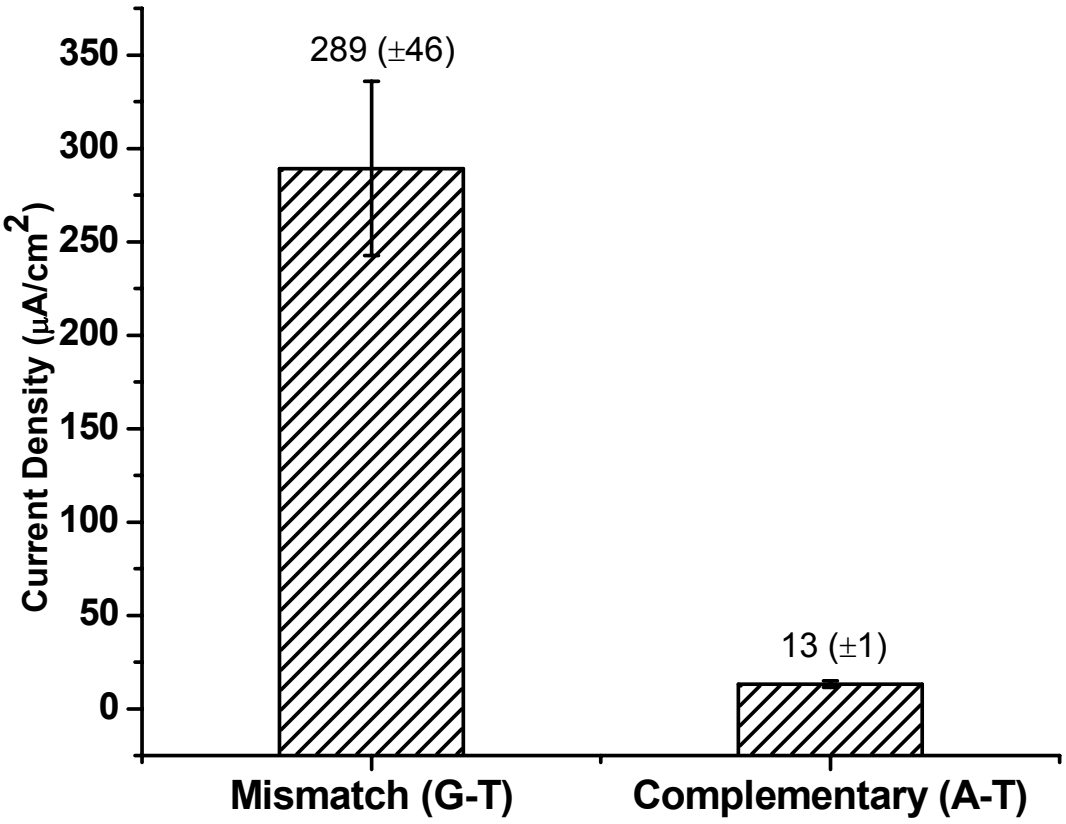

Figure 3.6 Comparison Bar graphs for the mismatched and complementary DNA electrodes.

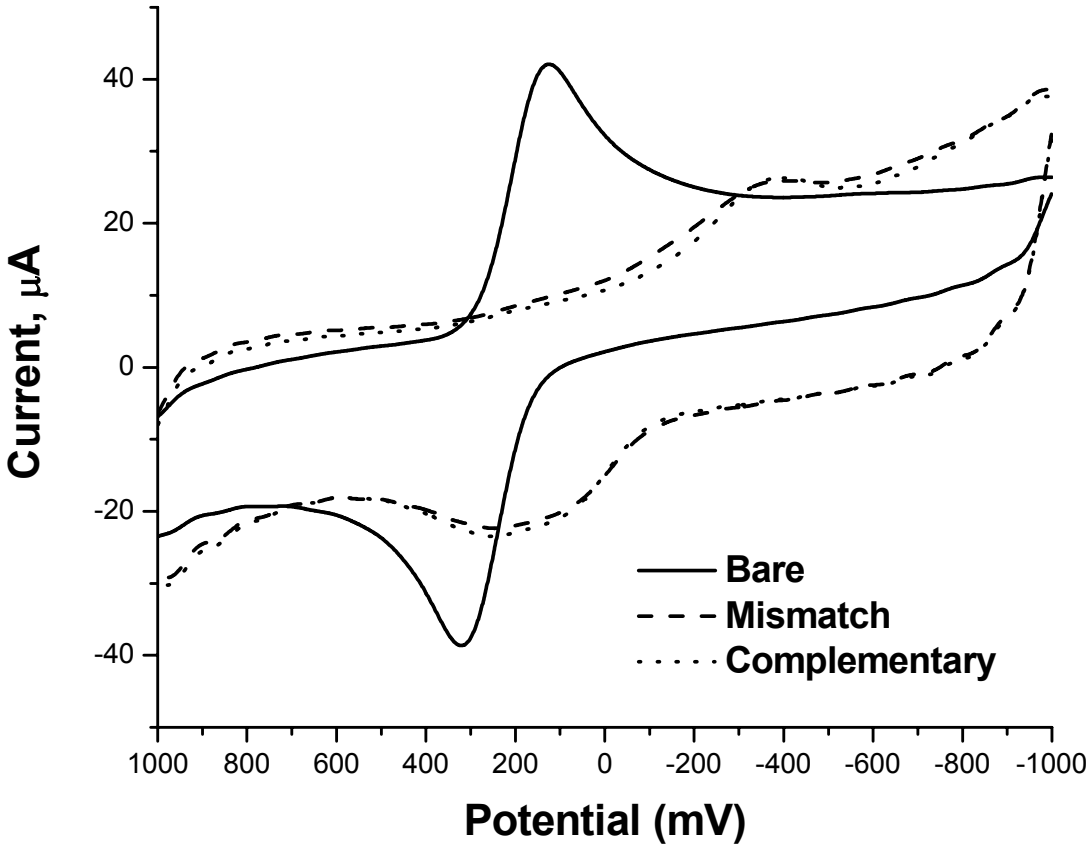

Figure 3.7 Overlaid cyclic voltamograms (vs Ag/AgCl) in 2μM MB-2mM $Fe(CN)_6^{3-}$ in pH 7.4 phosphate buffer for bare, and streptavidin modified electrodes incubated in mismatched and complementary DNA.

3.4 Conclusion

In this study, we developed a novel electrochemical biosensor for detecting DNA single-base mismatches through a catalytic reduction of potassium ferricyanide in the presence of electroactive methylene blue. We used a fusion MutS protein as the recognition element. In the cyclic voltammetric experiment, discussed in section 3.4, we observed a catalytic reduction peak for the electrode with mismatched DNA, whereas the electrode exposed to complementary DNA yields no visible catalytic peak. This result clearly shows that immobilized MutS is very much active on the electrode surface and readily interacts with mismatched DNA. This electrochemical method has a potential for applications in genetic diagnostics, and will enable us to detect gene mutations rapidly and with improved sensitivity. The method is very simple, fast, and potentially low-cost. Also, the method has a huge potential to be developed as a reusable miniaturized high-throughput device.

3.5 References

1. Liu, T. and J.K. Barton, DNA electrochemistry through the base pairs not the sugar-phosphate backbone. J Am Chem Soc, 2005. 127(29): p. 10160-1.
2. Lin, X.H., et al., Studies of the interaction between Aloe-emodin and DNA and preparation of DNA biosensor for detection of PML-RARalpha fusion gene in acute promyelocytic leukemia. Talanta, 2008. 74(4): p. 944-50.
3. Karaa, P.M., B,; Zeytinoglub, A; Ozsoz, M., Electrochemical DNA biosensor for the detection and discrimination of herpes simplex Type I and Type II viruses

from PCR amplified real samples. Analytica Chimica Acta, 2004. 518(1-2): p. 69-76.

4. Kelley, S.O., et al., Single-base mismatch detection based on charge transduction through DNA. Nucleic Acids Res, 1999. 27(24): p. 4830-7.

5. Blackwell, L.J.B., K.P.; Allen, D.J.; Modrich, P., Distinct MutS DNA-Binding Modes that are Differentially Modulated by ATP Binding and Hydrolysis. The Journal of Biological Chemistry, 2001. 276(36): p. 34339-34347.

6. Nag, N., B.J. Rao, and G. Krishnamoorthy, Altered dynamics of DNA bases adjacent to a mismatch: a cue for mismatch recognition by MutS. J Mol Biol, 2007. 374(1): p. 39-53.

7. Selmane, T., et al., Formation of a DNA mismatch repair complex mediated by ATP. J Mol Biol, 2003. 334(5): p. 949-65.

8. Joshi, A. and B.J. Rao, MutS recognition: multiple mismatches and sequence context effects. J Biosci, 2001. 26(5): p. 595-606.

9. Caswell, K.K.W., J.N.; Bunz, U.H.F.; Murphy, C.J., Preferential End-to-End Assembly of Gold Nanorods by Biotin-Streptavidin Connectors. Biochem J., 2005. 125(46): p. 13914-5.

10. Rosoff, M., Nano-surface Chemistry. CRC Press, 2002.

11. Anders, H.A., B; Olof, N.; Morten, L.; Joakim, L.; Mathias, U., The biotin-streptavidin interaction can be reversibly broken using water at elevated temperatures. lectrophoresis, 2005. 26(3): p. 501-10.

12. Ausdell, F.M., Brent, R., Kingston, R. E., Moore, D. D., Seitdman, J. G., Smith, J. G. and Struhl, K., Greene Publishing Associates and Willey/Inter science., 1994.

13. Geschwind, D.H., R. Rhee, and S.F. Nelson, A biotinylated MutS fusion protein and its use in a rapid mutation screening technique. Genet Anal, 1996. 13(4): p. 105-11.

14. Kase, Y. and H. Muguruma, Amperometric glucose biosensor based on mediated electron transfer between immobilized glucose oxidase and plasma-polymerized thin film of dimethylaminomethylferrocene on sputtered gold electrode. Anal Sci, 2004. 20(8): p. 1143-6.

15. Anzai, J.I.K.Y., Takeshita, H.;, Enzyme Multilayer-Modified Biosensors. Use of Streptavidin and Deglycosylated Avidin for Constructing Glucose Oxidase and Lactate Oxidase Multilayers. Analytical Sciences, 1997. 13(5): p. 859-861.

16. Sassolas, A., B.D. Leca-Bouvier, and L.J. Blum, DNA biosensors and microarrays. Chem Rev, 2008. 108(1): p. 109-39.

17. Seong, G.H., et al., Atomic force microscopy identification of transcription factor NFkappaB bound to streptavidin-pin-holding DNA probe. Anal Biochem, 2002. 309(2): p. 241-7.

PART II

SENSORS OR SENSING PLATFORMS FOR THE DETECTION OF GENERAL DNA DAMAGE

CHAPTER IV

DEVELOPMENT OF A NEW AFM METHOD TO DETECT DNA DAMAGE

4.1 Introduction

Environmental toxins, free radicals, radiation, and various chemical agents can cause major damage to DNA[1, 2]. The consequences of DNA damage are numerous and detrimental to the cell, and may lead to serious human diseases including cancer[3]. Among the types of damage that these agents inflict upon DNA are base lesions, sugar lesions, base modifications, single as well as double-strand breaks[4, 5]. DNA double-strand breaks are more harmful to the cell than any other type of DNA lesion. If not prevented or repaired promptly, DNA double-strand breaks will lead to mutagenesis and carcinogenesis[6].

4.1.1 Introduction to methods currently used in the detection of DNA damage

Various *methods* including gel electrophoresis, pulsed-field gel electrophoresis, neutral filter elution, and neutral sedimentation have been conducted to reveal the damaging effects of different chemical agents on DNA[7-12]. In addition, a couple of biochemical assays, comet assay and flare assay, are commercially available to assess DNA damage[13-15].

Though these biological techniques have proven merit, they give very little information regarding the location and nature of the damage. As a result, there is an increased demand for techniques that are capable of visualizing subtle alterations in the DNA molecule. Electron microscopy is one such technique that has been previously used in this field. Although electron microscopy produces very high-resolution images with a great deal of information, the technique is expensive. It is also complex as it needs chemical fixation and sample staining prior to imaging[16], as well as a large capital investment for the microscope.

AFM is a very useful tool in visualizing biological molecules at nanometer resolution[17, 18]. Use of AFM in DNA damage detection studies is expanding due to the ability of AFM to visualize biological molecules in their original form under native conditions. So far, the major obstacle for AFM in this field is that it cannot currently be used to clearly distinguish minor DNA damage such as single-base alterations that can eventually lead to double-strand breaks.

Some AFM-based methods exist that can detect UV-induced DNA damage, as this type of induced damage is easier to visualize. In most cases, exposure to UV radiation results

in DNA fragmentation, which can be directly distinguished from non-fragmented DNA using AFM. Krausch *et al* recently developed a method to screen for minor DNA damage by incorporating Human Replication Protein-A (HRP-A) to the damaged site[19] and imaging the DNA/HRP-A complex. Although this method was successfully able to discriminate damaged from undamaged DNA, the sensitivity of this method is compromised because the HRP-A binds even to undamaged DNA at a fairly high ratio.

In this chapter we propose a new AFM-based screening method to monitor minor DNA damage by labeling damaged sites with a biomarker. This site-specific biolabeling is achieved through well-established biotin-streptavidin chemistry. We use styrene oxide, a well-known DNA damaging agent[20], as a model agent to damage DNA. We also used sonication as another path to introduce DNA damage. Scheme 4.1 shows an illustration of the proposed DNA damage detection technique. We also investigate the possibility of combining the proposed site-specific biolabeled imaging method with electrochemical detection. The coupling of electrochemical detection and site-specific imaging is expected to produce both quantitative and qualitative information in a single experiment.

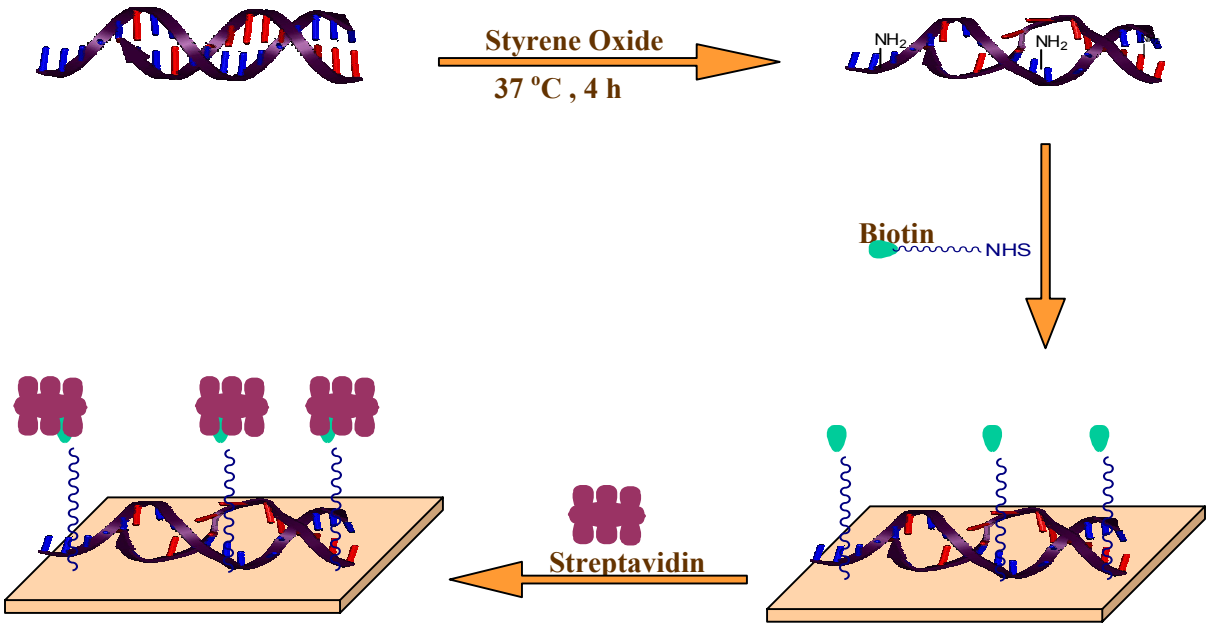

Scheme 4.1 Schematic illustration of the new detection method.

4.2 Experimental

4.2.1 Chemicals

Styrene oxide, Biotin-NHS, APTES, Streptavidin protein, and Calf thymus DNA were purchased from Sigma-Aldrich. De-ionized water (resistivity > 18 MΩ.cm) is provided by a Barnstead nanopure water system.

4.2.2 Apparatus

4.2.2.1 Ultrasound device

One-megahertz continuous ultrasound is applied for 20 minutes at an intensity of 1.5W/cm^2 by underwater technique. Sonication is provided by a commercially available transducer (Dynatron 850 Plus), with a 1.7-cm diameter treatment head and an effective radiating area of 0.75 cm^2. For ultrasound exposure, the cell culture flasks are immersed

in a water bath vertically and perpendicular to the axis of ultrasound beam emitted by the sonicator. The distance between sonicator's surface and samples subjected to ultrasound is kept constant for all experiments and is defined by the geometry of the water bath, which was used for all experiments.

4.2.2.2 UV-Vis spectroscopy

UV-Vis spectra are acquired on an 8453 Agilent Technologies spectrophotometer with a 1 cm pass-through quartz sample holder.

4.2.2.3 Atomic Force Microscopy imaging

AFM was performed with a pico-SPM® controlled by a MAC-mode® module and interfaced with a PicoScan® controller from Molecular Imaging, Tempe, Arizona (now Agilent Technologies). All of the AFM work was performed with a multi-purpose small scanner with a scan range 9 μm in x-y and 2 μm z height. Silicon Type II MACLevers® of 225 μm length, 2.8 N/m spring constant, and 60-90 kHz resonant frequencies (Molecular Imaging Corp.) were used in Acoustic AC mode in Air.

4.2.3 Culture of HEK-293 cells

HEK-293 Human Kidney cells are incubated in Dulbecco's Modified Eagle Medium (DMEM) supplemented with 2 mM L-glutamine, non-essential aminoacids, 5% penicillin/streptomycin and Earle's BSS adjusted to contain 1.5 g/L sodium bicarbonate. Cells are maintained at 37^{o}C in a humidified incubator containing 5% CO_2 in air.

4.2.4 Exposure of HEK-293 cells to ultrasound

HEK-293 cells are allowed to grow to confluence. Cell growth medium is then replaced with PBS buffer. Cell attachment to the dish is monitored before sonication. The bottom of the dish containing attached cells is then immersed in the water bath at room temperature with the sonicator head positioned as described above in "Apparatus." After exposure to ultrasound for 20 minutes, the cell container is removed and attached cells are collected and lysed for DNA extraction following standard protocols for DNA extraction, which include centrifugation followed by lysis of the cells with extraction buffer, proteinase K digestion of the lysate, and finally phenol:chloroform-isoamyl alcohol extraction.

4.2.5 Sample preparation for Atomic Force Microscopy (AFM) imaging to assess DNA damage.

Chemical DNA damage yields double helix openings and breaks in DNA strands. This process exposes the aromatic amines of DNA bases, which can be derivatized with biotin labels using biotin-NHS chemistry (see Results and Discussion section 4.3). The derivatization procedure is as follows: The DNA sample, either from the sonication flask or extracted from live cells which have been subjected to ultrasounds, is diluted to 10 μg/mL with pH 7.4 TE buffer. A 250 μL portion of this DNA solution is first reacted with 50 μL of biotin-NHS ester (0.2 mg/mL) in pH 7.4 TE buffer for 45 minutes. The resulting biotin-labeled DNA is filtered using a 10,000 MW cutoff filter to remove unreacted free biotin, followed by three sequential washings with buffer. The final DNA sample is diluted with TE buffer to a final concentration of 1μg/mL. A 50 μL drop of this final

solution is then carefully cast on a freshly cleaved HOPG and allowed to adsorb on the surface in an airtight, humidified, chamber for 15 minutes. The modified HOPG surface is then washed with buffer solution and incubated with 50 μL (10 μg/mL) streptavidin in pH 7.4 TE buffer for 10 minutes. The HOPG surface is thoroughly washed with the buffer to remove non-specifically bound streptavidin, and finally dried under a stream of nitrogen before AFM imaging. The same procedure is followed with intact DNA sample as controls. The extent of DNA damage is reflected by the number streptavidin features detected per unit of surface area.

4.3 Results & discussion

4.3.1 Application of the new method in detecting DNA chemical damage using styrene oxide as a damaging agent

Our new DNA damage detection method is tested using DNA that has been chemically treated with styrene oxide, which reacts with DNA bases to yield an adduct that results in double helix openings and breaks in the DNA strand. This process exposes the aromatic amines of DNA bases, which can be derivatized with biotin labels using biotin-NHS. These small biotin molecules, attached to damaged sites in the DNA, are then coupled to larger streptavidin molecules, which can be detected and visualized on the surface using AFM imaging. Similar concepts of detection of DNA damage using chemical derivatization, but coupled to other analytical methods such as HPLC, gas chromatography, and mass spectrometry are well known[21-23]. Here the derivatization and coupling with the larger streptavidin molecules allows for direct topographic imaging instead of relying on indirect detection associated with these other analytical techniques.

As a result, we can achieve direct assessment of chemical damage in DNA samples through the surface density of attached proteins.

Figure 4.1 illustrates 2D and 3D images of damaged and undamaged DNA after the biotin-streptavidin treatment, as discussed in the procedure. A high density of streptavidin features, which is a measure of damaged sites in DNA, can clearly be seen in the damaged DNA sample. In contrast, the surface immobilized with undamaged DNA has very few visible streptavidin features. This clearly indicates that the undamaged DNA bases are non-reactive with biotin-NHS molecules. In order to verify that the white spots found in the damaged-DNA AFM images are actually immobilized streptavidin, a cross-sectional analysis of the two images is performed. The average height of these white spots is about 5 nm, which is in agreement with the crystallographic height of streptavidin[24]. The topographical difference between the two images in the figure 4.1 is a clear indication of the validity and sensitivity of the new method in detecting DNA chemical damage.

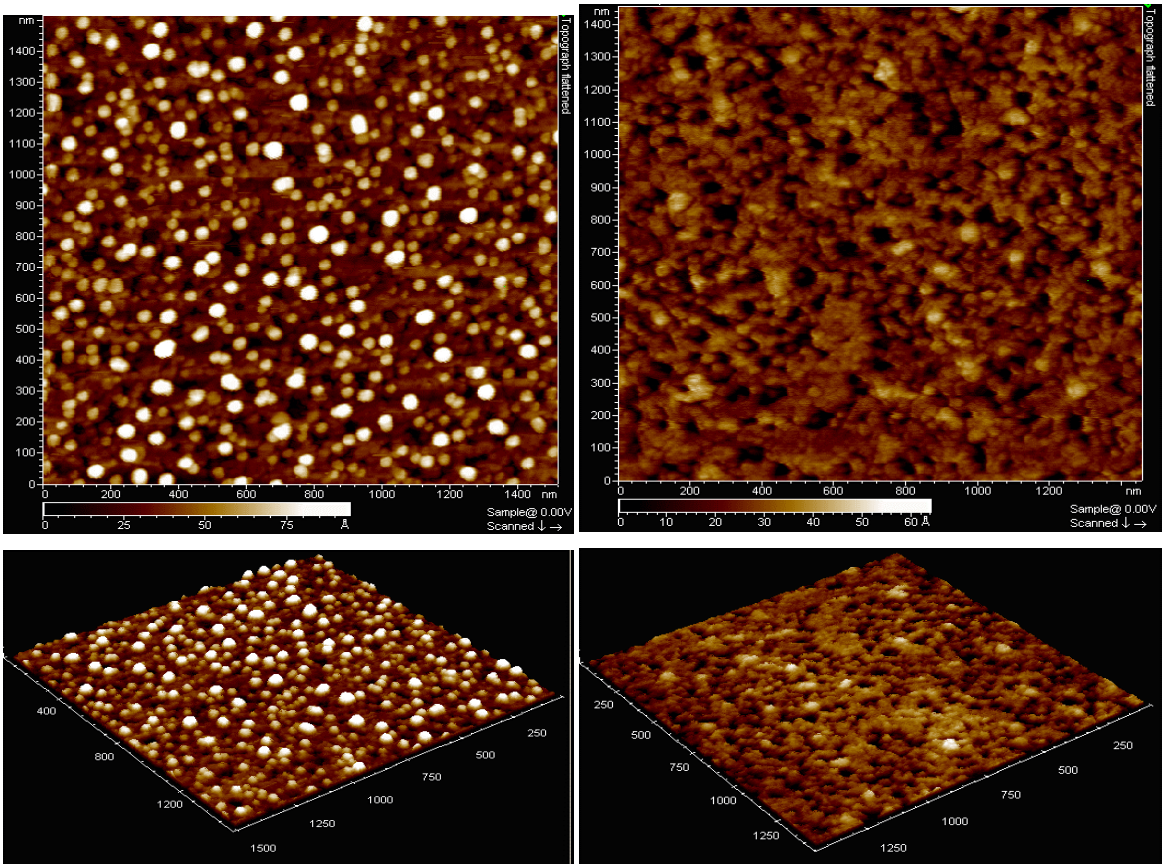

Figure 4.1 Tapping mode AFM images in Air for (a) Styrene Oxide damaged DNA after biotin-streptavidin treatment, and (b) Normal undamaged DNA after biotin-streptavidin treatment.

4.3.2 Application of the new method in ultrasound-induced DNA damage.

In vitro damage of DNA with styrene oxide yields a relatively high number of damage sites as a direct result of the absence of an active repair mechanism, as in living cells. Our previous study shows that our proposed method has the necessary sensitivity to detect

this *in vitro* DNA damage. We asked if our method can be expanded to DNA damage within live cells subjected to various levels of oxidative stress.

In order to test the applicability of this method in a real world situation, where the damage is minor and when the detection is challenging, we tested the method on DNA extracted from cultured HEK293 cells, which were previously subjected to controlled levels of ultrasounds. It has been reported that sonication creates hydroxyl radicals, which can react with DNA bases causing double-strand breaks[25].

The extracted DNA from ultrasound-treated cells and non-treated cells were incubated with biotin-NHS ester for a possible derivatization of damaged sites with biotin. These treated DNA were then immobilized on HOPG followed by linkage to larger streptavidin molecules in order to visualize the damage using AFM. Figure 4.2 shows two-dimensional AFM images of the ultrasound-treated and untreated DNA after streptavidin coupling. Two images, for treated and for untreated cells, show a distinguishable topographical difference, a clear indication that the proposed method is capable of detecting differential damage with high sensitivity. We were also able to obtain high-resolution 2-D and 3-D zoom images to confirm the size of streptavidin proteins actually immobilized on the DNA strand, but not on the surface (see Figure 4.3).

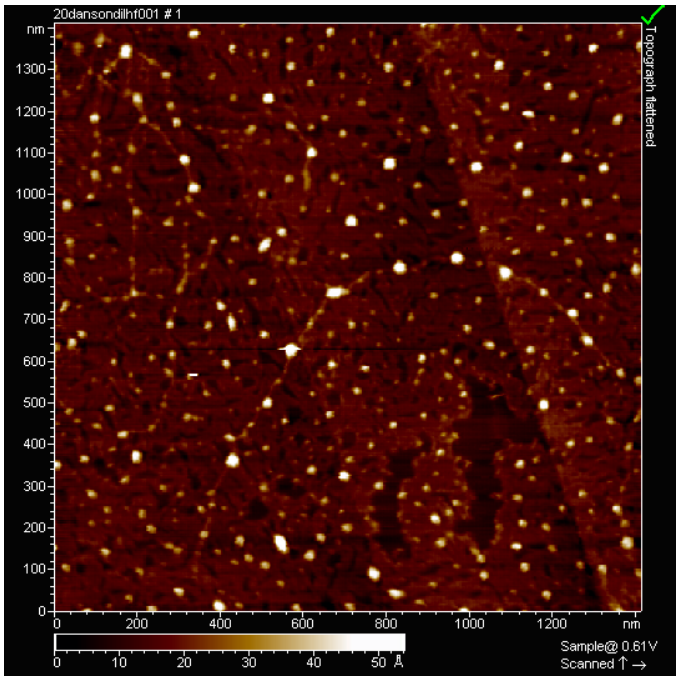

(a)

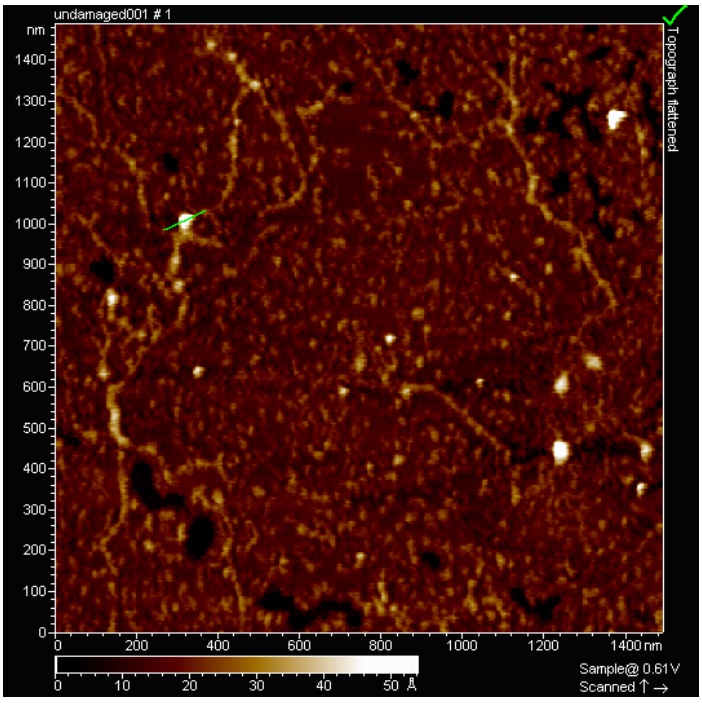

(b)

Figure 4.2 Tapping mode AFM images in Air for (a) Ultrasonically damaged DNA (for 20min) after biotin-streptavidin treatment, and (b) Normal undamaged DNA after biotin-streptavidin treatment.

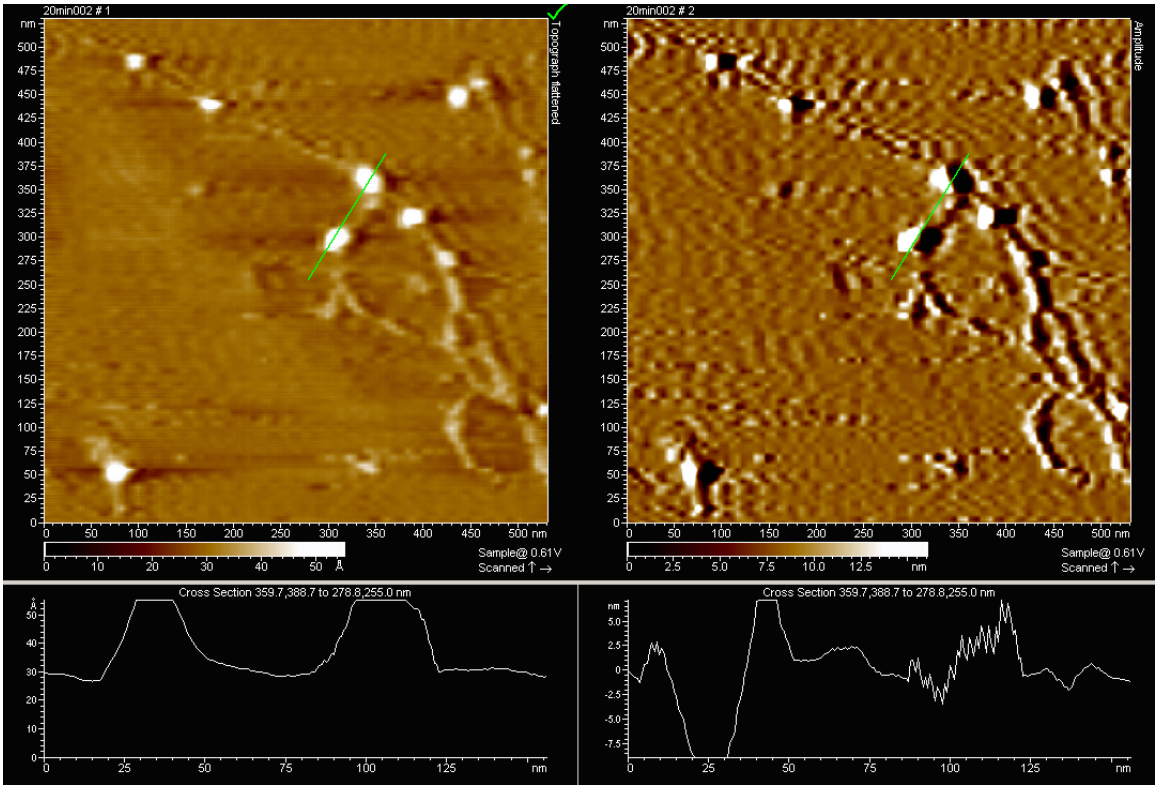

(a)

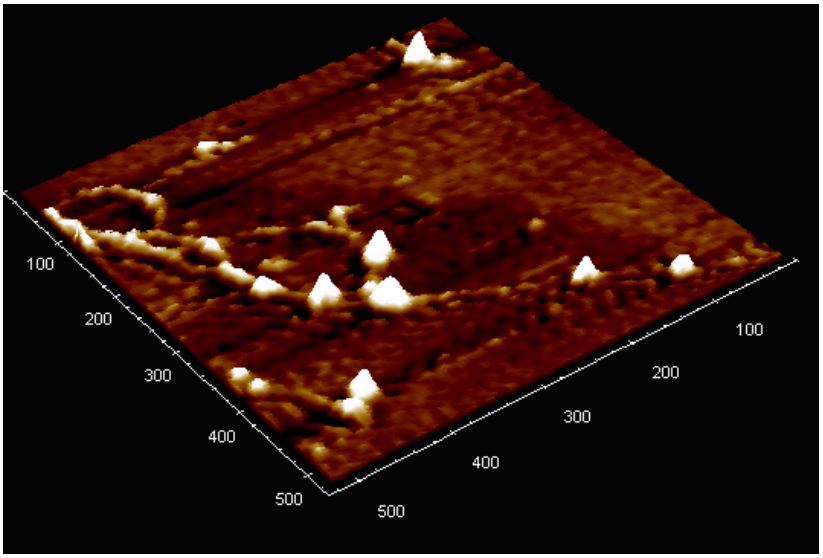

(b)

Figure 4.3 High-resolution zoom (a) 2-D and (b) 3-D AFM images for Ultrasonically damaged DNA after biotin-streptavidin treatment

To further confirm the validity of the method, we characterize intact and ultrasound-treated DNA samples using absorption spectroscopy after incubation in NHS-biotin. DNA samples subjected to ultrasound and control (intact) were treated with NHS-biotin as described in the experimental section. The samples are then washed multiple times with buffer on size-exclusion membranes allowing the elimination of nonattached small molecules (i.e. excess biotin not covalently bound to the target DNA molecules). Retained DNA samples from the size-exclusion filtration are then analyzed using UV-visible spectrophotometry. This analysis of ultrasound-treated DNA shows DNA absorbance at 260 nm, in addition to another band at around 200 nm that corresponds to covalently bound biotin labels. The control DNA sample not subjected to ultrasound, but similarly incubated with NHS-biotin, does not show the characteristic biotin band. Figure 4.4 shows wavelength scans for undamaged and ultrasonically damaged DNA after biotin-NHS treatment.

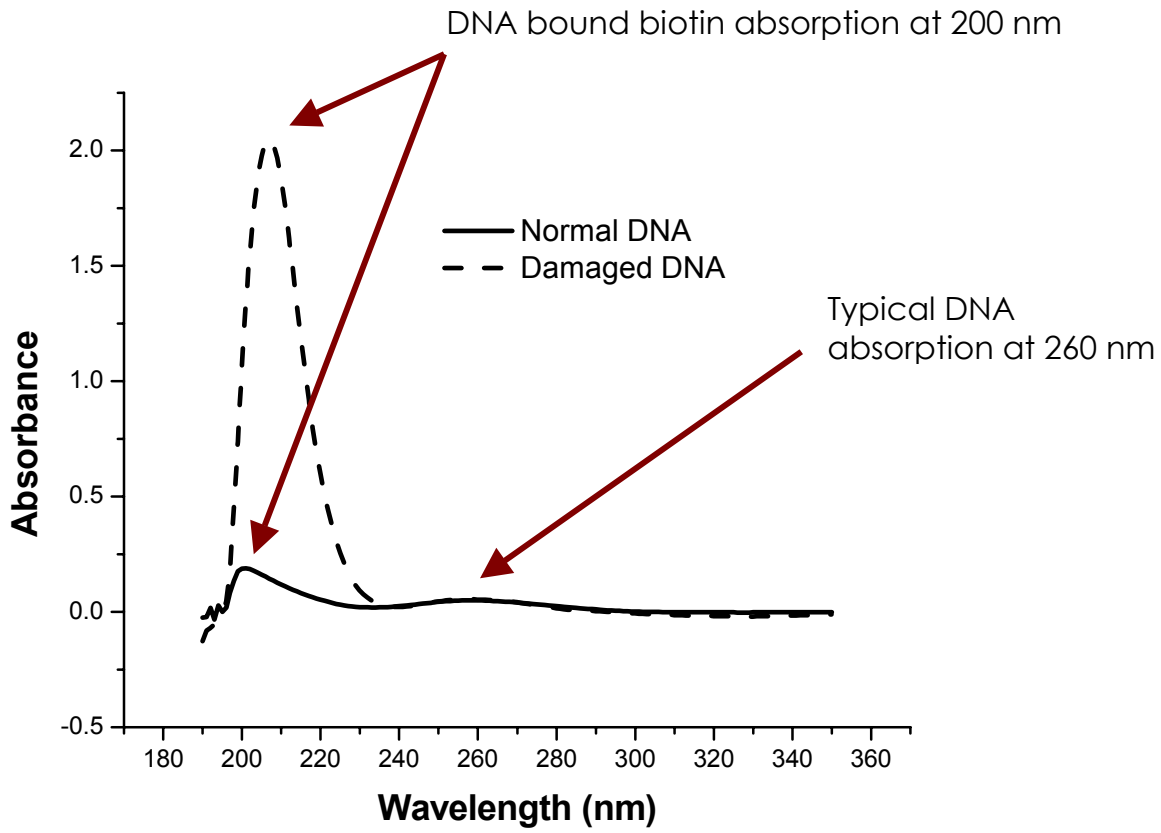

Figure 4.4 Wavelength scans for biotin-NHS treated undamaged DNA and ultrasonically damaged DNA.

4.3.3 Quantitative analysis of the damage using combined ECHEM/AFM technique.

Most of the current AFM-based detection methods produce only qualitative information. Our proposed method can be used to quantitatively evaluate the amount of DNA damage by counting observable streptavidin sites per unit area on the topographic image. In order to avoid erroneous quantification due to natural fluctuations of streptavidin density across the whole surface, we can easily take the average streptavidin density of three or more topographic images taken from random locations on the sample surface.

This additional work will have a slight negative effect on the total detection time of the assay. Another way to improve the detection time and to obtain more precise quantification, is to couple the AFM method to an electrochemical detector (ECHM), which will yield more accurate information. This combined technique will enable us to visually assess and electrochemically quantify DNA damage by performing AFM and ECHM in parallel.

Figure 4.5 shows combined AFM topographic images and their corresponding electrochemical signals obtained from sonicated DNA and normal DNA extracted from HEK 293 cells. $Ru(bpy)^{2+}$ complex was used in this experiment as an electrochemical probe. This ruthenium bipyridyl complex is known to catalyze electrochemical oxidation of DNA guanine bases[26]. In the first AFM image we clearly see that the number of streptavidin attachments in the undamaged DNA immobilized surface is negligible and the corresponding voltammogram gives a significant electro-catalytic signal for the ruthenium-mediated DNA oxidation.

In the second image we observe that the streptavidin density drastically increases upon exposure to ultrasound sonication. The electrochemical response for the damaged DNA-immobilized surface is significantly less due to attached streptavidin blocking ruthenium

probes from reaching DNA. The decrease in the electrochemical signal appears inversely proportional to the density of the streptavidin. While this is still in the development stage, the combined ECHEM/AFM method shows a potential to be developed into a good platform allowing topographic recognition as well as electrochemical quantification.

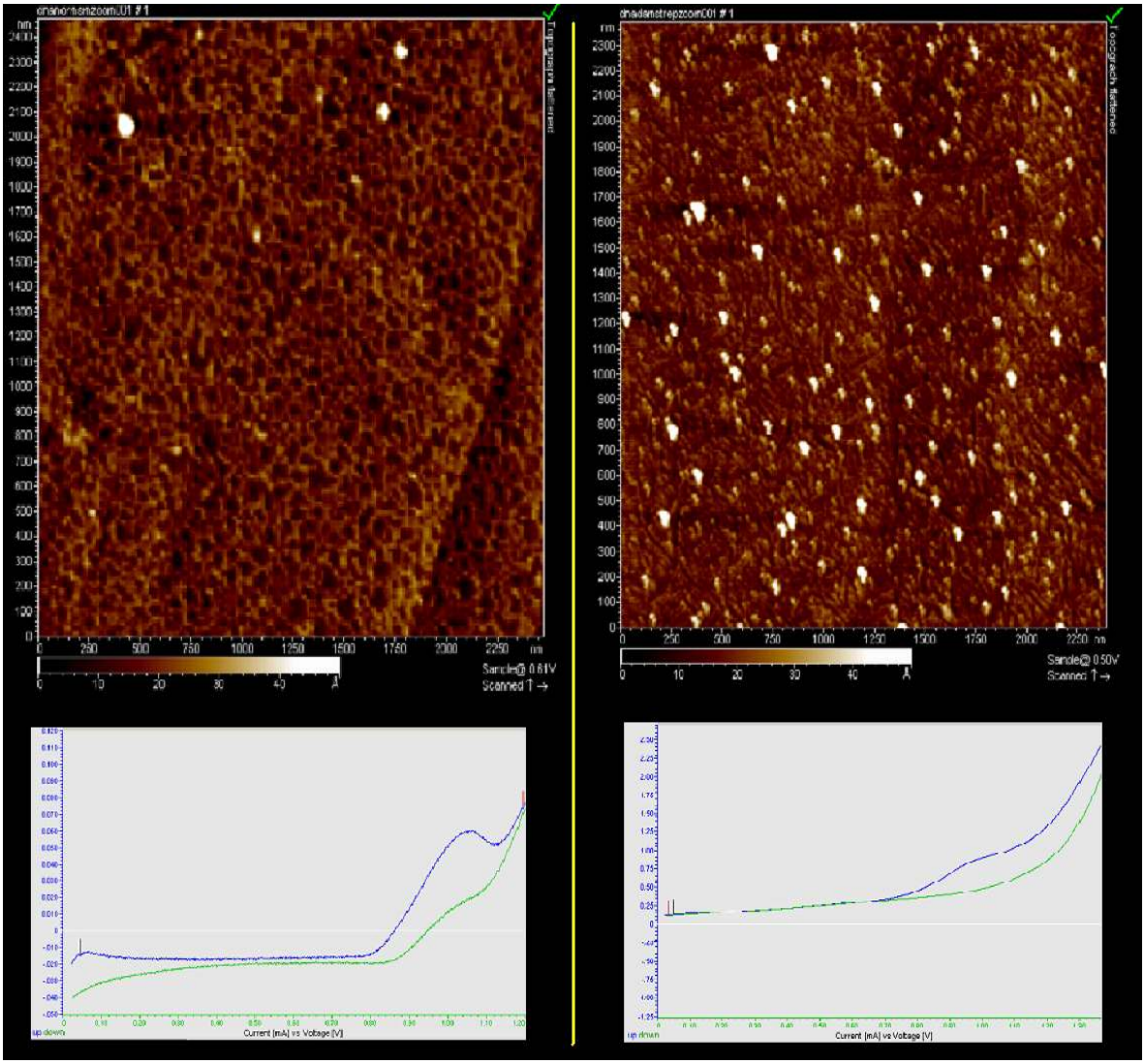

(a) **(b)**

Figure 4.5 Combined AFM/ECHEM images for (a) Normal undamaged DNA after biotin-streptavidin treatment, and (b) Ultrasonically damaged DNA after biotin-streptavidin treatment

4.4 Conclusion

The results described in sections 4.3.1 and 4.3.2 indicates that AFM imaging can be successfully used to detect and characterize DNA damage as a result of exposure to reactive chemicals and potential carcinogens. In the combined ECHEM/AFM method, the imaging provides the visual characterization with potential extension to high-resolution imaging to precisely characterize local damage on DNA strands and identify target spots of the damaging agent. The electrochemical component provides a highly sensitive quantification of the resulting DNA damage, and can be developed into a standard method of analysis to compare the relative damaging ability of chemical agents and/or DNA vulnerability.

4.5 References

1. Pogozelski, W.K. and T.D. Tullius, Oxidative Strand Scission of Nucleic Acids: Routes Initiated by Hydrogen Abstraction from the Sugar Moiety. Chem Rev, 1998. 98(3): p. 1089-1108.
2. Cardozo-Pelaez, F., et al., DNA damage, repair, and antioxidant systems in brain regions: a correlative study. Free Radic Biol Med, 2000. 28(5): p. 779-85.
3. Kastan, M.B. and J. Bartek, Cell-cycle checkpoints and cancer. Nature, 2004. 432(7015): p. 316-23.
4. Dizdaroglu, M., Free-radical-induced formation of an 8,5'-cyclo-2'-deoxyguanosine moiety in deoxyribonucleic acid. Biochem J, 1986. 238(1): p. 247-54.

5. Dizdaroglu, M., et al., Formation of cytosine glycol and 5,6-dihydroxycytosine in deoxyribonucleic acid on treatment with osmium tetroxide. Biochem J, 1986. 235(2): p. 531-6.

6. Dizdaroglu, M., Chemical Determination of Oxidative Damage to DNA. Handbook of Free Radicals and Antioxidants in Biomedicine, 1989. 3: p. 153-166.

7. Stamato, T.D.D., N., Asymmetric field inversion gel electrophoresis: a new method for detecting DNA double-strand breaks in mammalian cells. Radiat Res., 1990. 121(2): p. 196-205.

8. Murakami, M., K. Eguchi-Kasai, and K. Sato, Biological effects of active oxygen on an X-ray-sensitive mutant mouse cell line (SL3-147). Mutat Res, 1995. 336(3): p. 215-21.

9. Murakami, M., et al., Differences in heavy-ion-induced DNA double-strand breaks in a mouse DNA repair-deficient mutant cell line (SL3-147) before and after chromatin proteolysis. J Radiat Res (Tokyo), 1995. 36(4): p. 258-64.

10. Bradley, M.O. and K.W. Kohn, X-ray induced DNA double strand break production and repair in mammalian cells as measured by neutral filter elution. Nucleic Acids Res, 1979. 7(3): p. 793-804.

11. Frankenberg, D., et al., Effectiveness of 1.5 keV aluminium K and 0.3 keV carbon K characteristic X-rays at inducing DNA double-strand breaks in yeast cells. Int J Radiat Biol Relat Stud Phys Chem Med, 1986. 50(4): p. 727-41.

12. Herskind, C., Single-strand breaks can lead to complex configurations of plasmid DNA in vitro. Int J Radiat Biol Relat Stud Phys Chem Med, 1987. 52(4): p. 565-75.

13. Thomas, S.G., M.H.L.; Lowe, J.E.; Green, I.C., Measurement of DNA Damage Using the Comet Assay. Methods in Molecular Biology, 1997. 100: p. 301-310.

14. Olive, P.L., The comet assay: a method to measure DNA damage in individual cells. Nature Protocols, 2006.

15. Sanders, L., Pro-oxidant environment of the colon compared to the small intestine may contribute to greater cancer susceptibility . Cancer Letters, 2003. 208(2): p. 155 - 161.

16. Migheli, A., Electron Microscopic Detection of DNA Damage Labeled by TUNEL. Methods In Molecular Biology, 2002. 203: p. 31-39.

17. Hansma, H.G., et al., Atomic force microscopy of single- and double-stranded DNA. Nucleic Acids Res, 1992. 20(14): p. 3585-90.

18. Hansma, H.G., et al., Atomic force microscopy of DNA in aqueous solutions. Nucleic Acids Res, 1993. 21(3): p. 505-12.

19. Lysetska, M., et al., UV light-damaged DNA and its interaction with human replication protein A: an atomic force microscopy study. Nucleic Acids Res, 2002. 30(12): p. 2686-91.

20. Mbindyo, J., et al., Detection of chemically induced DNA damage by derivative square wave voltammetry. Anal Chem, 2000. 72(9): p. 2059-65.

21. Collins, A.R., Assays for oxidative stress and antioxidant status: applications to research into the biological effectiveness of polyphenols. Am J Clin Nutr, 2005. 81: p. 261S-267S.

22. Guetens, G.D.B., G.; Highley, M.; van Oosterom, A. T.; de Bruijn, E. A., Oxidative DNA damage: biological significance and methods of analysis. Crit Rev Clin Lab Sci, 2002. 39: p. 331-457.

23. Jenner, A.E., T. G.; Aruoma, O. I.; Halliwell, B., Measurement of oxidative DNA damage by gas chromatography-mass spectrometry: ethanethiol prevents artifactual generation of oxidized DNA bases. Biochem J, 1998. 331: p. 365-369.

24. Mascini, M., I. Palchetti, and G. Marrazza, DNA electrochemical biosensors. Fresenius J Anal Chem, 2001. 369(1): p. 15-22.

25. Milowska, K. and T. Gabryelak, Reactive oxygen species and DNA damage after ultrasound exposure. Biomol Eng, 2007. 24(2): p. 263-7.

26. Ontko, A.C., et al., Electrochemical Detection of Single-Stranded DNA Using Polymer-Modified Electrodes. Inorg Chem, 1999. 38(8): p. 1842-1846.

CHAPTER V

A NEW LAYER-BY-LAYER APPROACH FOR BIOMOLECULAR IMMOBILIZATION: APPLICATIONS IN DNA CHEMICAL DAMAGE DETECTION

5.1 Introduction

Immobilization of biomolecules has become an important aspect in biosensor development. Most of the currently available electrochemical and AFM-based biosensors, including the one we developed in the previous chapter, use weak hydrophobic interactions to immobilize recognition molecules on the sensor surface[1-3]. As a result, these recognition molecules are more susceptible to detach from the surface, reducing the overall sensitivity of the sensor. Leaching of these recognition molecules not only degrades the sensor's performance, but also can contaminate the test sample. In addition, some AFM probes are coated with hydrophobic materials that have a higher tendency to pick up these detached molecules during scanning. These contaminated tips are hard to clean and may become inoperable, adding more cost and time to the assay.

Employing a covalent modification method to immobilize the recognition molecules through linkers could rectify this problem, but it would also have a negative impact on the overall detection time, as most of the covalent methods are generally time consuming. In addition, the sensitivity of these covalent modifications can sometimes be limited as a direct result of chemical reactions between the biomolecules and the linker molecules[4, 5]. This can lead to a change in the structure of the immobilized biomolecule, eventually leading to conformational changes and subsequent alterations of activity.

A different method of immobilization needs to be found that will allow for better attachment of biomolecules without the unwanted side-reactions and other difficulties associated with the current methodologies. Other groups have used a "layer-by-layer" approach to sensor development that circumvents these problems by providing stronger attachments with fewer side-reactions, preserving the activity of the immobilized biomolecule[4-8].

The success of any layer-by-layer method is entirely dependent on the amount of charge or charge density the surface gains after modification (*vide supra)*. Higher charge density on the modified surface is a desired feature in this methodology, in that it results in tighter attachment of biomolecules to the surface. For this reason, it is important to use molecules or ions that have a high charge density. A major drawback associated with most of the current layer-by-layer immobilization methods are that they incorporate biomolecules with low charge densities[9-11], which results in poor surface attachment. In our study, we propose a novel layer-by-layer method to immobilize biomolecules with high charge densities, which will improve surface adhesion and overall retention.

Our proposed method uses electrochemical reduction of 4-diazonium salicylate to pre-activate the surface and Fe^{3+} ions to immobilize DNA or other biomolecular analytes for damage-detection analysis. Diazonium-based procedures offer the advantage of simplicity, efficiency and speed of the chemistry involved. A major advantage of using salicylic acid in this method is that it forms a very strong complex with Fe^{3+} ions[12]. The high active charge on Fe^{3+} facilitates the strongly bound immobilization of more biorecognition molecules on the surface, which is the key advantage of this method.

The method is first tested by immobilizing calf thymus DNA as a model negatively-charged biomolecule, which is then characterized by AFM and electrochemical methods. Our new method is also tested for its applicability in DNA damage detection using chemically damaged (styrene oxide) DNA. Scheme 5.1 shows an illustration of the proposed layer-by-layer method for biomolecular immoblization.

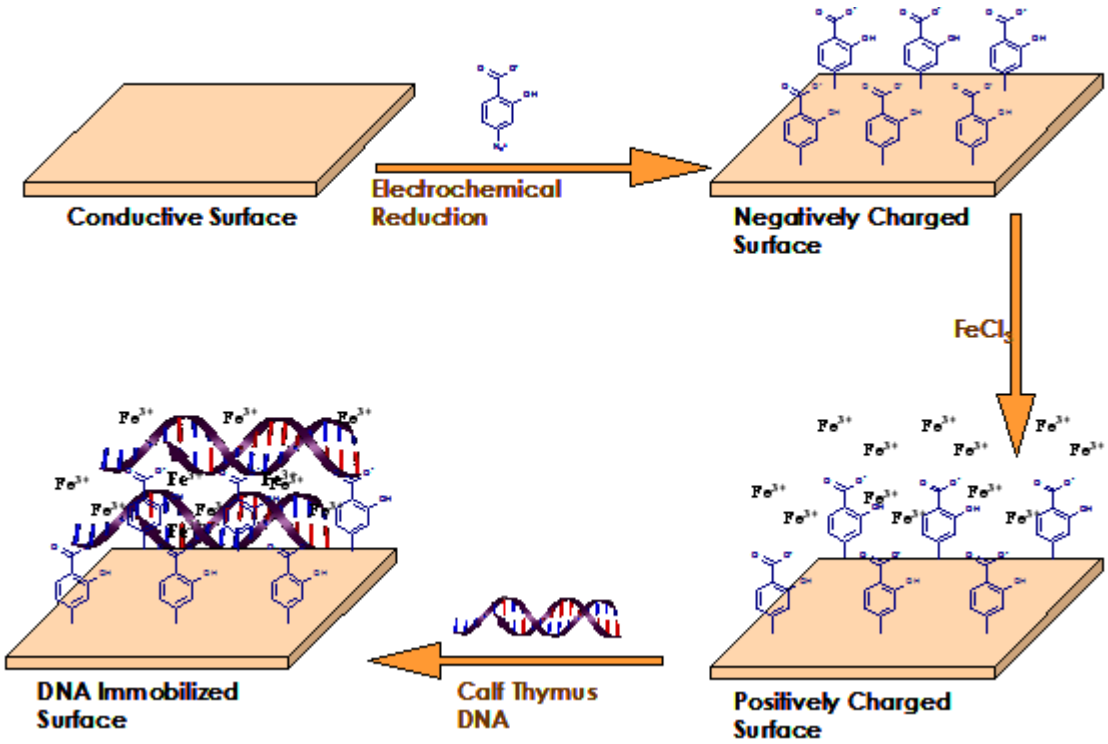

Scheme 5.1 Schematic illustration of the new layer-by-layer method.

5.2 Experimental

5.2.1 Chemicals

Styrene oxide and Calf thymus DNA were purchased from Sigma-Aldrich. De-ionized water (resistivity > 18 MΩ.cm) was provided by a Barnstead nanopure water system.

5.2.2 Electrochemical measurements

A BAS 100W (Bio-Analytical Systems) electrochemical workstation is used for all electrochemical experiments. All electrochemical measurements are carried out at room temperature in buffers that are purged for 10 min with nitrogen immediately before readings and blanketed with nitrogen throughout the experiment. Cyclic Voltammetry (CV) and Square Wave Voltametry (SWV) are performed in a three-neck electrochemical cell with Ag/AgCl reference electrode, platinum counter electrode, and 3.0 mm diameter glassy carbon working electrodes.

5.2.3 Atomic Force Microscopy

AFM is performed with a pico-SPM® controlled by a MAC-mode® module and interfaced with a PicoScan® controller from Molecular Imaging, Tempe, Arizona (now Agilent Technologies). All AFM work is performed with a multi-purpose small scanner with a scan range 9 μm in the x-y plane and 2 μm z height. Silicon Type II MAClevers® of 225 μm length, 2.8 N/m spring constant, and 60-90 kHz resonant frequencies (Molecular Imaging Corp.) were used in Acoustic AC mode in air.

5.2.4 DNA immobilization procedure for AFM and electrochemical characterizations

Cyclic voltammetry is used to create a layer of salicylic acid on freshly prepared HOPG or glassy carbon surface; this is done by cycling the applied potential two times between +0.6V and -0.8V at a scan rate of 0.1 V/sec in a 5 mM aqueous solution of 4-diazonium salicylate. After the second cycle, the observed current decays almost to the level of the background current, indicating the formation of a layer of salicylic acid on the surface, possibly a full monolayer. The electrochemical reduction process shows irreversible one-electron reduction of the diazonium group at around –0.2 V vs. Ag/ AgCl.

After electrochemical modification, the salicylic acid-modified surface is thoroughly washed with ultra-pure deionized water. The surface is then incubated in 5 mM $FeCl_3$ solution for 1 minute, thoroughly washed with deionized water, and then dried under a stream of dry nitrogen for 10 minutes. Finally, 50 μl of normal calf thymus DNA (0.1 mg/ml in pH 7.4 phosphate buffer) is cast on the positively charged surface and allowed to stand for 5 minutes before again being thoroughly washed with deionized water. The same procedure is repeated using damaged calf thymus DNA for the detection of DNA damage.

5.3 Results & discussion

5.3.1 Characterization of the DNA modified electrode

5.3.1.1 AFM characterization of HOPG surface modified with normal DNA

AFM characterization is performed to examine the effectiveness of immobilizing biomolecules using our new salicylic acid method. The results from this set of characterizations are shown by the AFM images in Figure 5.1, which shows the topographic images of (a) Bare HOPG, (b) Salicylate/Fe^{3+} modified HOPG, (c) and DNA immobilizaed HOPG.

The bare HOPG in figure 5.1a is extremely smooth, with a *z* height of only 0.3 nm, which permits the identification of any topographical changes that occur when the surface is modified with salicylate/Fe^{3+} or salicylate/Fe^{3+}/DNA. The salicylate/Fe^{3+} grafted surface (figure 5.1b) shows a relatively cratered topography with a peak height of 1 nm, which is very close to the theoretical height of immoblized salicylate, indicating the formation of a fine monolayer on the HOPG. The appearance and the z height for both bare HOPG and salicylate/Fe^{3+} modified HOPG are compatible with other published experiments[13-15]

The salicylate/Fe^{3+}-modified surface is then exposed to normal calf thymus DNA. AFM imaging (figure 5.1c) shows this fully modified surface has developed a “string-like” appearance, indicative of the presence of a fairly dense layer of the DNA. Further AFM imaging of the film after several washings indicates little or no change in film characteristics, adding credence to the robust adherence of DNA using this method. A control experiment was performed by incubating salicylic acid-modified HOPG in DNA, without exposing the surface to Fe^{3+}. AFM imaging shows no attachment. This is as

expected, as charge-charge repulsions between the negatively charged salicylate surface and negatively charged DNA will prevent the DNA from binding.

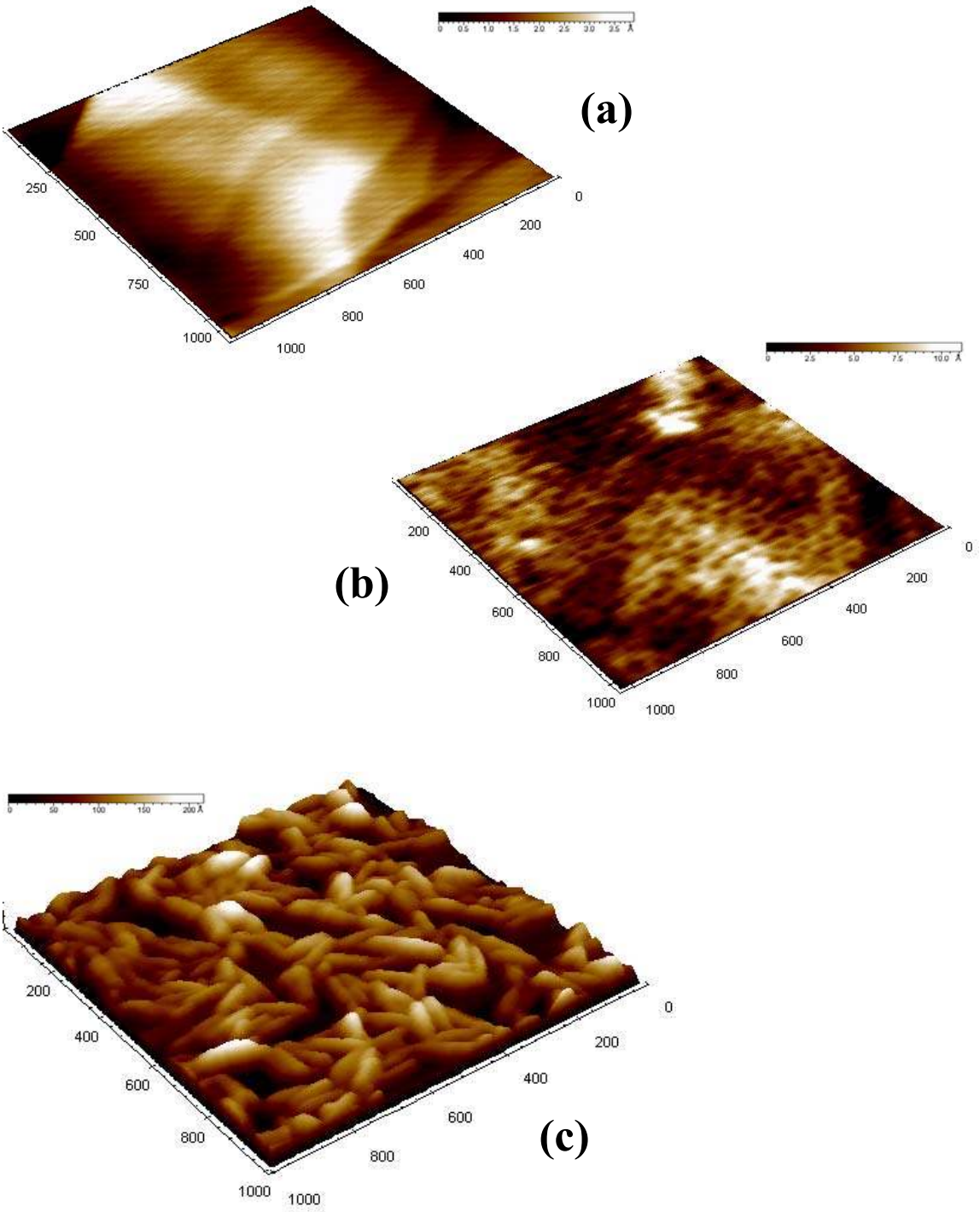

Figure 5.1 Tapping mode AFM images of (a) Bare HOPG, (b) HOPG modified with salicylic/Fe^{3+}. (c) Calf Thymus DNA immobilized HOPG.

5.3.1.2 Characterization of normal DNA immobilized electrodes using electro-active probes

A second set of characterizations was carried out using electrochemical techniques in the presence of two different electro-active probes. The results obtained for each probe are discussed in the following sections.

5.3.1.2.1 Characterization using ruthenium bipyridyl electro-active probe

Figure 5.2 shows the square wave voltammograms for the bare, salicylate/Fe^{3+} modified, and calf thymus DNA immobilized electrodes in 50 μM $Ru(bpy)_3^{2+}$ complex in pH 5.5 acetate buffer. The oxidation peak for ruthenium bipyridyl complex appears at about 1.05 V for the bare electrode. Derivatization of the electrode with salicylate/Fe^{3+} complex significantly reduces the oxidation peak, indicating repulsions between the positively charged electrode surface and the positively charged ruthenium probe. A huge oxidative response is seen after DNA immobilization on the salicylate/Fe^{3+} modified electrode. This increase in oxidative current is due to the guanine-mediated catalytic oxidation of ruthenium bipyridyl complex[14], providing solid evidence for the efficiency of the immobilization process.

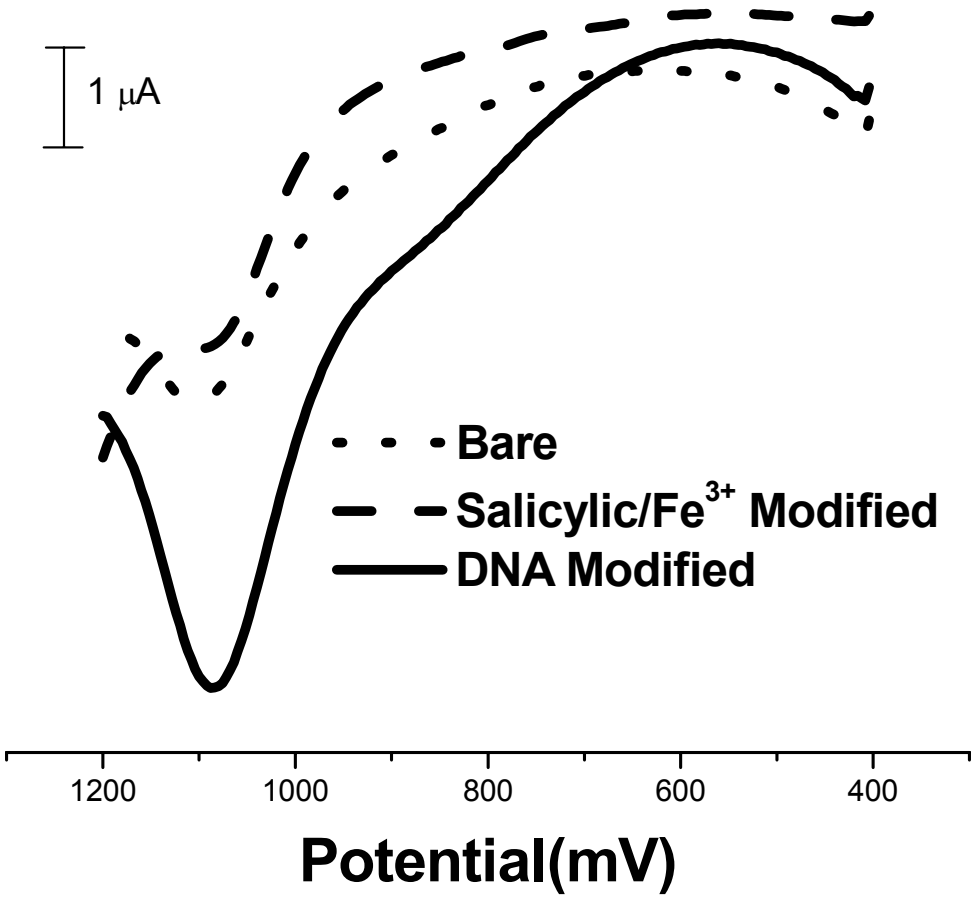

Figure 5.2 Square wave voltammograms for 50μM ruthenium complex in pH=5.5 acetate buffer.

5.3.1.2.2 Characterization using cobalt bipyridyl electro-active probe

We use another electrochemically active, positively charged metal ion complex, $Co(bpy)_3^{3+}$, to further characterize the DNA immobilized electrode. $Co(bpy)_3^{3+}$ binds to the negatively charged DNA backbone predominantly via electrostatic interactions at low ionic strength[16, 17]. Figure 5.3 shows overlaid square wave voltammograms for each modified electrode surface in 1mM $Co(bpy)_3^{3+}$ in pH 5.5 acetate buffer.

The reduction peak for $Co(bpy)_3^{3+}$ appears at about 0.1 V using bare electrode. As we observed in the $Ru(bpy)_3^{2+}$ system, derivatization of the electrode with salicylate/Fe^{3+} complex creates high positive charge density on the surface that electrostatically repulses $Co(bpy)_3^{3+}$, resulting in a significant reduction of the peak height, as shown in the overlaid voltammogram.

The reduction peak should increase significantly if DNA has been successfully immobilized on the surface, due to the electrostatic attraction between the positively charged $Co(bpy)_3^{3+}$ and the negatively charged DNA. The high peak current associated with the voltammogram for the DNA-immobilized electrode is consistent with this principle and further supports the successful immobilization of the DNA.

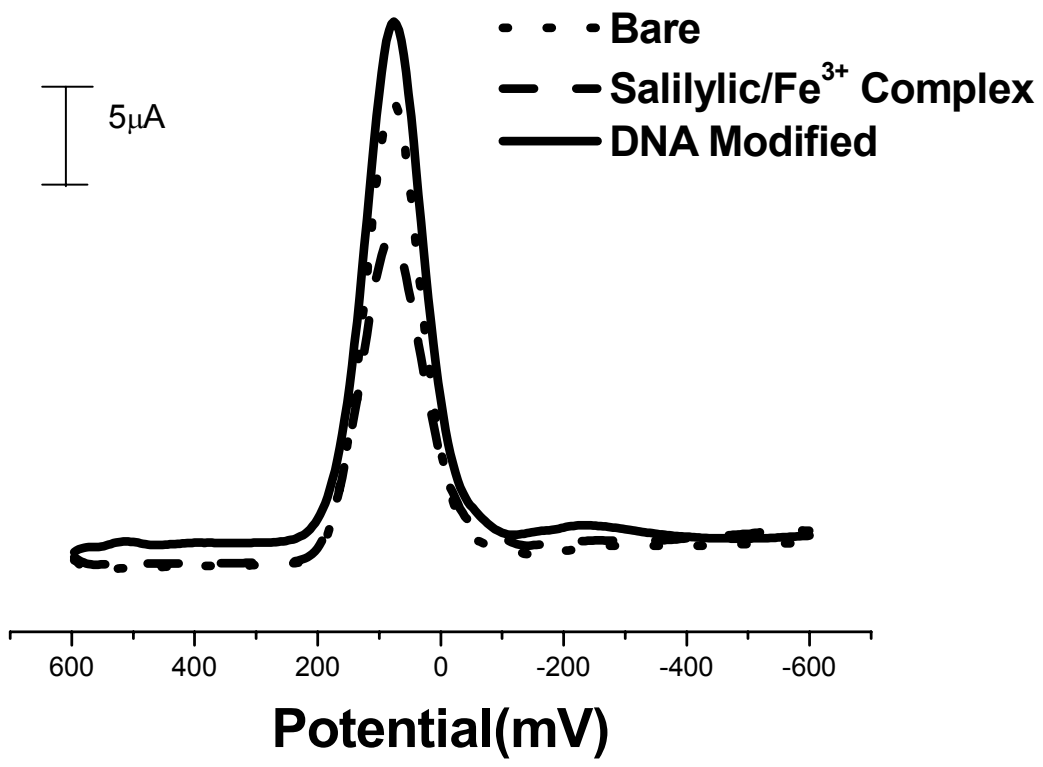

Figure 5.3 Square wave voltammograms for 1 mM cobalt complex in pH 5.5 acetate buffer.

5.3.2 Application of the new method in DNA chemical damage detection

We demonstrated earlier in section 5.3.1.2.1 that a ruthenium bipyridyl electro-active probe could be used to detect immobilized DNA via an increase in oxidative current. This current is observed during SWV mainly due to positive-negative charge interactions coupled with the guanine-mediated catalytic oxidation of ruthenium bipyridyl complex.

DNA damage is known to unwind the helices and expose DNA bases, including guanines, making them more accessible to the electro-active probe and providing additional oxidative catalysis. This leads to a significant increase in catalytic current, essentially amplifying the chemical damage, providing greater sensitivity. We take advantage of this difference in catalytic current to apply our new methodology to the detection of DNA damage.

Our new salicylic acid based layer-by-layer method was tested for its applicability in DNA chemical damage detection. Normal DNA and chemically damaged DNA using styrene oxide are immobilized on two identical glassy carbon electrodes. The two electrodes are then characterized using $Ru(bpy)_3^{3+}$ in pH 5.5 acetate buffer, as shown in the voltammogram for the DNA modified electrodes.

The overlaid square wave voltammograms (Figure 5.4) clearly shows a difference between the oxidation peaks of damaged DNA and normal DNA, indicating that our salicylate-based immobilization technique, in conjunction with the use of $Ru(bpy)_3^{3+}$ as an electro-active probe, is clearly capable of differentiating between normal and damaged DNA.

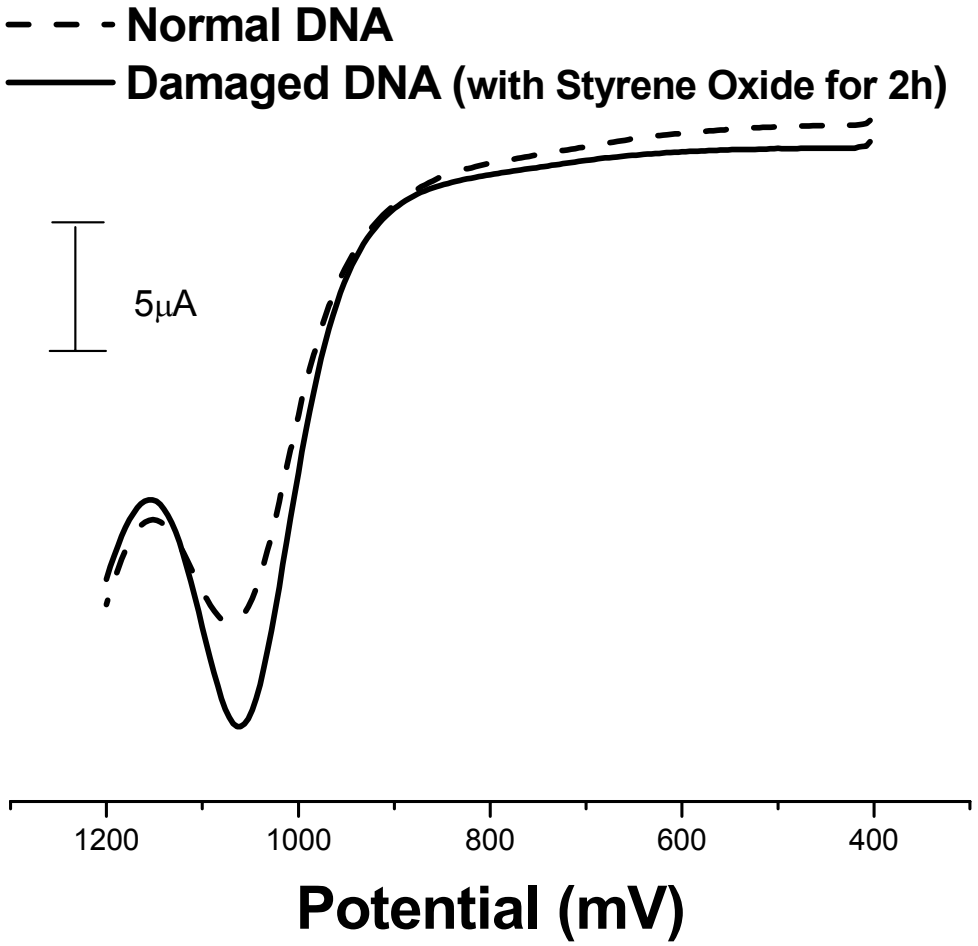

Figure 5.4 Square wave voltammograms for normal and damaged DNA in 50 μM ruthenium complex in pH 5.5 acetate buffer.

5.4 Conclusion

Our new layer-by-layer method brings the capability of creating a considerable high charge density on the surface, using molecular-size control of coverage. Both electrochemical and Atomic Force Microscopic results show promising discrimination between each modification step. Both of these tools show that creating a surface with higher charge density will lead to strong and efficient immobilization of DNA on the surface. Our new immobilization method, in conjunction with the use of $Ru(bpy)_3^{3+}$ as an electro-active probe, can discriminate between normal and damaged DNA, and can be further developed into a highly sensitive tool to study chemical DNA damage at the molecular level.

5.5 References

1. Zhang, Q. and V. Subramanian, DNA hybridization detection with organic thin film transistors: toward fast and disposable DNA microarray chips. Biosens Bioelectron, 2007. 22(12): p. 3182-7.
2. Zhang, L., et al., Direct electrochemistry and electrocatalysis based on film of horseradish peroxidase intercalated into layered titanate nano-sheets. Biosens Bioelectron, 2007. 23(1): p. 102-6.
3. Grigorenko, E.V., DNA Arrays. CRC Press, 2002.
4. Ahuja, T., et al., Biomolecular immobilization on conducting polymers for biosensing applications. Biomaterials, 2007. 28(5): p. 791-805.
5. Rusling, J.F., Biomolecular Films. CRC Press, 2003.

6. Benítez, M.J.J., J.S., A Method of Reversible Biomolecular Immobilization for the Surface Plasmon Resonance Quantitative Analysis of Interacting Biological Macromolecules. Analytical Biochemistry, 2002. 302(2): p. 161-168.

7. Cosnier, S., Biosensors based on immobilization of biomolecules by electrogenerated polymer films. New perspectives. Appl Biochem Biotechnol, 2000. 89(2-3): p. 127-38.

8. Crespilho, F.N.Z., V.; Oliveira, O.N.; Nart, F.C., Electrochemistry of Layer-by-Layer Films: a review. Int. J. Electrochem. Sci, 2006. 1: p. 194-214.

9. Ding, B., ; Kim, J.; Kimura, E.; Shiratori, S., Layer-by-layer structured films of tio2 nanoparticles and poly(acrylic acid) on electrospun nanofibers. Nanotechnology, 2004. 15: p. 913-917.

10. Pedano, M.L.M., L.; Desbrieres, J.; Defrancq, E.; Dumy, P.; Coche-Guerente, L.; Labbe, P.; Legrand, J.; Calemczuk, R.; Rivas, G. A., Analytical Letters, 2004. 37(11): p. 2235-2250.

11. Ivanova, E.P.P., D.K.; Brack, N.; Pigram, P.; Dcolau, D.V., Poly(-lysine)-mediated immobilisation of oligonucleotides on carboxy-rich polymer surfaces. Biosensors and Bioelectronics, 2004. 19(11): p. 1363-1370.

12. Shohei, I.A., H.; Jin, M., Electronic Structure of an Iron Complex of Salicylic Acid Derivative. Nippon Kagakkai Koen Yokoshu, 2004. 84: p. 122.

13. Brett, A.M.O.P., A.M.C., DNA imaged on a HOPG electrode surface by AFM with controlled potential. Bioelectrochemistry, 2005. 66(1-2): p. 117-124.

14. Ontko, A.C., Electrochemical Detection of Single-Stranded DNA Using Polymer-Modified Electrodes. Inorg Chem, 1999. 38(8): p. 1842-1846.

15. Tang, Z.L., S.; Dong, S.; Wang, E., Electrochemical synthesis of Ag nanoparticles on functional carbon surfaces. Journal of Electroanalytical Chemistry, 2001. 502(1-2): p. 146-151.

16. Yang, J., Zhang, Z., Rusling, J. F.,, Detection of Chemically-Induced Damage in Layered DNA Films with Co(bpy)3 by Square-Wave Voltammetry. Electroanalysis, 2002. 14: p. 1494-1500.

17. Carter, M., Voltammetric Studies of the Interaction of Metal Chelates with DNA. 2. Tris-Chelated Complexes of Cobalt (III) and Iron (II) with 1,10-Phenanthroline and 2,2'-Bipyridine. J. Am. Chem. Soc, 1989. 111: p. 8901-8911.

CHAPTER VI

CONCLUSIONS AND FUTURE DIRECTIONS

A review of the most current literature suggests that there is a fundamental gap between the current state-of-the-art in DNA mismatch and damage detection and the desired characteristics of low-cost, high-speed, simplicity, versatility, and potential for miniaturization.

We began this study focused on two main goals: The first goal being to advance the existing sensor technologies for mismatch and damage detection so that they meet market demand. The second goal is to narrow the aforementioned fundamental gap by developing new approaches that satisfy all desired characteristics. Our results clearly demonstrate the potential of our proposed new methods in developing low-cost, high-throughput miniaturized devices that have increased versatility as compared to current detection methods.

In the first approach we successfully advanced the current state-of-the-art, the thiol-gold sensor developed by the Barton group. Our proposed diazonium ion-based immobilization has many distinct advantages over other conventional methods including

speed, simplicity, reliability, and cost effectiveness. Also, this method has no surface restrictions and can be used with any conductive surface, increasing versatility, which is a big plus for new sensor development.

Though vastly improved, our method still has some limitations common with other methodologies that we would like to continue to improve upon. One such limitation is the requirement of using DNA sequences with amino labels at the 5` end, which can be a major obstacle in real world situations where a patient's gene is obviously not 5'-amino labeled. In the future, we will investigate the possibility of using unlabeled DNA with a 5'- sticky end. The sticky end can be easily created by removing the nucleotide base at the 3' end of the sequence using restriction enzymes. The removal of the 3' end base exposes free amino functionalities in the complementary 5' end base, which can then be used to immobilize the sequences.

Our second approach, immobilization of biotin-tagged MutS protein, is a versatile platform for fabrication of a miniaturized electrochemical device that can be effectively used in future cancer diagnostics. This method proved to be low-cost, fast, simple, and more importantly label free, as it doesn't require fluorescent labels or radioactive labels for detection. Moreover, the ability of MutS to recognize various types of base mismatches and deletions will enable this method to detect gene mutations rapidly and with improved sensitivity. MutS-DNA complexes exhibit a high degree of dissociation in high ionic-strength buffers; in the future, we can exploit this characteristic to make a reusable mismatch detection sensor. This will be investigated by exposing MutS-DNA complex to different ionic-strength buffers on the sensor surface and measuring the electrocatalytic signal for ferricyanide/MB solution. We will also explore the possibility

of using this new technology to engineer a low-cost, high-throughput micro-device coupled to an electrochemical detector for the screening of mutations. In making such a device, we could utilize similar technologies currently used in commercially available glucose sensors and protein array chips. Fabrication of this device can be initiated by making a MutS immobilized array chip and connecting each site of the chip to an electrochemical detector. A concept design for such a device is shown in scheme 6.1.

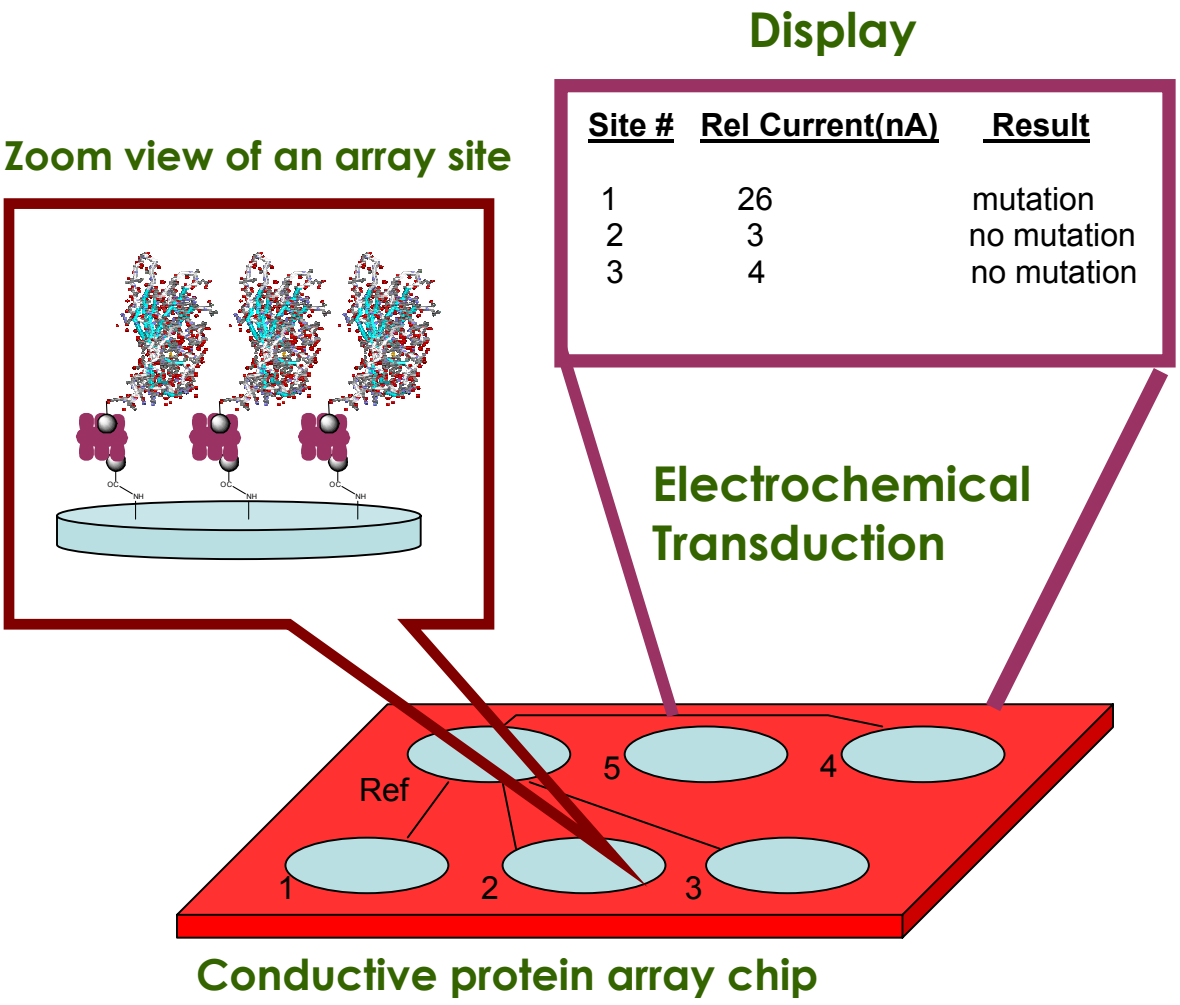

Scheme 6.1 A concept design of a MutS-based array chip device.

The AFM-based, site-specific biolabeling approach described in chapter 4 has shown to be a promising visualization method to monitor minor DNA damage. As indicated in our results, this method has very high sensitivity, with a proven ability to detect damage on individual molecules. In addition, the method can be easily adapted to acquire more information such as the location and type of damage.

Used by itself, AFM can only produce limited information in order to quantitatively evaluate DNA damage. Our combined AFM/ECHEM approach improves upon this limitation by demonstrating a high potential to obtain both qualitative and quantitative data in a single experiment. Further optimization and characterization of this combined method in the course of the current study was limited by time constraints, but the AFM/ECHEM approach is needed to optimize detection of damage in real world samples. In the future we will explore the possibility of attaching a redox-active molecule or particle to the damage site in order to enhance the sensitivity of the electrochemical assay. The best choice would be to use gold nanoparticles, as they are redox active and large enough to visualize.

The sensitivity of the combined AFM/ECHEM assay can be further enhanced by introducing our new layer-by-layer method we developed in chapter 5. Characterization of this new method clearly showed that it creates high charge density on the surface so that it can tightly hold immobilized DNA. This increased bonding strength significantly enhances the sensitivity of the assay.

There is still a need for future improvements in the current technology, ensuring that continued development in this direction will be of great benefit to bridging the current gap in DNA mismatch/damage sensors. Among the proposed possible future directions, it

seems most likely that development of the MutS-based array chip device will be of the greatest benefit.

We began this study with the goal of advancing existing sensor technologies for DNA mismatch and damage detection. Our results clearly demonstrate that we succeeded in developing low-cost, high-throughput miniaturized devices that have increased versatility as compared to current detection methods.